

DA FORM

(2)

# NAVAL POSTGRADUATE SCHOOL

## Monterey, California

AD-A214 468



# THESIS

FLOWFIELD EFFECTS OF LAUNCH  
ON A VERTICALLY-LAUNCHED MISSILE

by

John J. Viniotis

June 1989

Thesis Advisor:

Richard M. Howard

Approved for public release; distribution unlimited

DTIC  
ELECTED  
NOV 22 1989  
S B D

89 11 20 105

## Unclassified

Security Classification of this page

## REPORT DOCUMENTATION PAGE

1a Report Security Classification		Unclassified		1b Restrictive Markings	
2a Security Classification Authority		3 Distribution/Availability of Report Approved for public release; distribution is unlimited.			
2b Declassification/Downgrading Schedule					
4 Performing Organization Report Number(s)		5 Monitoring Organization Report Number(s)			
6a Name of Performing Organization Naval Postgraduate School		6b Office Symbol (If Applicable) 67		7a Name of Monitoring Organization Naval Postgraduate School	
6c Address (city, state, and ZIP code) Monterey, CA 93943-5000		7b Address (city, state, and ZIP code) Monterey, CA 93943-5000			
8a Name of Funding/Sponsoring Organization		8b Office Symbol (If Applicable)		9 Procurement Instrument Identification Number	
8c Address (city, state, and ZIP code)		10 Source of Funding Numbers Program Element Number Project No Task No Work Unit Accession No			
11 Title (Include Security Classification)		FLOWFIELD EFFECTS OF LAUNCH ON A VERTICALLY-LAUNCHED MISSILE			
12 Personal Author(s) John J. Viniotis					
13a Type of Report Master's Thesis		13b Time Covered From To		14 Date of Report (year, month, day) 1989 June	
16 Supplementary Notation		The views expressed in this thesis are those of the author and do not reflect the official policy or position of the Department of Defense or the U.S. Government.			
17 Cosati Codes		18 Subject Terms (continue on reverse if necessary and identify by block number) Vertical Launch, Surface-to-Air Missile; High-Angle-of-Attack Aerodynamics; Turbulence, Body of Revolution; Vortex Asymmetry.			
19 Abstract (continue on reverse if necessary and identify by block number) The flowfield about a Vertically-Launched Surface-to-Air Missile model at an angle of attack of 50° and a Reynold's number of $1.1 \times 10^5$ was investigated in a low speed wind tunnel at the Naval Postgraduate School. The goal of this thesis is to determine the location and intensity of the asymmetric vortices in the wake of the VLSAM model and to display these vortices by velocity mapping and pressure contours. The two model configurations tested were for a cruciform missile with wings and tails; one at 0° roll angle ("plus" aspect) and the other at a 45° roll angle ("cross" aspect). Two flowfield conditions were treated: the nominal ambient wind tunnel condition and a condition with a grid-generated turbulence of length scale 1.08 inches and 1.88% turbulence intensity. The turbulence length scale is 61.7% of the model diameter and 4.7% of the model length. The following conclusions were reached: 1) An increase in turbulence intensity tended to reduce the strength of the asymmetric nose-generated vortices; 2) the two asymmetric vortices remained in approximately the same position for an increase in turbulence; 3) "cross" aspect vortices were more diffused, slightly larger and centered further away from the model surface than those of the "plus" aspect body configuration, which correlates with the differences in induced side forces for these configurations observed by Rabang; 4) the top vortex of the two asymmetric vortices was closer to the model surface and appeared to be stronger for both configurations; and 5) the addition of wings and tails did not greatly alter the vortex pattern around the nose of the missile model.					
20 Distribution/Availability of Abstract <input checked="" type="checkbox"/> unclassified/unlimited <input type="checkbox"/> same as report <input type="checkbox"/> DTIC users			21 Abstract Security Classification Unclassified		
22a Name of Responsible Individual Richard M. Howard			22b Telephone (Include Area code) (408) 646-2870		22c Office Symbol Code 67Ho

DD FORM 1473, 84 MAR

83 APR edition may be used until exhausted

security classification of this page

All other editions are obsolete

Unclassified

Approved for public release; distribution is unlimited.

Flowfield Effects of Launch  
on a Vertically-Launched Missile

by

John J. Viniotis  
Lieutenant, United States Navy  
B.S. United States Naval Academy, 1982

Submitted in partial fulfillment of the  
requirements for the degree of

MASTER OF SCIENCE IN ENGINEERING SCIENCE

from the

NAVAL POSTGRADUATE SCHOOL  
June 1989

Author:



John J. Viniotis

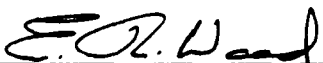
Approved by:



Richard M. Howard, Thesis Advisor



J. Val Healey, Second Reader



E. R. Wood, Chairman,  
Department of Aeronautics and Astronautics



Gordon E. Schacher,  
Dean of Science and Engineering

## ABSTRACT

The flowfield about a Vertically-Launched Surface-to-Air Missile model at an angle of attack of  $50^\circ$  and a Reynolds number of  $1.1 \times 10^5$  was investigated in a low speed wind tunnel at the Naval Postgraduate School. The goal of this thesis is to determine the location and intensity of the asymmetric vortices in the wake of the VLSAM model and to display these vortices by velocity mapping and pressure contours. The two model configurations tested were for a cruciform missile with wings and tails; one at  $0^\circ$  roll angle ("plus" aspect) and the other at a  $45^\circ$  roll angle ("cross" aspect). Two flowfield conditions were treated: the nominal ambient wind tunnel condition and a condition with a grid-generated turbulence of length scale 1.08 inches and 1.88% turbulence intensity. The turbulence length scale is 61.7% of the model diameter and 4.7% of the model length. The following conclusions were reached: 1) An increase in turbulence intensity tended to reduce the strength of the asymmetric nose-generated vortices; 2) the two asymmetric vortices remained in approximately the same position for an increase in turbulence; 3) "cross" aspect vortices were more diffused, slightly larger and centered further away from the model surface than those of the "plus" aspect body configuration, which correlates with the differences in induced side forces for these configurations observed at Rabang; 4) the top vortex of the two asymmetric vortices was closer to the model surface and appeared to be stronger for both configurations; and 5) the addition of wings and tails did not greatly alter the vortex pattern around the nose of the missile model.

For _____	
I	<input checked="" type="checkbox"/>
d	<input type="checkbox"/>
Justification _____	
By _____	
Distribution/	
Availability Codes	
Dist	Avail and/or Special
R-1	

## TABLE OF CONTENTS

I.	INTRODUCTION -----	1
A.	BACKGROUND -----	1
B.	HIGH ANGLE OF ATTACK AERODYNAMICS -----	3
1.	Aerodynamic Regimes -----	3
2.	Asymmetric Vortex Theory -----	5
3.	Two-Dimensional Crossflow -----	6
4.	Three-Dimensional Vortices -----	11
C.	TURBULENCE -----	13
D.	LIFTING SURFACE EFFECTS -----	14
E.	VLSAM LAUNCH ENVIRONMENT -----	16
1.	Marine Environment -----	16
2.	Launch and Crosswind Velocities -----	17
3.	Additional Launch Considerations -----	18
II.	EXPERIMENT AND PROCEDURES -----	19
A.	PURPOSE -----	19
B.	APPARATUS -----	21
1.	Wind Tunnel -----	21
2.	Turbulence-Generating Grids -----	23
3.	VLSAM Model and Support Equipment -----	29
4.	Velmax 8300 3-D Traverser -----	29
5.	5-Hole Pressure Probe -----	32
6.	Scanivalve and HP Data Acquisition System -----	32

C. EXPERIMENTAL CONDITIONS -----	34
D. SOFTWARE AND PROCEDURES -----	37
1. PPROBE Program -----	38
2. CALP Program -----	40
3. CONVERT Program -----	42
4. TECPLLOT System -----	43
E. PRELIMINARY TESTS -----	43
1. Dynamic Pressure Calibration -----	43
2. Yaw and Pitch Angle Corrections -----	44
III. RESULTS -----	45
A. CONFIGURATION 0A ("PLUS" WITHOUT TURBULENCE) -----	45
B. CONFIGURATION 3A ("PLUS" WITH TURBULENCE GRID 3)-----	48
C. CONFIGURATION 0C ("CROSS" WITHOUT TURBULENCE)-----	52
D. CONFIGURATION 3C ("CROSS" WITH TURBULENCE GRID 3)-----	57
E. COMPARISONS -----	57
1. Between Body Configurations (A and C) -----	57
2. Between Turbulence Levels (0 and 3) -----	61
3. With Body-Only Configuration (B) -----	62
IV. CONCLUSIONS AND RECOMMENDATIONS -----	66
APPENDIX A. PPROBE Program -----	68
APPENDIX B. CALP Program -----	79
APPENDIX C. CONVERT Program -----	84
APPENDIX D. RESULT 00.DAT -----	87
APPENDIX E. RESULT 0A.DAT -----	90
APPENDIX F. RESULT 3A.DAT -----	100

<b>APPENDIX G. RESULT 0C.DAT</b>	-----	110
<b>APPENDIX H. RESULT 3C.DAT</b>	-----	120
<b>LIST OF REFERENCES</b>	-----	130
<b>INITIAL DISTRIBUTION LIST</b>	-----	133

## LIST OF FIGURES

### Figure

1.	Airflow Regimes -----	4
2.	Vortex Flow About a Slender Nose Cylinder -----	6
3.	Two-Dimensional Crossflow About a Cylinder -----	7
4.	Side Force to Normal Force Ratio -----	9
5.	Effect of Reynold's Number on Maximum Side Force at $\alpha=55^\circ$ -----	10
6.	Side Force Variations with Nose Roll Angle -----	11
7.	The Planar Survey Grid -----	20
8.	Naval Postgraduate School Wind Tunnel -----	22
9.	Planview of VLSAM Model With Pressure Probe and Grid In the Test Section of the Wind Tunnel -----	24
10.	Square-mesh Turbulence-Generating Grid -----	25
11.	Grid Turbulence Intensities -----	26
12.	Grid Turbulence Length Scales -----	27
13.	Turbulence-Generating Grids -----	28
14.	Specifications of VLSAM Model -----	30
15.	Velox 8300 Traversing Assembly -----	31
16.	5-Hole Pressure Probe and Measuring Tip -----	33
17.	HP Data Acquisition System -----	35
18.	VLSAM Model Body Configurations -----	36
19.	Program/Data File Flowchart -----	37
20.	Calibration Manometer -----	41
21.	Velocity Vector Plot – Configuration 0A -----	46

22.	Total Pressure Coefficient – Configuration 0A -----	47
23.	Static Pressure Coefficient – Configuration 0A -----	49
24.	Velocity Vector Plot – Configuration 3A -----	50
25.	Total Pressure Coefficient – Configuration 3A -----	51
26.	Static Pressure Coefficient – Configuration 3A -----	53
27.	Velocity Vector Plot – Configuration 0C -----	54
28.	Total Pressure Coefficient – Configuration 0C -----	55
29.	Static Pressure Coefficient – Configuration 0C -----	56
30.	Velocity Vector Plot – Configuration 3C -----	58
31.	Total Pressure Coefficient – Configuration 3C -----	59
32.	Static Pressure Coefficient – Configuration 3C -----	60
33.	Velocity Vector Plot – Configuration 0B -----	63
34.	Total Pressure Coefficient – Configuration 0B -----	64
35.	Static Pressure Coefficient – Configuration 0B -----	65

## **LIST OF TABLES**

### **Table**

1. Grid Specifications -----	25
2. Grid Turbulence Parameters -----	27

## NOMENCLATURE

$C_p$	Static Pressure Coefficient
$C_T$	Total Pressure Coefficient
$d$	Base diameter of missile body
$K$	Wind tunnel calibration factor
$l_N$	Nose length
$L_d$	Missile diameter scale
$L_l$	Missile length scale
$L_u$	Longitudinal turbulence length scale
$Q$	Freestream dynamic pressure
$P_s$	Freestream static pressure
$P_t$	Freestream total pressure
$P_{sL}$	Local static pressure
$P_{tL}$	Local total pressure
$P_1$	Total pressure
$P_2$	Lateral static pressure
$P_3$	Lateral static pressure
$P_4$	Pitch angle pressure
$P_5$	Pitch angle pressaure
$R_e$	Reynold's number
$T_u$	Turbulence intensity
$u'$	Root-mean-square (rms) velocity fluctuation
$U_M$	Measured velocity

$U_\infty$	Longitudinal mean velocity
$Z_c$	Roughness length
$\alpha$	Angle of attack (AOA)
$\alpha_{AV}$	AOA for the formation of asymmetric vortices
$\epsilon$	Blockage correction factor
$\theta_A$	Nose semi-vertex angle
$\phi$	Angle from crossflow
$\phi_R$	Roll angle
$\rho$	Air density

## **ACKNOWLEDGEMENTS**

Sincere graditude goes to my thesis advisor, Dr. Richard M. Howard, for his guidance and encouragement throughout the course of my study. I have been provided with a rewarding learning experience by being afforded the chance to conduct wind tunnel experiments.

I would also like to thank the following Naval Postgraduate School personnel for their support in this research:

Mr. Jack King, Aerolab

Mr. John Moulton, Aeronautics Shop

Capt. Dan Johnson, USA, NPS Student

Lt. Jim Pinaire, USN, NPS Student.

## I. INTRODUCTION

### A. BACKGROUND

The development of the Vertical Launch Surface-to-Air Missile (VLSAM) has provided greater weapon system reliability, availability and flexibility over its predecessors. Earlier systems, such as trainable launchers and box launchers, were rather cumbersome and required excessive deck space, thus limiting the number of missiles per ship. Additionally, these systems were slow to reload since trainable launchers required cycling of rounds to get the desired one in position for launch, while box launchers were reloaded by hand. The vertical launcher provides for quick access to any round without cycling, rapid reloading and, due to its design and the fact that the missile blast is kept in a concentrated area near the launcher, it requires less deck space. [Refs. 1, 2 and 3]

The VLSAM's trajectory allows it to point to its target after launch and subsequently guide itself to the correct heading. Its aerodynamic characteristics may significantly change as it operates from subsonic to supersonic speeds during the launch, midcourse and terminal phases of its flight. [Ref. 2] The varying flight control requirements and the airflow about the missile during these phases provide for different flight regimes.

When launched, the VLSAM enters an open ocean environment and is subject to potentially significant cross-winds, the result of which is a missile flying at relatively low velocities at a high angle of attack. [Refs. 1 and 2] In particular, an example of this low velocity/high angle of attack condition is the Standard Missile 2-Block 4, or AEGIS Extended Range version, which

has an added sustainer section and leaves its launcher at a much lower speed than the unboosted SM-2 version. A missile flying at relatively low velocities at a high angle of attack may bring with it the formation of asymmetric vortices about the missile nose and afterbody which can generate unpredictable and undesired side forces, thereby affecting overall missile flight stability. The airflow around a ship's superstructure, the ocean surface conditions and the atmospheric boundary layer conditions during launch may also provide turbulent flow over the missile. [Ref. 2] The advent of the VLSAM and the desire to have highly maneuverable supersonic missiles have increased the need for further studies in high angle of attack research under various flowfield conditions.

This thesis continues experiments and research conducted to date at the Naval Postgraduate School (NPS) to understand the effects of turbulence on the VLSAM aerodynamic characteristics. Previously, Roane [Ref. 1] developed a system model to measure flowfield turbulence through the use of four different grids which generate varying turbulence levels in the NPS low speed wind tunnel. Rabang [Ref. 2] studied the effects of this turbulence on the asymmetric vortex forces on the missile model. Lung [Ref. 3] determined the location and intensity of the asymmetric vortices in the wake of the model by experimental flowfield measurements about a body-only missile configuration with and without freestream turbulence. Similarly, the goal of this study is to determine vortex locations and intensities, through a series of wind tunnel experiments, for two missile configurations, both with and without turbulence. The configurations considered are for a cruciform missile with wings

and tails; one at  $0^\circ$  roll angle ("plus" aspect) and the other at a  $45^\circ$  roll angle ("cross" aspect).

## B. HIGH ANGLE OF ATTACK AERODYNAMICS

In high angle of attack aerodynamics, flow separation from the body, wing and tail surfaces is important due to the strong normal and side forces which may be generated. Major factors which influence flow separation are nose shape, angle of attack, crossflow Reynolds number and nose fineness ratio. Other factors include roll angle and roll rate, free stream turbulence, surface roughness, acoustic environment and VLSAM model vibrations [Ref. 4].

### 1. Aerodynamic Regimes

As the angle of attack,  $\alpha$ , of a slender body of revolution ranges from  $0^\circ$  to  $90^\circ$ , there are at least four distinct airflow regimes through which the missile body transitions. [Ref. 4]

- (1) Regime I ( $0^\circ < \alpha < 5^\circ$ ): At very low angles of attack, the axial flow dominates and there is no discernable boundary layer separation (flow is attached).
- (2) Regime II ( $5^\circ < \alpha < 20^\circ$ ): At intermediate angles of attack, boundary layer separation occurs on the lee side of the body. This becomes a free shear layer which rolls up into a symmetric vortex pair that is steady with time. No side forces or yawing moments are induced.
- (3) Regime III ( $20^\circ < \alpha < 60^\circ$ ): At high angles of attack, crossflow effects start to dominate and vortices are now shed asymmetrically. These vortices induce side forces (out-of-plane forces) and yawing moments. The more asymmetric the vortex, the greater the side force magnitude. There are some flow instabilities toward the higher end of this angle of attack range.

- (4) Regime IV ( $60^\circ < \alpha < 90^\circ$ ): At very high angles of attack, the crossflow completely dominates and flow separation is unsteady. The Reynolds number, Mach number and geometry determine whether the boundary layer is shed as a von Karman vortex street or a random wake-like flow. [Refs. 1, 2 and 3]

Figure 1 shows sketches of all four vortex-generation regimes.

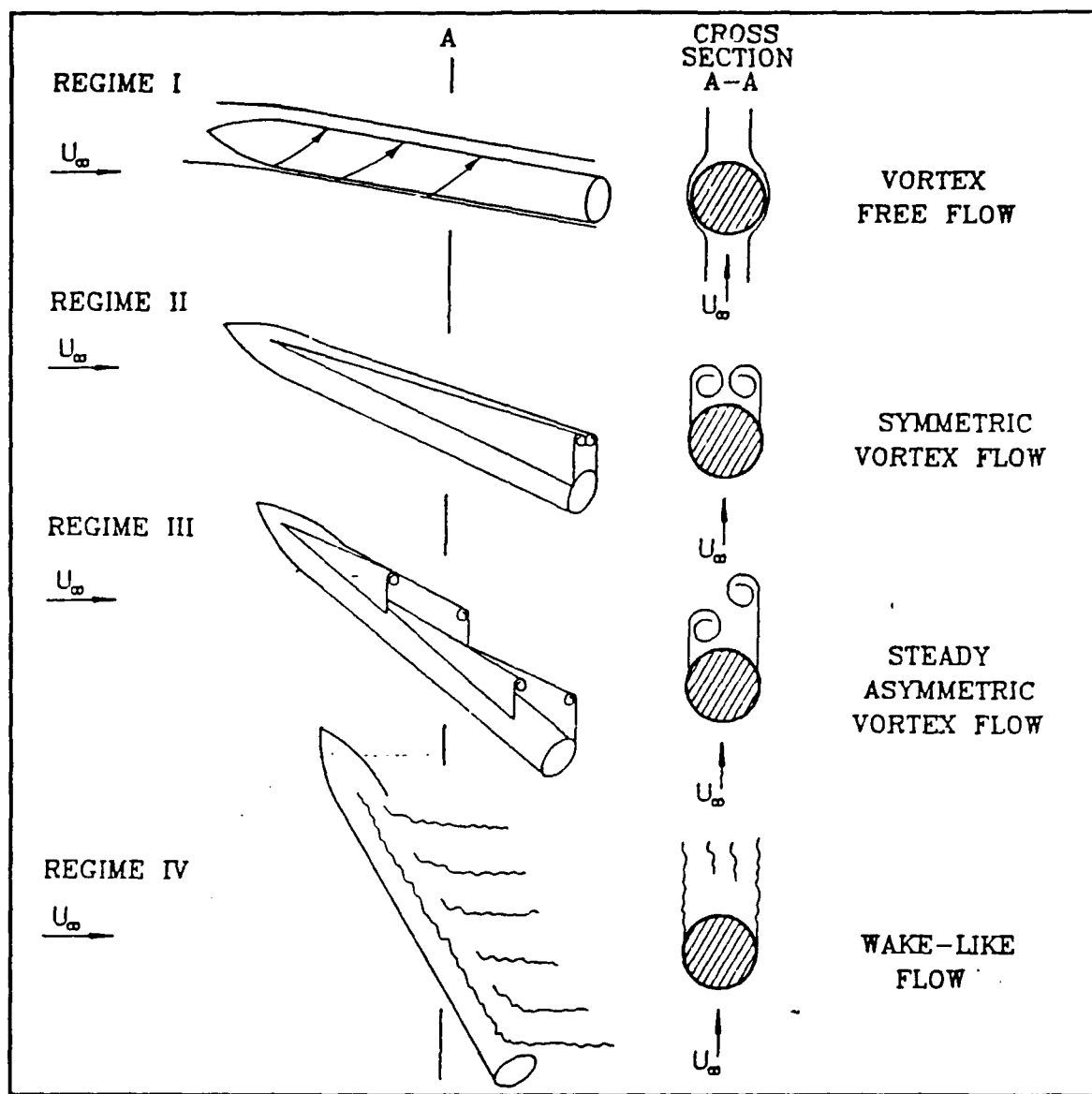


Figure 1. Airflow Regimes [Ref. 2]

## **2. Asymmetric Vortex Theory**

The principal cause of the formation of asymmetric vortices is still not completely understood and may be attributed to many factors. One idea is that boundary-layer-induced asymmetry in the location of flow separation causes the vortex flowfield to become asymmetric. These boundary layer asymmetries may result from transition and separation differences on each side of the missile body. Another proposition is that a hydrodynamic (inviscid) instability in the pair of initially symmetric vortices causes the asymmetry. [Refs. 5, 6 and 7] These vortices, which increase in strength with angle of attack, interact with the surrounding potential flowfield to provide the asymmetric configuration. A vortex-switching phenomenon has also been observed in which the vortex pattern rapidly switches from an almost symmetric to a highly asymmetric configuration, which may possibly relate to a second inviscid solution in the leeward flowfield. [Refs. 8 and 9] At any rate, even though their major cause has not been determined, the behavior of asymmetric vortices has been well documented for a large number of models and shapes.

Nose-generated asymmetric vortices appear in the flowfield around an ogive-nosed, slender, cylindrical body. The vortex formation occurs along the entire body length and induces a significant side force on the body. Figure 2 shows this vortex flow along the length of an unyawed, slender nose cylinder.

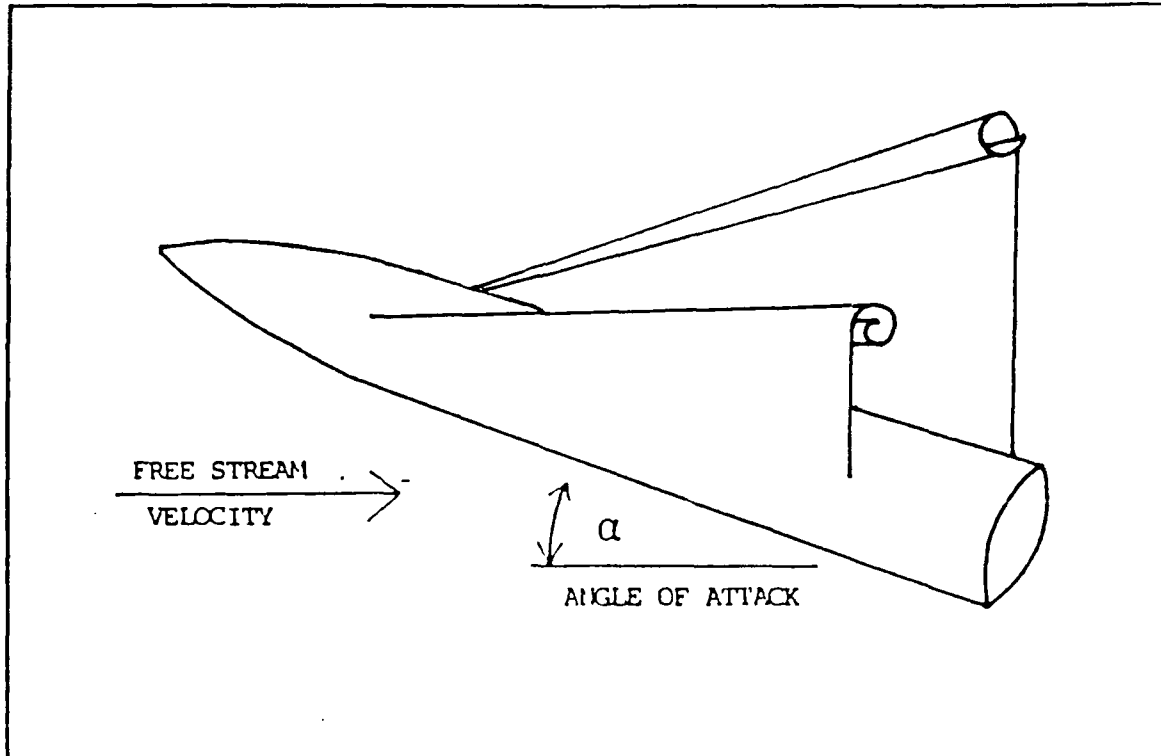


Figure 2. Vortex Flow About a Slender Nose Cylinder [Ref. 1]

### 3. Two-Dimensional Crossflow

Airflow over a slender body can be divided into normal and axial components. Axial flow is along the missile body length while crossflow is essentially a two-dimensional flow normal to a cylinder. The crossflow analogy provides information for cylinder lift and drag which act in the crossflow direction. Depending on the type of flow separation on either side of the cylinder, side forces (at right angles to the crossflow) may exist. [Ref. 2]

Boundary layer transition and separation mechanisms may provide an explanation for flow separation and subsequent asymmetric vortex generation. The primary factor which influences the separation location of the

boundary layer is the crossflow Reynolds number. Other factors include surface roughness and turbulence.

Flow around a cylinder in incompressible flow can be classified into four regions, represented by differing flow separation and drag behavior, as depicted in Figure 3. [Refs. 10, 11 and 2] In the subcritical range, the boundary layer is laminar and flow separation occurs close to the lateral meridian

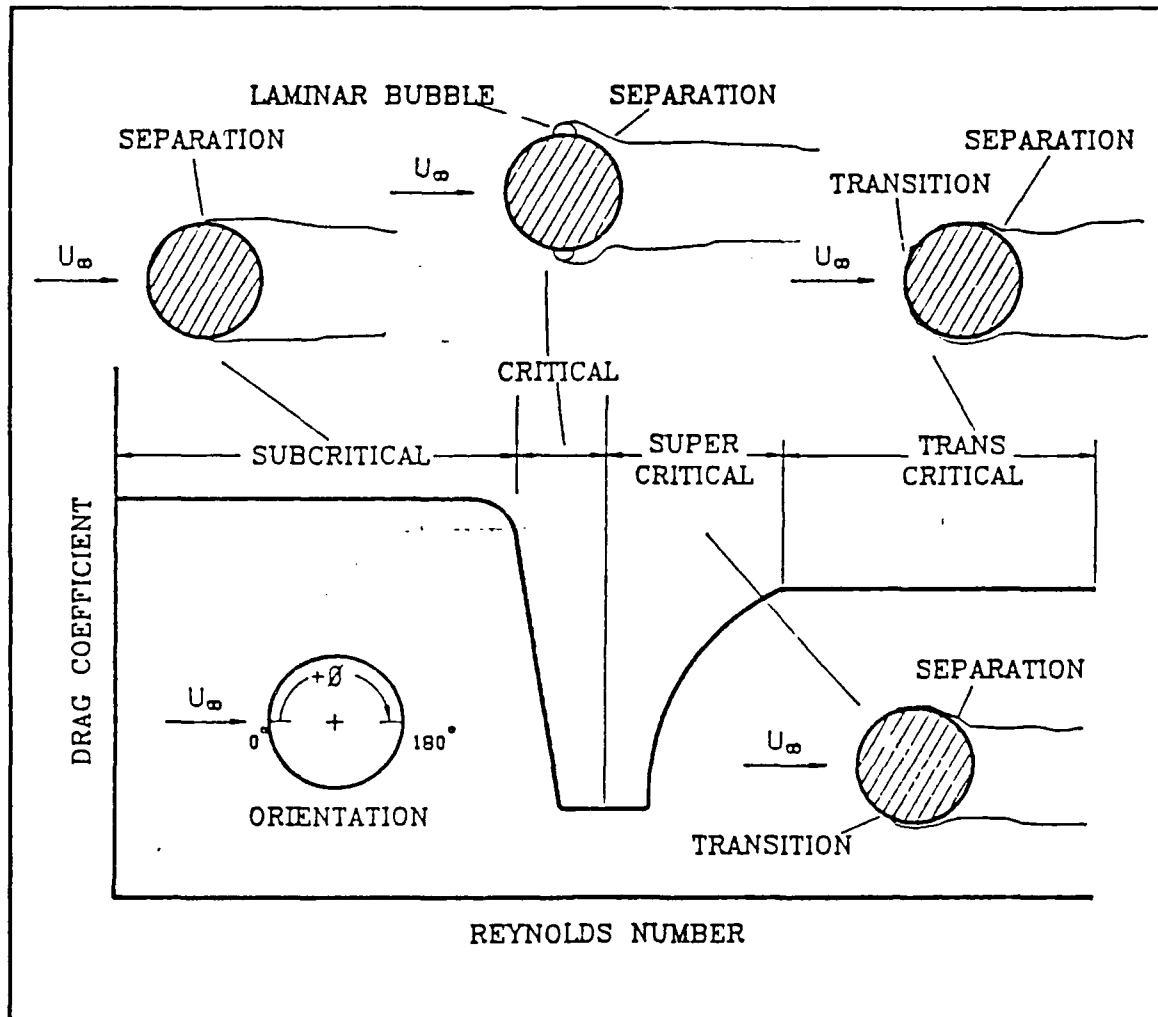


Figure 3. Two-Dimensional Crossflow About a Cylinder [Ref. 2]

where the angle ( $\phi$ ) from the crossflow direction varies from  $80^\circ$  to  $90^\circ$ .

[Ref. 12] In the critical Reynolds number region, a drag bucket is produced. The laminar boundary layer separates from the body at  $\phi = 90^\circ$  and reattaches as a turbulent boundary layer which is more energetic. Separation is delayed to  $\phi \approx 140^\circ$ , resulting in a reduction of the drag. [Ref. 3] A laminar bubble is formed between the laminar separation and the turbulent reattachment. At this point, the flow separation may easily fluctuate from critical to subcritical for small changes in Reynolds number. From Figure 4 [Ref. 10], when critical separation exists on one side of the body while subcritical separation is on the other, a large difference in  $\phi$  is possible. Therefore, vortices will be at maximum asymmetry and the side force at the highest magnitude. Since maximum side force occurs at the critical Reynolds number, it is a noteworthy parameter. [Ref. 13]

As the Reynolds number is further increased, turbulent separation moves forward to  $\phi < 140^\circ$  and the laminar bubble no longer exists. At  $\phi > 140^\circ$ , asymmetric vortices are ineffective at producing a significant side force, thus the sudden decrease in magnitude ( $C_y/C_n$ ) as shown in Figure 4. For supercritical and transcritical Reynolds numbers, the laminar transition point moves towards  $\phi \approx 0^\circ$  and turbulent separation occurs at  $\phi \approx 100^\circ$ . The asymmetric transcritical separation point moves towards the lateral meridian, where the vortices once again produce a significant side force. [Refs. 5 and 2] The Reynolds number provides the greatest influence on the normal force and drag characteristics, particularly within the critical range where the maximum normalized side force and maximum vortex asymmetry occur. [Ref. 12]

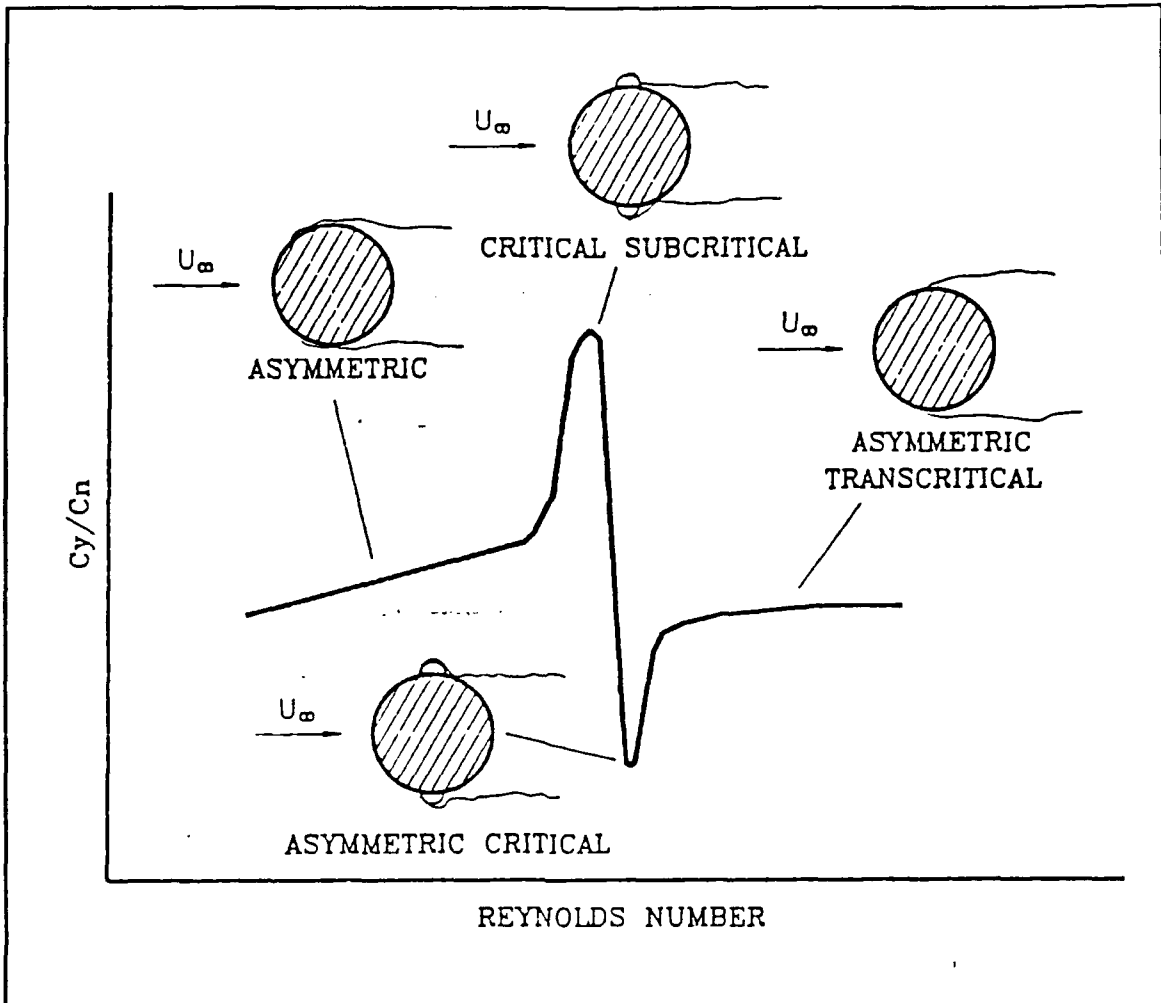


Figure 4. Side Force to Normal Force Ratio [Ref. 5]

Another study by Lamont [Ref. 14] describes a different effect of Reynolds number on the maximum side force as illustrated by Figure 5, where the side force at an angle of attack of  $55^\circ$  is plotted. The maximum side force falls from a high value at laminar separation to almost zero in the middle of the transition region before climbing again to higher levels at fully

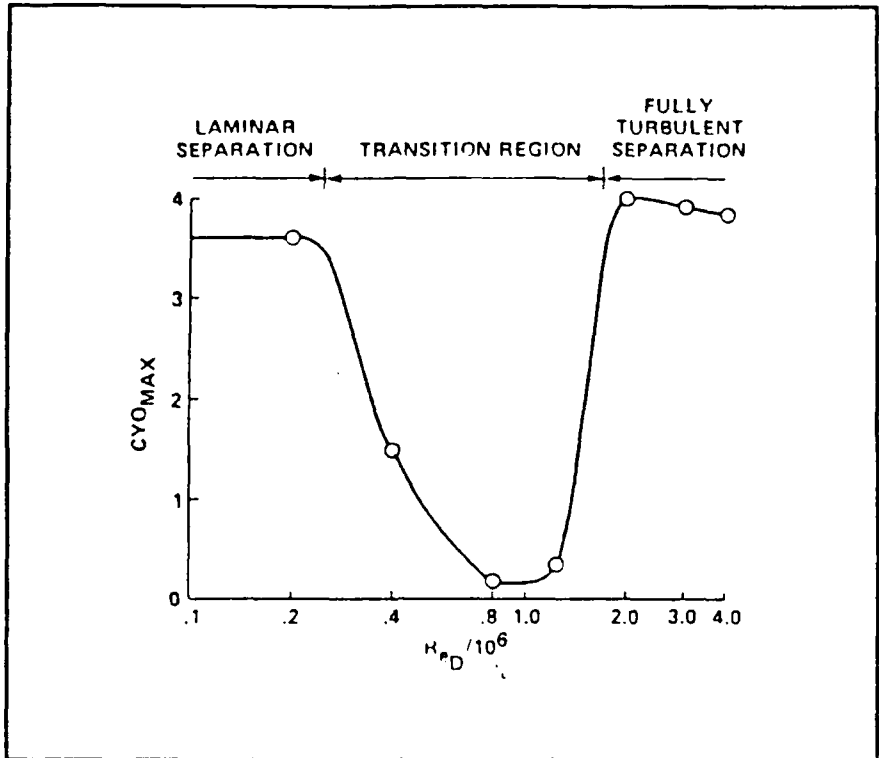


Figure 5. Effect of Reynold's Number of Maximum Side Force at  $\infty = 55^\circ$  [Ref. 14]

turbulent separation. Thus, there appears to be two different mechanisms for producing asymmetric flow and, hence, a side force on an ogive-cylinder. One mechanism operates in both the laminar and the fully turbulent separation regimes, in which the side force results from asymmetric vortex patterns in the wake of a body. The other mechanism occurs only in the transitional separation regime. Here, the Reynolds number at which the near-zero side forces were recorded, is the same range of Reynolds number in which the minimum drag coefficient on a 2-D cylinder occurs and in which no coherent vortex shedding can be detected.

#### 4. Three-Dimensional Vortices

The missile nose geometry is an important factor in vortex generation and disposition since vortices shed at the nose tend to dominate other vortices along the body length. [Ref. 15, 8 and 16]

Nose-generated vortices are sensitive to the nose roll angle due to surface imperfections and nose geometric deviations [Ref. 17]. Rabang varied the roll angle in  $45^\circ$  increments and investigated the resulting side force coefficients, shown in Figure 6. The vortex system generated by the nose dominates afterbody vortices for body configurations with and without wings regardless of the turbulence conditions [Refs. 2, 18, and 19].

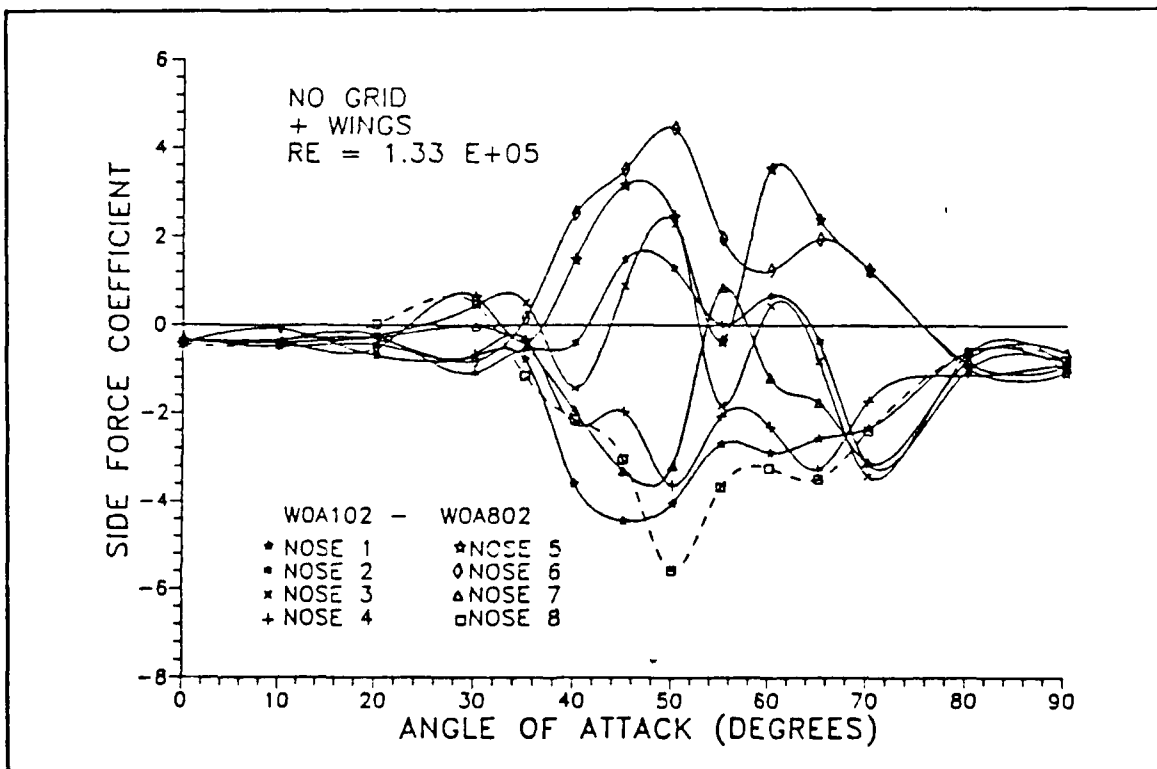


Figure 6. Side Force Variations With Nose Roll Angle [Ref. 2]

Nose geometry may be pointed or blunt for cones and ogives. For pointed noses, angle of attack for the onset of asymmetric vortices ( $\alpha_{AV}$ ) is a function of the semi-vertex angle ( $\theta_A$ ). Asymmetric vortices start at the nose and are rapidly shed, yielding unsteady side forces. [Ref. 3] At all Mach numbers, asymmetric vortex shedding starts when  $\alpha_{AV}$  is greater than  $\theta_A$ .

For a conical nose:

$$\theta_A \approx \alpha_{AV}/2 \text{ (approximation)} \quad (1)$$

For a tangent ogive nose:

$$\theta_A = \tan^{-1} \left[ \frac{l_N/d}{l_N^2/d - 0.25} \right] \quad (2)$$

where  $l_N$  is the nose length and  $d$  is the base diameter, or

$$\theta_A = l_N/d \text{ (approximation)} \quad (3)$$

Nose fineness ratio also affects the asymmetric vortex induced side forces in that as this ratio increases, the side force also increases. With an increasing ratio, both the nose apex angle ( $\theta_A$ ) and the angle of attack for the onset of asymmetric vortices ( $\alpha_{AV}$ ) will decrease, making the missile more susceptible to induced side forces at lower angles of attack. [Refs. 15 and 20] Decreasing nose fineness ratio has been found to be more beneficial in reducing side forces than blunting the nose [Ref. 15]. Side force decreases with an increasing Mach number to nearly zero at supersonic speeds [Refs. 18 and 21].

### C. TURBULENCE

Turbulence denotes the presence of random, short duration variations in a flowfield with a given mean velocity. When calculating turbulence effects on a body in the flowfield, a comparison between the scale of the body and that of the turbulence must be made. The energy in the turbulence flowfield should also be considered. [Ref. 1]

Turbulence intensity,  $T_u$ , is the measure of the relative magnitude of velocity fluctuations in the flowfield. For a horizontal flowfield or crosswind, it is the ratio of the root-mean-square (rms) velocity fluctuation,  $u'$ , to the mean velocity component in the flowfield,  $U_\infty$ .

$$T_u = u'/U_\infty \quad (4)$$

Turbulence length scales describe the time-averaged measure of the size of the constantly changing fluid disturbance eddies. An increase in the spatial length of the turbulence corresponds to an increase in the time the body is exposed to the fluctuation. Large and small scale turbulence length scales are both found in a flowfield.

From a single source, the cascade effect produces turbulence eddies of different length scales. This "cascade" effect is caused by a strain in one direction ( $x$ ,  $y$ ,  $z$  plane) which affects the orthogonal components due to the conservation of angular momentum. For example, an increase in the  $x$  and  $y$  velocity components of a vortex rotating in the  $x$ - $y$  plane will have an effect on the velocity and length scales of the  $y$ - $z$  components. [Ref. 1] Cascading continues until the smaller eddies disappear due to the viscosity. As turbulence decreases, the energy transfer decreases and the individual intensities of

each eddy will decrease at a faster rate. [Ref. 22] Thus, the larger scale turbulence predominates.

The length scale to body size ratio may determine the manner in which turbulence affects the VLSAM flowfield. It may be compared to missile length,  $L_u:L_l$ , or missile diameter  $L_u:L_d$ . [Refs. 1 and 2]

For length scales much greater than the body,  $L_u \gg L_l$ , the effect is like a steady-state flowfield, where deviations in speed and direction would be of long duration. The flowfield effects on vortex development are mainly dominated by the same factors and conditions as for a two-dimensional cylinder.

In contrast, unwanted rolling, pitching and yawing motion of the body is primarily caused when the turbulence length scale is comparable to the body length,  $L_u \approx L_l$ . [Ref. 23] The flowfield is distinctly non-steady for this case.

When the length scale is of a dimension much smaller than the body, most significantly, when it is smaller than the missile diameter,  $L_u \ll L_d$ , it has a magnitude comparable to the boundary layer thickness on the missile surface. Thus, boundary layer development and flow separation over the body may be affected by the presence of small scale turbulence. An increase in turbulence intensity with a length scale on the order of the boundary-layer scale tends to reduce the magnitude of induced side forces. [Refs. 2, 24, and 25] A goal of the current investigation is to determine the effect of vortex-scale turbulence on the asymmetric vortices and resulting induced side forces.

#### D. LIFTING SURFACE EFFECTS

The complete vortex structure of the missile is a net result of the individual contributions from the body, wings, strakes and tails. In general, missiles use low aspect ratio wings (when compared with aircraft). Since some

missiles have wing spans that approach body diameter, it is important to consider the joint effects from a wing-body combination. Nose vortices dictate flow behavior over a missile body at high angles of attack and, consequently, these vortices may also be felt by the wings. Nose and body vortices move away from a missile body without wings but, when wings are added, they move closer to the body. This result is comparable to increasing the effective angle of attack causing unsteady asymmetric vortices. For wings with low aspect ratio, a major portion of the lift produced by the wing will be a result of vortex lift. The net effect of the wing-body combination appears to be a reduction in the effective angle of attack for the onset of asymmetric vortices and side forces. [Refs. 2, 3, and 26]

Vortex lift effects are improved by incorporating strakes with low aspect ratio wings. The strakes produce additional strong vortices. Some researchers have found that placing long strakes on a missile would induce interference with the crossflow component around the body, thus decreasing the effect of the forces and moments generated by asymmetric body vortices. [Ref. 6] Rabang has shown that the addition of typical VLSAM wings and strakes tend to preserve the induced side force for all levels of turbulence intensities and length scales. [Ref. 2]

The addition of tails has a minor influence on forebody flowfields and maximum side forces, in particular, at low angles of attack. At higher angles of attack, nose and wing vortices may have a slight effect on the tailflow, depending on the wing placement and afterbody length between the wings and tails.

## **E. VLSAM LAUNCH ENVIRONMENT**

### **1. Marine Environment**

Turbulence conditions which exist within the atmospheric boundary layer (ABL) may significantly impact the VLSAM. The ABL is the lowest portion of the atmosphere and is formed by its interaction with the surface over which it flows. Turbulence in this layer is the result of the transfer of heat, momentum and mass.

The surface layer, the lowest segment of the ABL, can vary in height from 5 to 200 meters but is typically on the order of 50 meters. It is also characterized by mechanically produced, small-scale turbulence resulting from surface roughness or friction from waves on the ocean surface. This small-scale turbulence is larger than the missile length. This region is described by variations in wind speed, nearly vertical heat and mass fluxes, and other meteorological fluctuations with height. [Refs. 27 and 23] Furthermore, the majority of the flow in the surface layer itself can be considered horizontally homogeneous and two-dimensional [Ref. 23].

A measure of the roughness of the surface is called the roughness length,  $Z_0$ , which is a function of the mean wind velocity at various heights above the surface. By combining the roughness length with the elevation and wind speed, both the turbulence intensity and length scale can be empirically determined. [Refs. 2, 3 and 28] Typical open ocean surface roughness lengths are in the range of  $0.001 < Z_0 < 0.01$ , with  $Z_0$  in meters. For a 10 meter elevation and a mean wind speed of 25 m/sec in a neutral atmosphere, turbulence intensities may range from 13 to 17 percent. [Ref. 28] The longitudinal turbulence length scale would then range from  $262 < L_u < 295$  feet ( $80 < L_u < 90$

meters). Therefore, for a typical missile with a 1.1 foot diameter, the turbulence length scale to missile diameter length scale ratio is  $L_u:L_d \approx 280:1$ . [Ref. 28] This represents a length scale very much larger than a conventional missile length and, therefore, would have little effect on its boundary layer development. However, the cascade effect from large scale turbulence and from crosswind interaction with a ship's superstructure allows length scales, initially much larger (85 meters) than the dimension of a missile, to decrease (cascade) to scales where they could affect the missile boundary layer development and the development of vortices from the missile nose. The actual amount of such small-scale turbulence present in the marine atmosphere is largely unknown, however. [Ref. 23]

## **2. Launch and Crosswind Velocities**

A typical VLSAM at launch (vertical velocity = 164 ft/sec) is still well within the surface layer environment and is subject to both crosswind and turbulence effects. [Ref. 29] Crosswind velocity depends on both the ambient wind speed and the speed of the launch platform. A ship speed of 20 knots with a head wind of 20m/sec, combined with the VLSAM launch velocity, results in an effective angle of attack of  $31^\circ$  at 191 ft/sec, which places the missile in the asymmetric vortex region (Regime III) almost immediately after clearing the exit plane of the launcher, 0.2 seconds after launch. [Refs. 1 and 2]

When the missile first leaves its launcher it will experience an even greater effective angle of attack due to its slower velocity. A ship's hull and superstructure can dictate changing flow fields and turbulence at this initial launch altitude. The ship airwake may increase crosswind velocities and

cause significant crosswind gradients in the flowfield, thus increasing turbulence intensities while decreasing turbulence length scales. [Ref. 2]

Later in its launch profile, when the VLSAM pitches over towards a target, it may reach effective angles of attack of up to 50°. [Refs. 2 and 30] Thus, during the launch phase there exists a definite possibility of asymmetric vortex induced side forces on a VLSAM.

### **3. Additional Launch Considerations**

During launch, a missile is influenced by many factors which are dependent on missile design, ship's orientation, launcher mechanics and missile flight control. Shipboard roll, pitch and yaw are directly transmitted to the launch platform and must be taken into account. Inherent factors, such as the plume (jet) effect of the missile's engine and blast effects of the vented exhaust gases, can also affect VLSAM aerodynamics. Exhaust gases can impinge directly on the missile surfaces or they can impact the flowfield in which the missile is launched, especially if the gases are vented upward into the vicinity of the accelerated missile. [Ref. 1] The manner in which control systems respond to missile orientation changes is another factor. Should the missile change its flight attitude, the flowfield around it will also be altered. Obviously, the considerations discussed in this section are not all-encompassing. There are many other factors that affect missile flight behavior during launch, but they are beyond the scope of this thesis and will not be included.

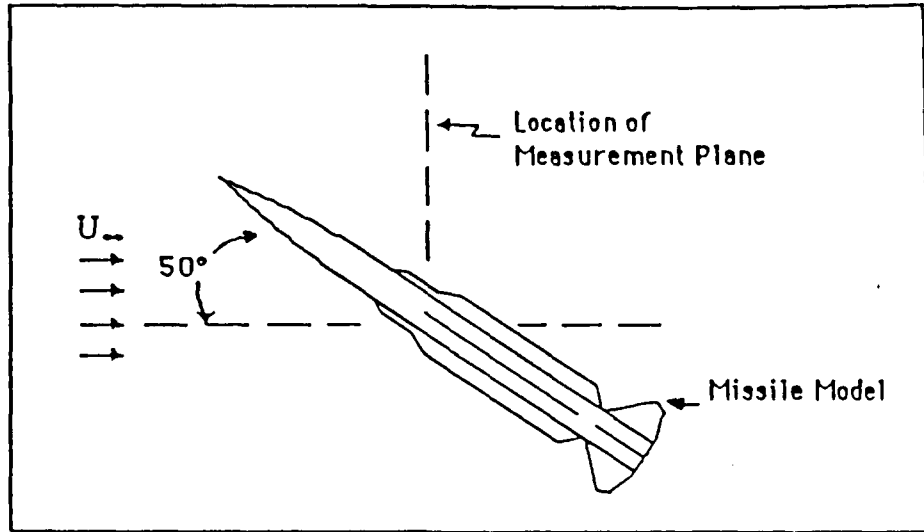
## II. EXPERIMENT AND PROCEDURES

### A. PURPOSE

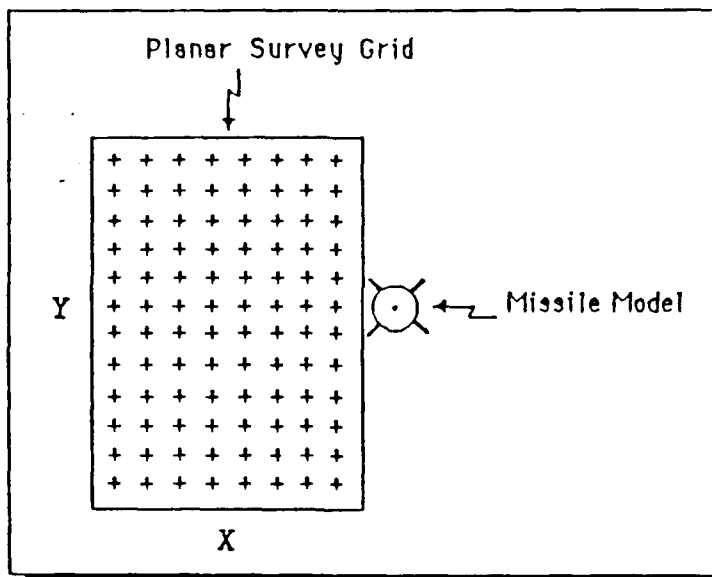
In this study, the location and intensity of asymmetric vortices in the wake of the VLSAM model were determined for varying levels of turbulence. This turbulence was generated by the placement of a series of grids in the wind tunnel. The vortices were displayed by velocity mapping and pressure contours. To accomplish this, wind tunnel flowfield pressure measurements were taken for a specified survey grid using a scanivalve/probe data acquisition system.

Figure 7 [Ref. 3] shows the planar survey grid, the x-y plane, which was perpendicular to the freestream velocity and located 10.5 inches downstream from the missile model's nose. The model body was centered on the y dimension. For the actual data acquisition runs, 23 points were measured in the y direction. There were 11 points above and below the model centerline, with point 12 directly at the centerline. Along the x axis, 13 points were measured. The x-y dimension for the experiment was 3x5.5 inches, with a step distance (increment) of 0.25 inch ( $22 \times 0.25 = 5.5$  and  $12 \times 0.25 = 3$  inches). This dimension covered the main portion of asymmetric vortices.

Pressure measurements were obtained by the 5-hole probe throughout the survey plane. The data from the pressure probe was reduced through the use of computer programs to obtain isobars of total pressure coefficient and static pressure coefficient, and to map the crossflow velocity vectors. These



(a) Top View



(b) Front View

Figure 7. The Planar Survey Grid [Ref. 3]

results were correlated with the force measurements of Rabang and with the previous experiments by Lung to provide a greater understanding of the vortex flowfield. The following sections further discuss the equipment and software used, and the experimental procedures followed.

## B. APPARATUS

Information about the construction, specifications and configurations of the major pieces of equipment used in this study is described in this section.

### 1. Wind Tunnel

The low-speed, single return, horizontal-flow tunnel located in Halligan Hall at NPS was utilized. (Figure 8, [Ref. 31]) . It is powered by a 100 horsepower electric motor coupled to a three-blade variable-pitch fan via a 4-speed Dodge truck transmission. Aft of the fan blades are a set of stator blades which help straighten flow. Two fine wire mesh screens located upstream of the settling chamber plus turning vanes at all four corners reduce turbulence. A heavy wire screen behind the test section prevents foreign object damage to the fan blades [Refs. 1, 2 and 31] The tunnel is 64 feet long and ranges from 21.5 to 25.5 feet wide.

The wind tunnel test section measures 45 inches by 32 inches. The walls diverge slightly to prevent reduction in freestream pressure due to boundary layer growth. The settling chamber area to test section area contraction ratio is approximately 10:1. Corner fillets, which house the lighting, reduce the section area from  $10 \text{ ft}^2$  to  $9.88 \text{ ft}^2$ . Fillets are found at wall intersections throughout the tunnel to help reduce boundary layer effects. [Ref. 31]

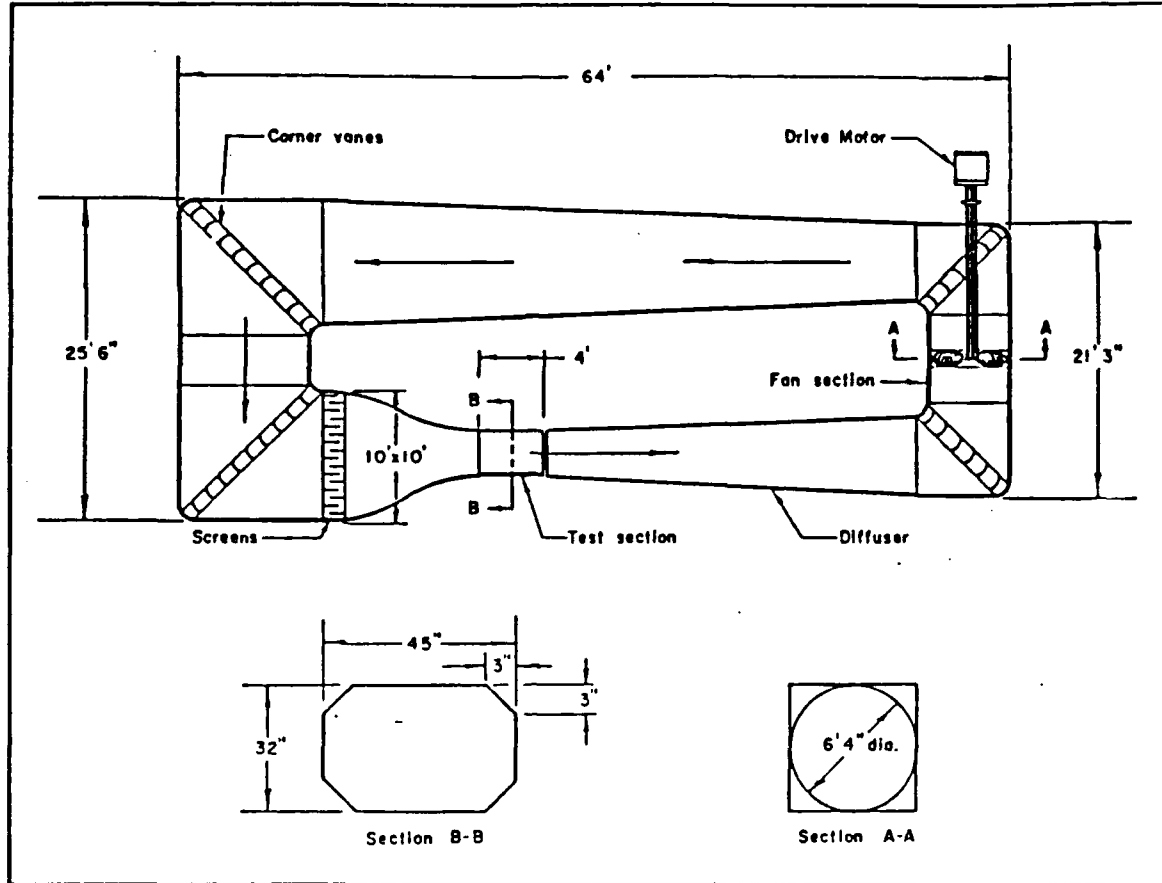


Figure 8. Naval Postgraduate School Wind Tunnel [Ref. 31]

A reflection plane installed in the test section reduces the available height to 28 inches. A flush-mounted turntable allows for changes in model pitch angle or angle of attack via a remotely controlled electric motor beneath the tunnel. Since the test section operates at atmospheric pressure, breather slots are installed around the tunnel perimeter to replenish air lost through leaks and to ensure a uniform test section pressure. The tunnel was designed to provide test section velocities of up to 290 ft/sec. [Ref. 31]

Wind tunnel temperature is measured by a dial thermometer extending into the settling chamber. Dynamic pressure is measured by the static pressure difference between the test section and the settling chamber using a water filled manometer. The static pressure is measured by four pressure taps located upstream from the test section to avoid interference from the model. These taps are connected via a common manifold prior to feeding into the manometer. Pressure differences are measured in centimeters of water. Equation (5) is used to convert to the actual wind tunnel velocity.

[Ref. 3]

$$U_m = \left[ \frac{(2)(2.0475)(P_{cm} H_2 O)}{K(\rho)} \right]^{1/2} \quad (5)$$

where:

$U_m$  = measured velocity (ft/sec)

2.0475 = conversion factor

$P_{cm} H_2 O$  = manometer reading

K = calibration factor (for specific grid)

$\rho$  = air density ( $lb/ft^2$ )

## 2. Turbulence-Generating Grids

Four grids are used to create turbulence of varying intensities and length scales. Each is mounted in a wooden frame and placed 73 inches forward of the pivot axis of the model support system (see Figure 9). Three of the grids are constructed from wood and the fourth is made of wire. Grid specifications are listed in Table 1 and are shown in Figure 10. They are

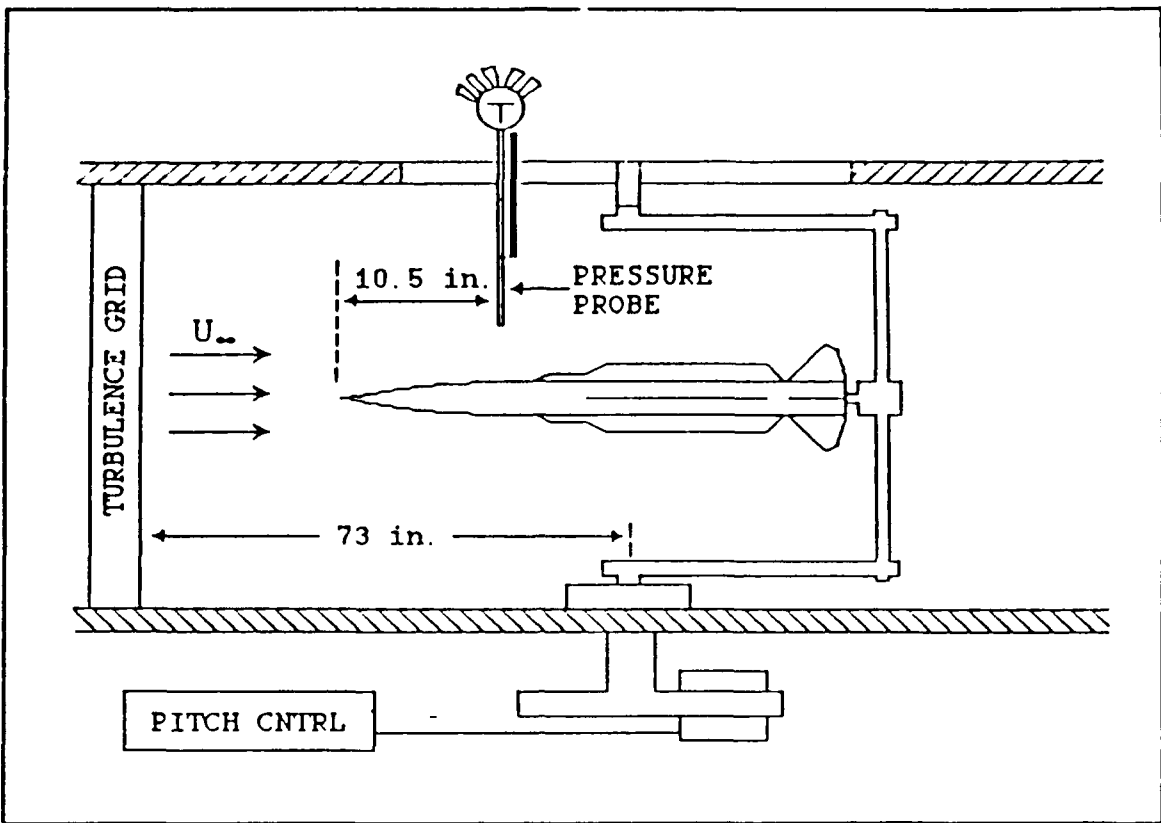


Figure 9. Planview of VLSAM Model With Pressure Probe and Grid In the Test Section of the Wind Tunnel (not drawn to scale) [Ref. 2]

TABLE 1. GRID SPECIFICATIONS [REF. 2]

Grid	Mesh Width (in.)	Bar Diameter (in.)	Mesh/Diameter	Material
One	5.00	1.00	5	Wood
Two	3.75	0.75	5	Wood
Three	2.50	0.50	5	Wood
Four	1.00	0.0625	16	Wire

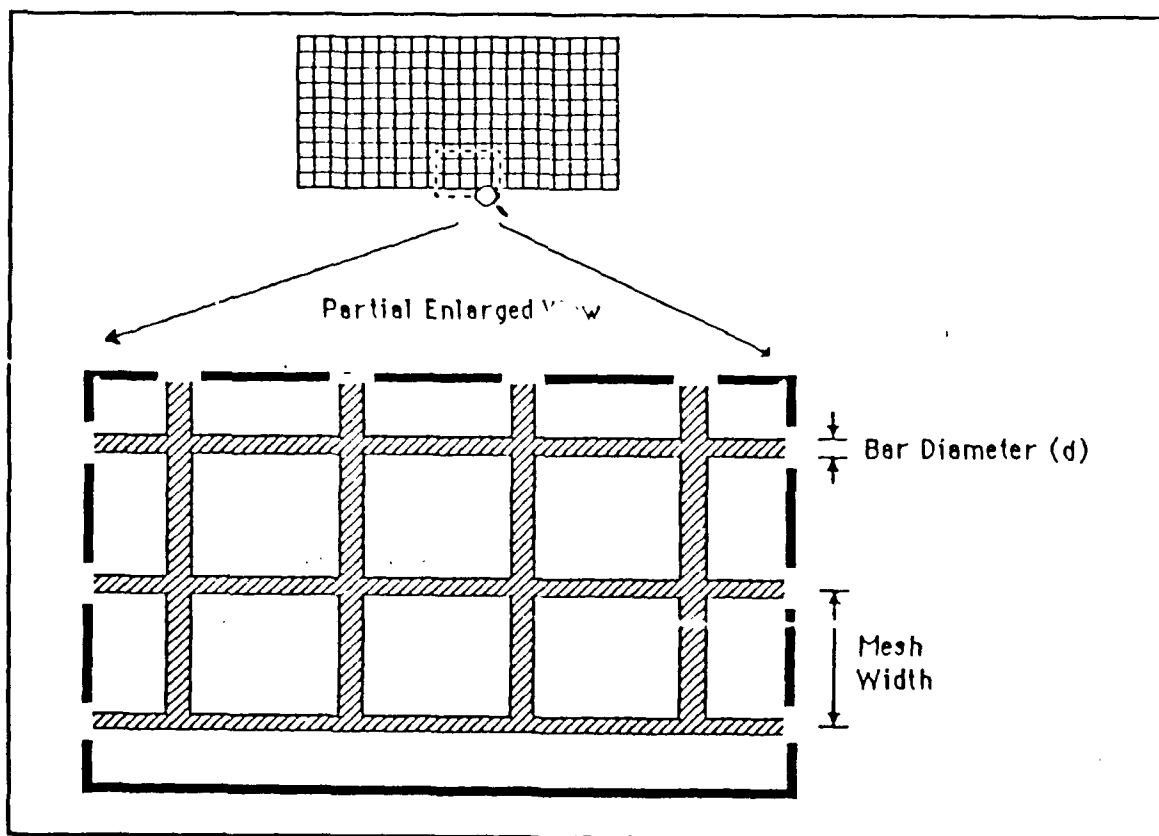


Figure 10. Square-Mesh Turbulence-Generating Grid [Ref. 3]

square-mesh square-bar biplanar grids which generate nearly isotropic homogeneous turbulence. [Ref. 29] Roane measured turbulence intensities and estimated length scales, shown in Figures 11 and 12. [Ref. 1] The grid turbulence parameters taken by Roane are summarized in Table 2. Grid turbulence effects, with respect to changing length scales at constant intensity or constant length scales with changing intensities, can not be investigated with the present grid geometries. [Ref. 3] Figure 13 shows photographs of the grids.

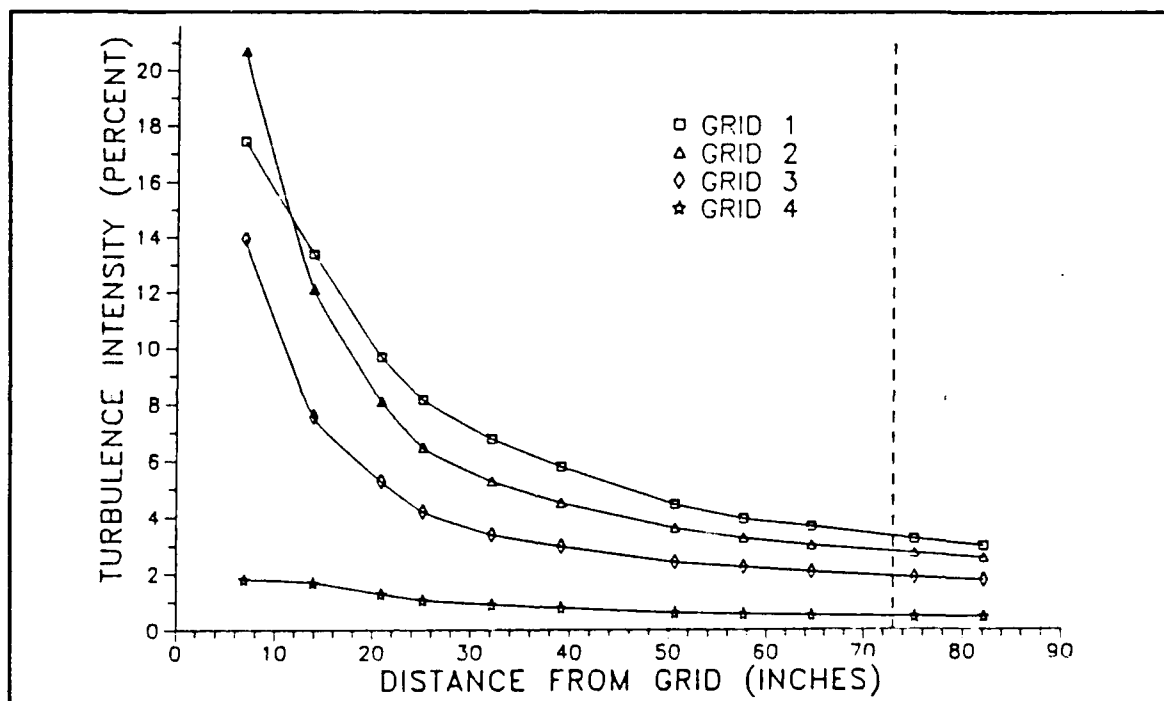


Figure 11. Grid Turbulence Intensities (dashed line indicates model pivot axis) [Ref. 2]

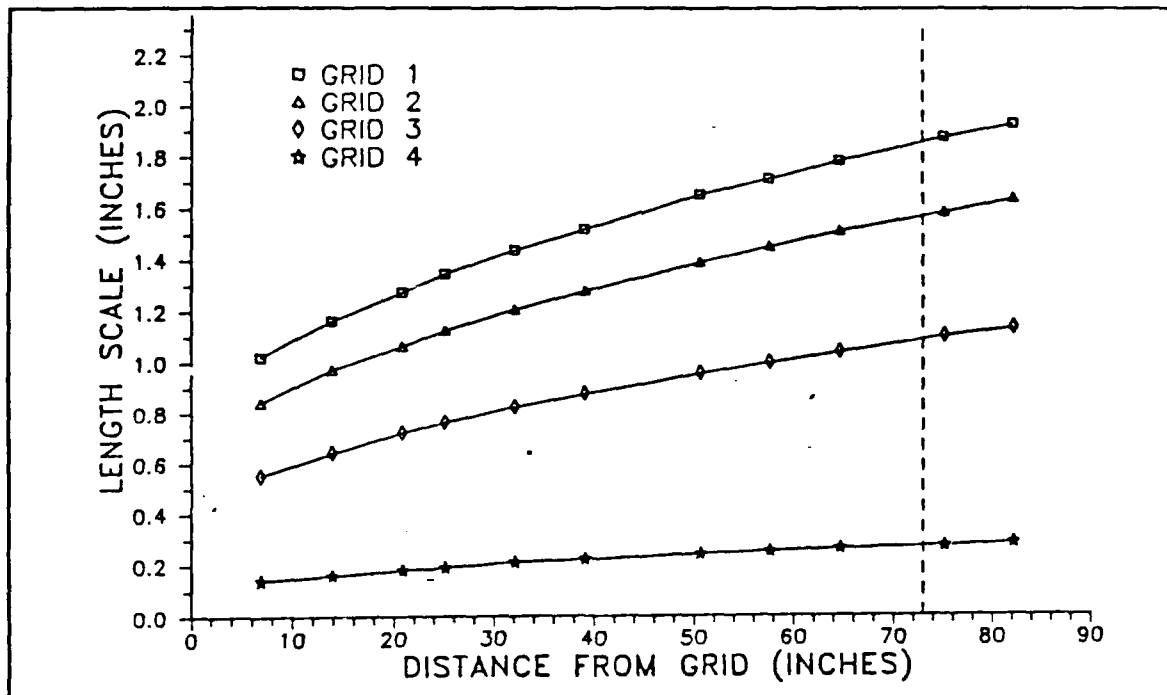


Figure 12. Grid Turbulence Length Scales [Ref. 2]

TABLE 2. GRID TURBULENCE PARAMETERS  
(AT MODEL PIVOT AXIS) [REF. 1]

Grid	Intensity (percent)	Length Scale (in.)	Turbulence/ Model Dia.	Dynamic Pressure (lb/ft <sup>2</sup> )
One	3.31	1.84	1.05	15.35
Two	2.78	1.56	0.89	14.88
Three	1.88	1.08	0.62	16.38
Four	0.47	0.27	0.15	15.61
None	0.23	-	-	15.85

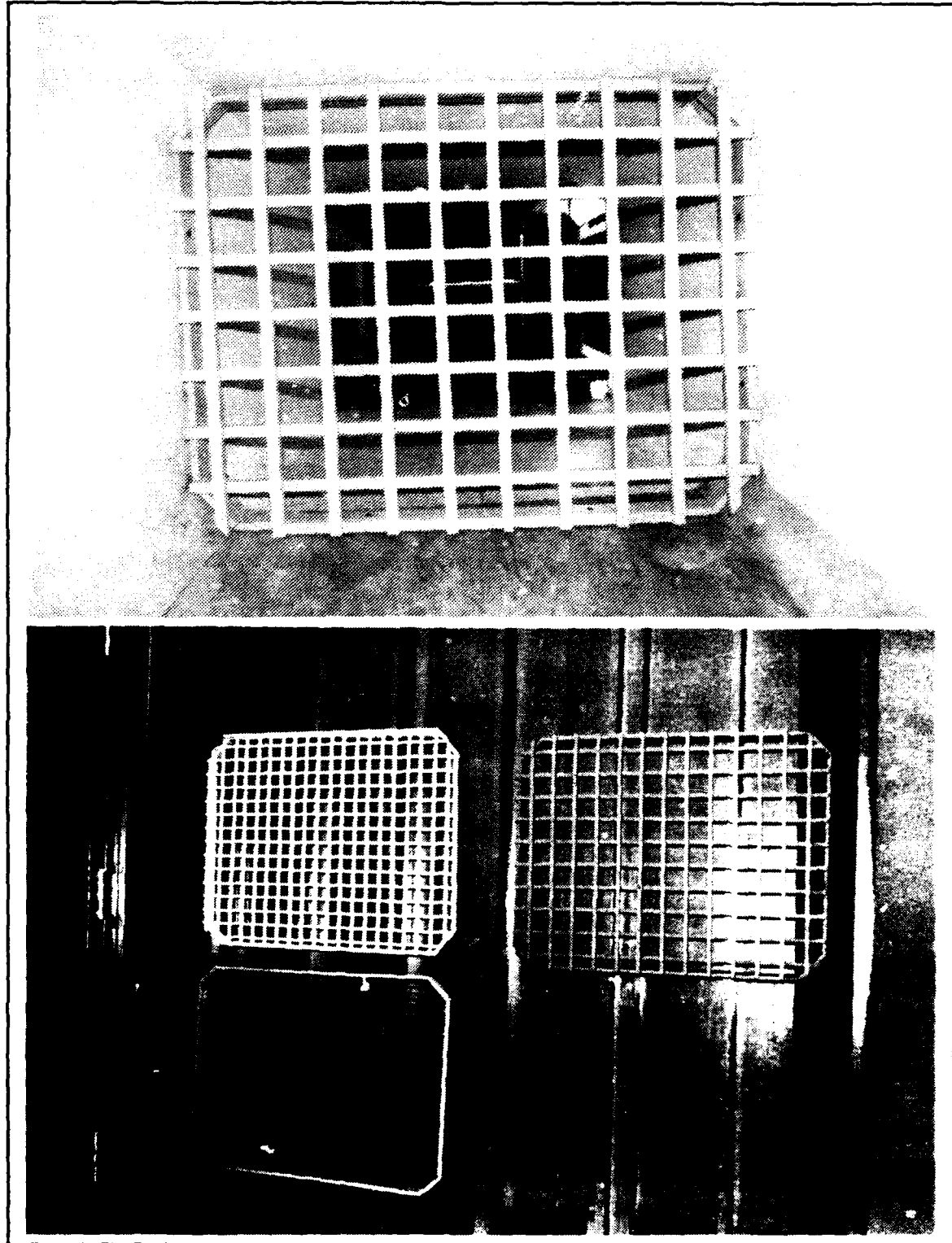


Figure 13. Turbulence-Generating Grids

### **3. VLSAM Model and Support Equipment**

The model was designed to represent a current cruciform tail-control missile with very low aspect ratio wings (long dorsal fins). It was constructed from 6061 and 2024 aluminum alloy by NPS personnel. [Ref. 1]

The hollow cylinder body section contains locating pin attachment points for the balance, sleeve, wings and tails. The machined sleeve provides a close tolerance fit between the balance gage and the interior of the model. [Ref. 3] Both body roll angle and nose roll angle may be varied in 45° increments. The wings with strakes and the tail control fins are rigidly connected to the model body by countersunk screws. Figure 14 depicts the dimensions and specifications of the VLSAM model. [Ref. 2] The model's surface is polished and free of protruberances.

The model support is rigidly fixed in the test section by the reflection plane turntable at the base and an aluminum reinforced clear plexiglass section at the top. The pivot point of this rotating support coincides with the approximate center of the VLSAM model. The plexiglass has three slots (7-, 8- and 10-inches long) cut in it, each 5/4 inches wide. These slots correspond to the positions of model length to diameter ratios of 3, 6 and 9; i.e., 5.25, 10.5 and 15.75 inches from the nose. [Refs. 2 and 3]

### **4. Velmex 8300 3-D Traverser**

The Velmex 8300 is composed of a motor controller assembly and a traversing assembly, and uses three microcomputer-controlled stepping motors (one for each axis of movement). The motor controller assembly is capable of interpreting motor movement commands from a host computer,

Total length = 22.85 in.  
 Base diameter = 1.75 in.  
 Length/diameter ratio = 13.06  
 Ogive nose length = 4.0 in.  
 Ogive/diameter ratio = 2.29  
 Wing span/root chord = 3.13 in./13.55 in.  
 Tail span/root chord = 5.50 in./1.70 in.  
 Center of pressure = 13.5 inches aft of nose tip (approx.)

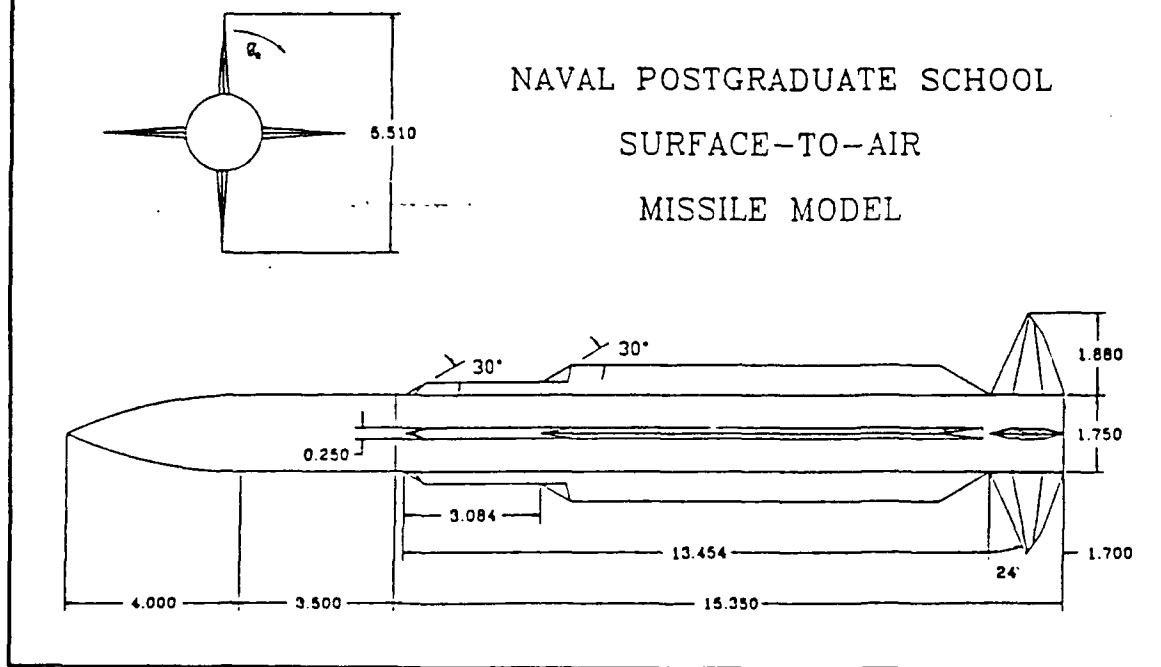


Figure 14. Specifications of VLSAM Model [Ref. 2]

programmable control or terminal. Software commands allow the operator to select motor variables such as velocity, acceleration, increment distance and units (motor steps or inches). [Ref. 32]

The stainless steel and aluminum traverser assembly (Figure 15) consists of three separate motor/jackscrew assemblies.

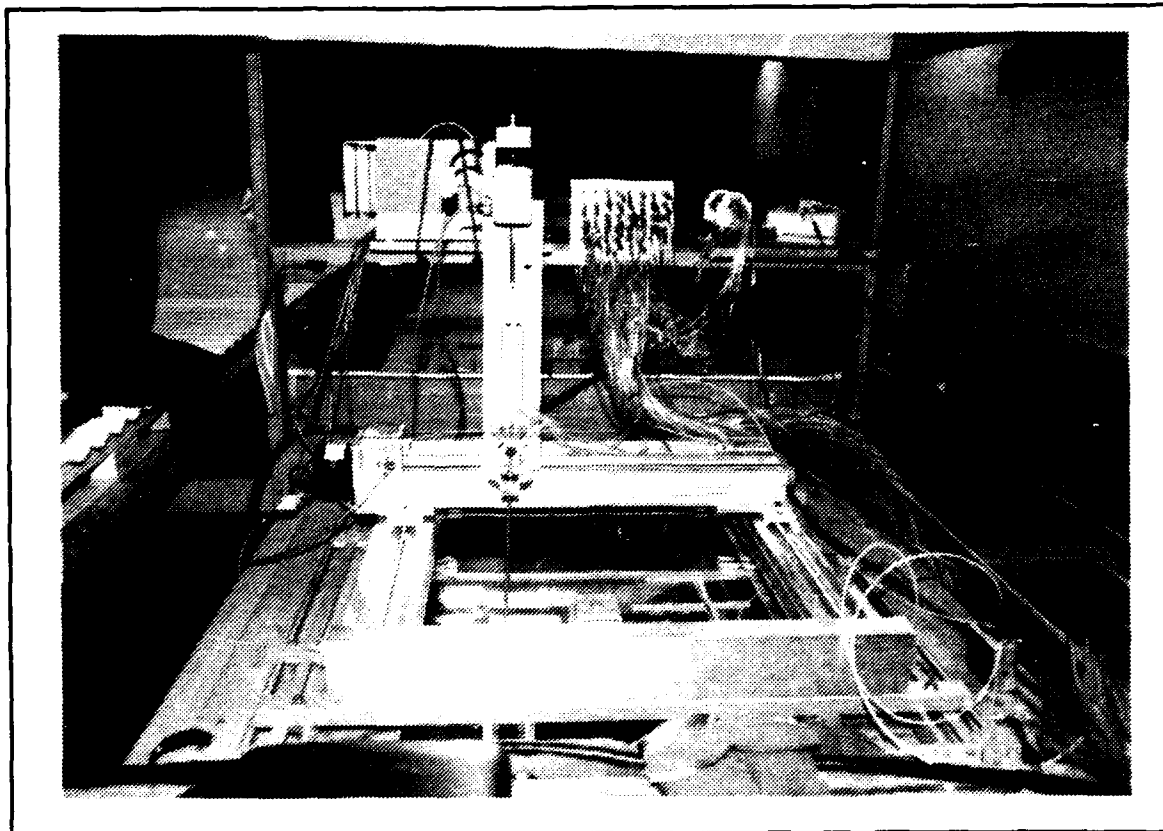


Figure 15. Velmex 8300 Traversing Assembly

The traverser was mounted to existing hardware on top of the tunnel so as to minimize tunnel-induced vibrations. A 5-hole pressure probe, attached to the 8300 control drive, can be accurately and effectively moved through the test section.

## **5. 5-Hole Pressure Probe**

The three-dimensional 5-hole probe, Figure 16 [Ref. 33], is made of corrosion resistant non-magnetic stainless steel. It is 0.125 inch in diameter and 24 inches in total length with 22 inches of reinforcement tubing. The probe has five measuring holes located on its prism-shaped tip. A centrally located hole ( $P_1$ ) measures total pressure, while two lateral pressure holes ( $P_2, P_3$ ) are used to determine yaw angle of flow. Pitch angle is determined by pressure holes ( $P_4, P_5$ ) located above and below the total pressure hole. The probe is usable for speeds up to Mach 0.7.

The speed of reading depends on the length and diameter of the pressure passage inside the probe, the size of the pressure tubes to the manometer, and the displacement volume of the manometer. [Ref. 33] For smaller diameter tubes, the time constant increases rapidly. For this experiment, the tube diameter was 1/4-inch O.D. and the tube lengths were three feet, so the time delay was about 0.15-0.26 second. [Ref. 3]

## **6. Scanivalve and HP Data Acquisition System**

One 48-port scanivalve was used to measure each of the 5-hole probe pressures. The Hewlett-Packard (HP) data acquisition system consists of a combination of hardware and software that enables the IBM PC-AT computer to act as a fully automated instrumentation system. [Ref. 34] Individual instruments include the Relay Multiplexer, Digital Multimeter and Relay Actuator.

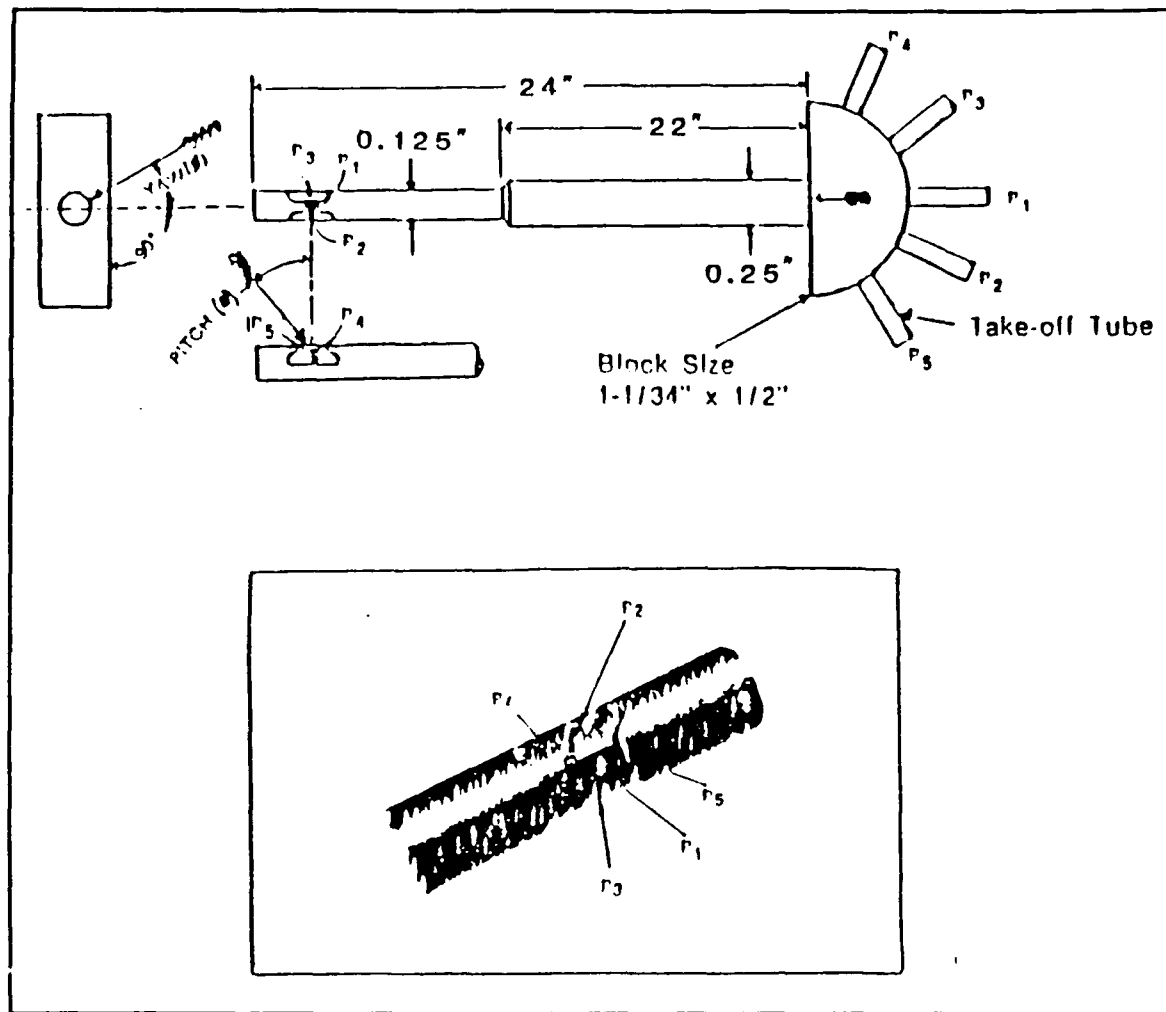


Figure 16. The 5-Hole Pressure Probe and Measuring Tip [Ref. 33]

The scanivalve mechanism puts out a 7-bit binary coded decimal (BCD) signal that corresponds to the port (1-48) currently connected to the scanivalve transducer. This allows remote electronic monitoring of the port assembly configuration. [Ref. 3] The scanivalve consists of a transducer, motor drive, port assembly and solenoid controller, which actually regulates the scanivalve. Two commands allowed by this solenoid are STEP, which

moves the scanivalve to one port location, and HOME, which sends the scanivalve to port number 48. The Relay Actuator is used solely in controlling the scanivalve to STEP or HOME. [Ref. 3]

The HP Data Acquisition System is shown in Figure 17. The scanivalve signal, containing probe port pressure information, passes to the Relay Multiplexer which provides one common output channel for the Digital Multimeter (DMM). The signal is conditioned by a low pass filter prior to being measured by the multimeter. The DMM automatically converts input analog voltage signals into a digital (binary) form which can be read by the computer.

### C. EXPERIMENTAL CONDITIONS

To facilitate data correlation, the conditions for this experiment were similar to the conditions of the previous studies by Lung and Rabang.

- (1) Test section reference dynamic pressures were set at 7.2 cm H<sub>2</sub>O for the no grid run and at 10.0 cm H<sub>2</sub>O for grid #3, which yielded a subcritical Reynolds number of  $R_e = 1.1 \times 10^5$ . These reference pressures are the same as those used in the turbulence mapping by Roane [Ref. 1] and were duplicated in this study in order to ensure comparable test section velocities and turbulence grid length scales and intensities.
- (2) The VLSAM model nose geometry was held fixed at nose position eight, which Rabang showed gave the maximum side force magnitude. [Ref. 2]
- (3) Afterbody roll angles were as follows:
  - Body A: wings and tails at roll angle  $\phi_R = 0^\circ$  in a "+" configuration
  - Body B: no wings or tails at roll angle  $\phi_R = 45^\circ$
  - Body C: wings and tails at roll angle  $\phi_R = 45^\circ$  in an "x" configuration.Figure 18 shows these three configurations. Only Bodies A and C were tested in this study.

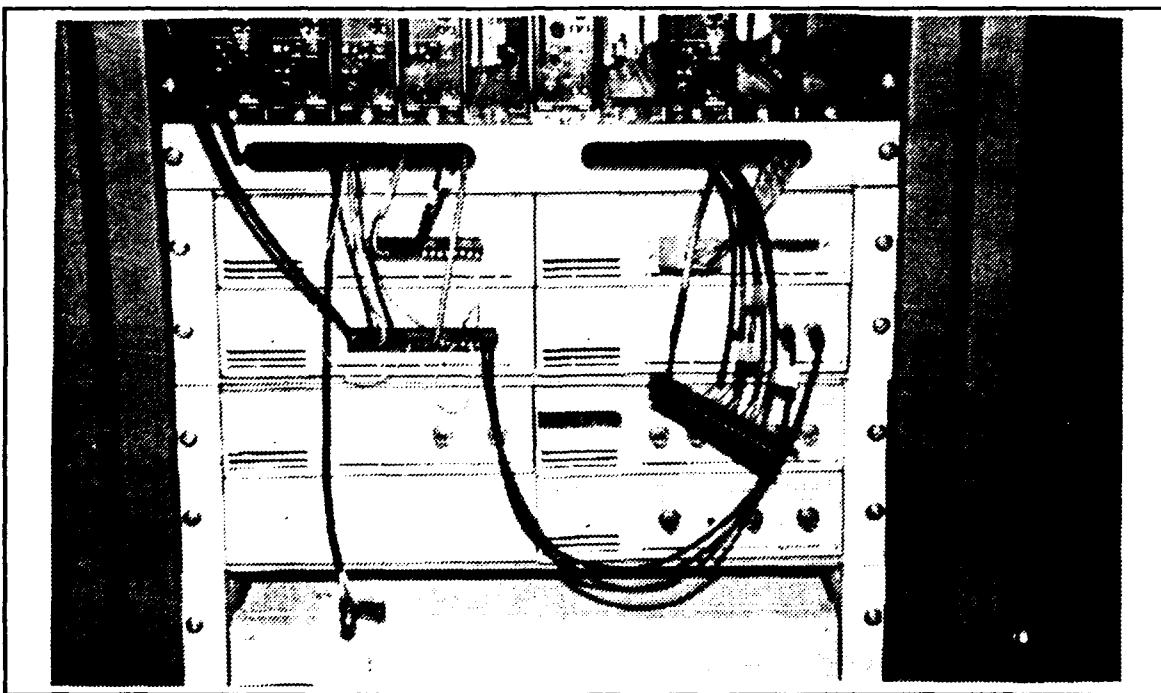
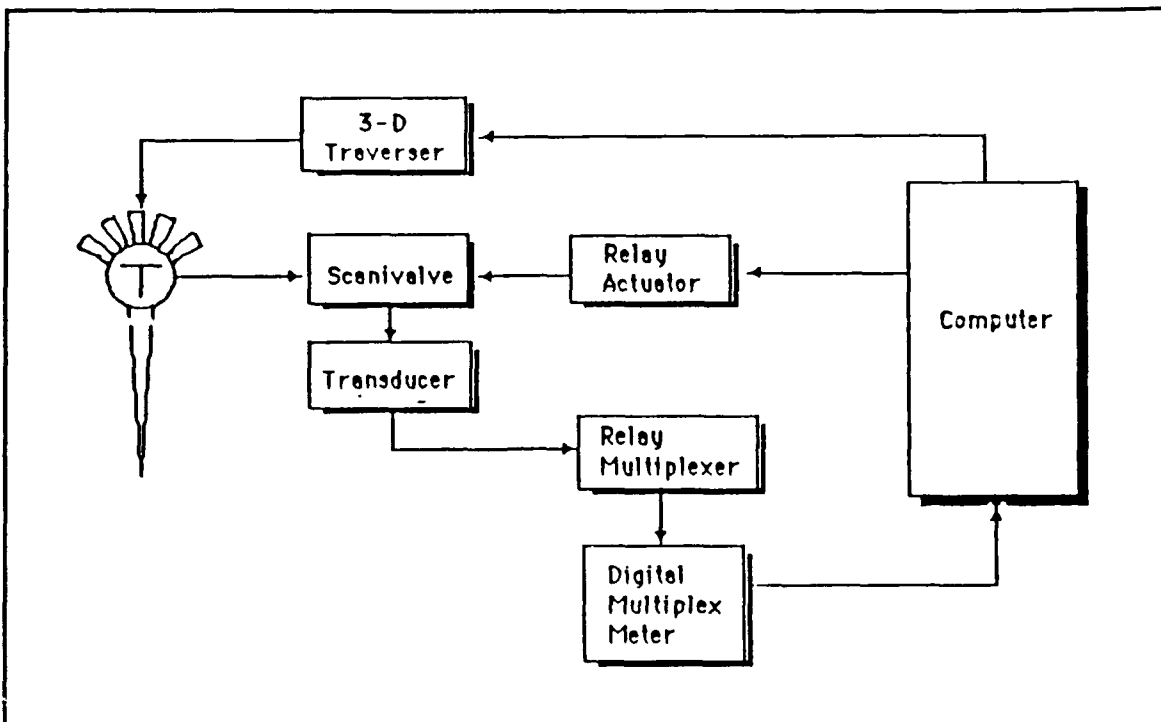


Figure 17. HP Data Acquisition System [Ref. 3]

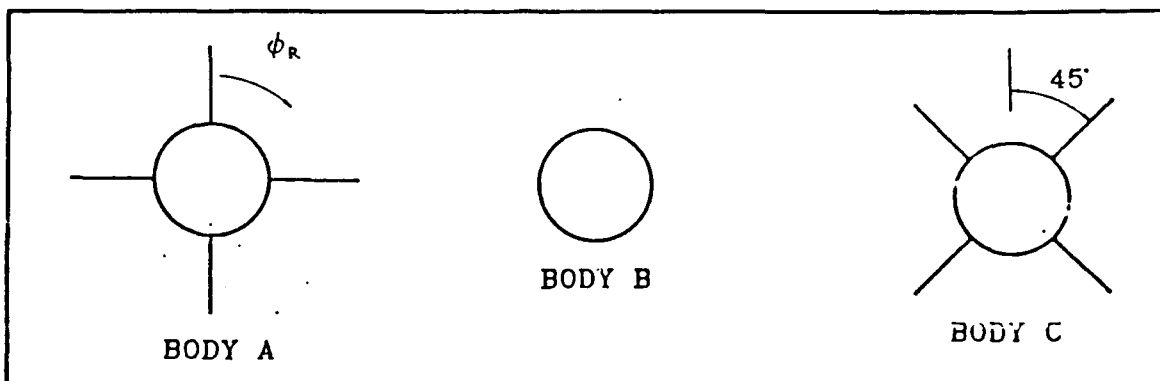


Figure 18. VLSAM Model Body Configurations [Ref. 2]

- (4) Model blockage factor corrections were calculated by Rabang for each body configuration. These factors are a function of the model angle of attack. For this experiment, the angle of attack was fixed at 50°, where the total blockage correction  $\epsilon$  equalled 0.0123. This factor was implemented in data conversion programs.
- (5) The longitudinal position for data acquisition was at a length/body diameter ratio of 6, which was 10.5 inches from the nose of the missile model.
- (6) Wind tunnel temperatures were not allowed to vary by more than 20°F from the beginning to the end of a run. Wind tunnel settling chamber temperatures tended to rise quickly due to air friction, particularly when the grid was added. When temperatures were excessive, the tests were stopped and the air in the tunnel was circulated until it cooled down sufficiently before tests were continued.

## D. SOFTWARE AND PROCEDURES

In order to correlate results with previous data, the computer programs used (or developed) by Lung to acquire and reduce data were also used for this study. Figure 19 [Ref. 3] is a schematic flowchart of the various programs and their resulting data files. The following sections provide further elaboration on these programs.

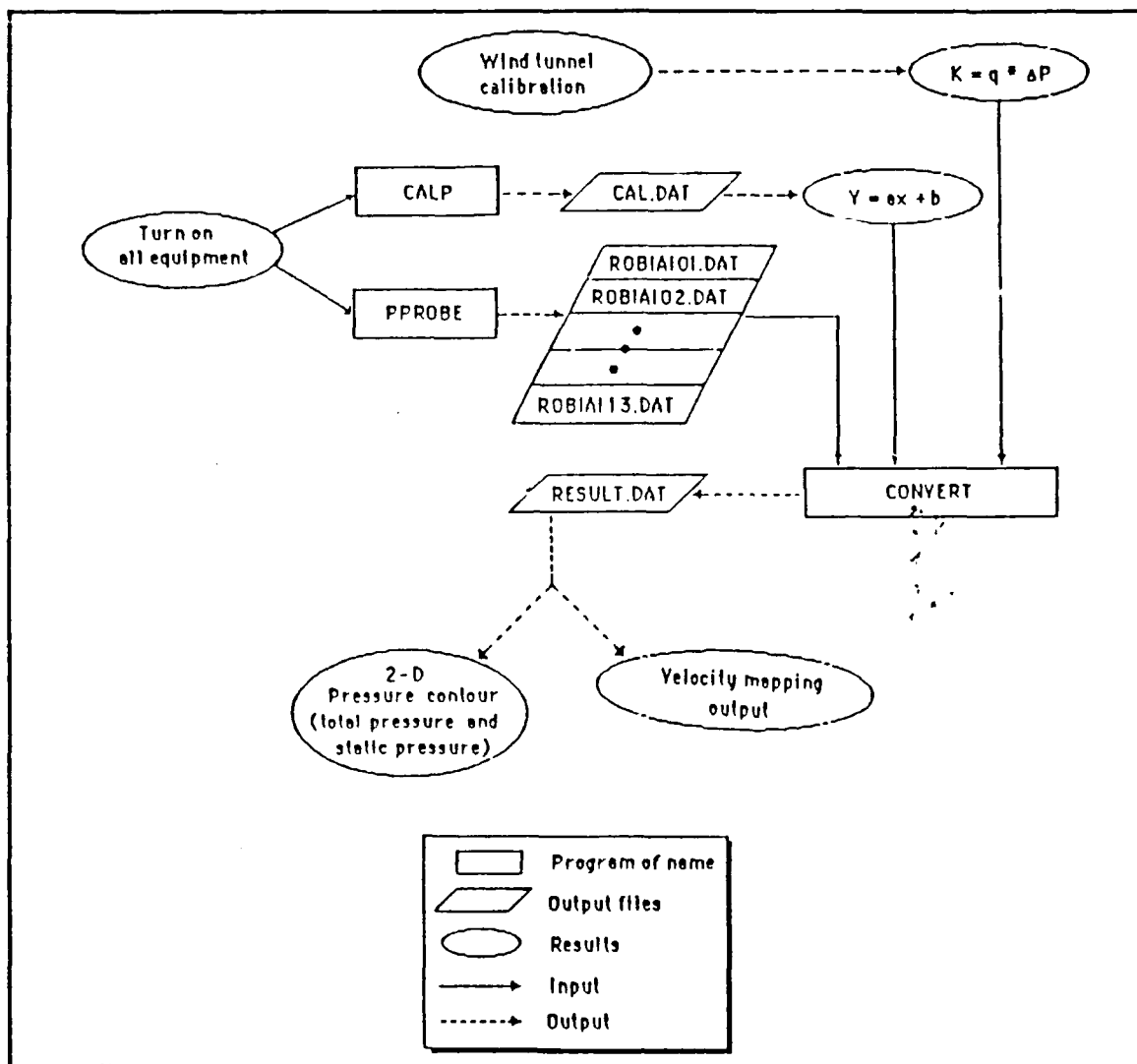


Figure 19. Program/Data File Flowchart [Ref. 3]

## **1. PPROBE Program (Data Acquisition)**

The BASIC A application program which runs the VLSAM experiment is comprised of STATEFILE, PGMSHEL and traverser programs. STATEFILE gives the computer configurations of the data acquisition instruments, while PGMSHEL informs the computer of all the functions available at each of these instruments. STATEFILE and PGMSHEL perform initialization chores and allow communication between the HP instruments and the IBM computer. [Ref. 34]

The traverser program is the actual application code which allows the operator to precisely control pressure probe movement by either manual or computer-controlled input. The traverser program was written by Kindelspire [Ref. 35] in the Advanced Basic Language. The PPROBE program is shown in Appendix A.

Manual control was used to initialize the pressure probe position prior to collecting data for the actual run, which utilized computer-controlled movements. While in the manual mode, the program asked a series of questions which enabled the operator to test motor movements and set traverser motor velocity and acceleration default values. Through manual inputs, the probe was positioned such that the  $P_1$  (total pressure) hole was centered on the lengthwise axis of the VLSAM model body and placed as close as possible to it. From this point, the probe was moved vertically downward to the position of the first point in the data collection plane. For this experiment, the origin was located 2.75 inches below the model axis, and the data field dimensions were 2.75 inches above and below and 3 inches outward from the model.

After this initial probe position was set, the computer-controlled motor movement option was selected. The field dimensions (x, y coordinates), the traverser motor step distance, and the input file name were entered into the program. The data plane was 3.0" by 5.5" with a 0.25-inch step distance for this study. From this input, PPROBE then reiterated the total number of points to be measured (299 this case) and assigned filenames for each column of data. An example of how data files were named is as follows:

example: R0A1A3

where:

R	=	run
0	=	grid number (type)
A	=	VLSAM model configuration
1	=	field dimension (3, 5.5)
A	=	step distance (0.25)
3	=	test number

Thus, from the example above, the program assigned filenames R0A1A301.DAT through R0A1A313.DAT, which represented the 13 columns of data (23 points per column).

The 5-hole pressure probe scale wheel was then adjusted until the  $P_2$  and  $P_3$  (lateral) pressures were nearly equal (nulling), as measured by a portable digital manometer/calibrator. The measured yaw angle was read off the wheel and typed into the computer. Once this was accomplished, PPROBE moved the scanivalve from port 1 to port 4 via the Relay Actuator. There was a one-second delay to allow pressure equalization before the Digital Multimeter sampled the output voltage from the scanivalve transducer via the Relay Multiplexer. After ten samples were taken at port 4, the Relay Actuator stepped the scanivalve to the next port (5), where another ten

samples were taken. This process was repeated until all five channel pressures (ports 4 through 8) were measured. [Ref. 3] Note that scanivalve port 4 represents probe pressure  $P_1$ , port 5 is  $P_2$ , port 6 is  $P_3$ , port 7 is  $P_4$ , and port 8 is  $P_5$ .

The Relay Actuator homed the scanivalve to port 48 after all the pressures were measured, and then PPROBE displayed the measurements and average values for each channel on the computer screen. The program either moved the probe upward one step (0.25") or remeasured the same point, depending on whether the data was within tolerance or not, as determined by the operator. For this study, the following tolerances were used:  $P_2$  and  $P_3$  differed by 0.09 psf or less, and  $P_1$  was a positive number (or a very small negative number on the order of -0.5 psf). Once a column of data was measured, PPROBE would store the average values for each point in a file (23 pts) and move the traverser to the next column position. The data acquisition process was continued until all 299 points were completed.

## 2. CALP Program (Scanivalve Transducer Calibration)

The CALP program (Appendix B) was the other data acquisition program utilized in this study. It was run both before and after the actual test (PPROBE) to account for any change in experimental conditions which might have occurred over the 8-10 hour period it took to run PPROBE.

The transducer voltage was first adjusted to approximately zero millivolts. Calibration manometer (Figure 20) readings were then entered into the computer. The manometer provided a known pressure source for scanivalve calibration. From the transducer output voltage and pressure data

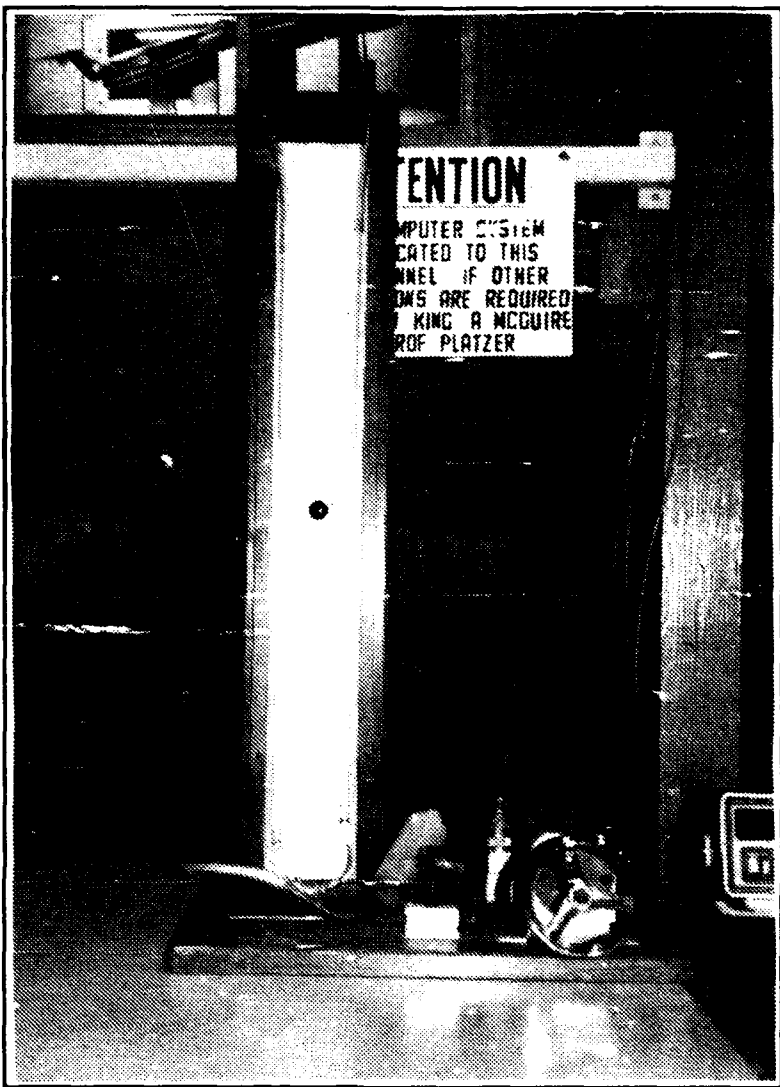


Figure 20. Calibration Manometer [Ref. 3]

provided by CALP, two calibration curve equations were calculated (before/after PPROBE runs). An averaged slope equation was then used in data reduction computations to minimize errors. This slope equation was used by the CONVERT program to change voltage data into dynamic pressure data.

### 3. CONVERT Program

This program (Appendix C) was used to reduce data. It read the PPROBE data files (ex: R0A1A303.DAT) containing average pressures ( $P_1$ – $P_5$ ) and converted them into x–y coordinates, velocity, yaw angle, pitch angle (alpha), total local pressure, total pressure coefficient, local static pressure, and static pressure coefficient. The x, y coordinates and yaw angle were simply read from the PPROBE data files and input into CONVERT. The pitch angle coefficient was determined by a ratio of the pressures measured by the 5-hole probe. This coefficient was then used in an equation developed by Lung [Ref. 3] using commercial curve-fitting software in order to find the corresponding pitch angle. Calibration curves provided by the probe manufacturer were used for the curve-fit. The program also obtained velocity pressure coefficients for particular pitch angles, from which the local velocity was calculated after addition of a wind tunnel calibration factor, K, and other unit conversion factors. Additionally, the total and static pressure coefficients were obtained for different pitch angle regions.

Room ambient pressure was used as the reference pressure for these coefficients, which are functions of total and static pressures and are non-dimensionalized by the tunnel dynamic pressure:

$$C_{PS} = (P_{sL} - P_s)/Q \quad (6)$$

$$C_{PT} = (P_{tL} - P_t)/Q \quad (7)$$

where

$C_{PS}$	=	Static pressure coefficient
$C_{PT}$	=	Total pressure coefficient
$Q$	=	Freestream dynamic pressure
$P_s$	=	Freestream static pressure
$P_t$	=	Freestream total pressure
$P_{sL}$	=	Local static pressure
$P_{tL}$	=	Local total pressure

The actual dynamic pressure is (nearly) the same for the two cases.

For this experiment, the reference dynamic pressure values were 7.2 cm H<sub>2</sub>O for grid 0 and 10.0 cm H<sub>2</sub>O for grid 3. Temperature input for the CONVERT program was an average of the initial and final wind tunnel temperatures for the entire run time. Similarly, barometric pressure values were recorded before and after each run. CONVERT also added yaw and pitch angle (alpha) corrections to the data. These factors are +5.0° for yaw and -17.942° for pitch. They were determined from a preliminary run conducted with no grid and no missile model in the wind tunnel. Further explanation of this run is discussed in the Preliminary Tests section. The output of the CONVERT program was stored in a file named RESULT.DAT, which, in turn, was used as input to the TECPLOT system.

#### 4. TECPLOT

The commercial TECPLOT software system was used to generate crossplane velocity vector plots and pressure contour plots. These plots could be tailored in many different ways by choosing scale factors, arrowhead wedge angles, contour levels and spacing, and many other parameters. A Hewlett-Packard 7470A x-y pen plotter was utilized in conjunction with TECPLOT to provide both the vector and contour plots.

### E. PRELIMINARY TESTS

#### 1. Dynamic Pressure Calibration

All of the turbulence grids were previously calibrated in the wind tunnel. Readings from the tunnel calibration manometer and from a pitot-static tube inserted in the center of the test section were recorded over a speed range and wind tunnel calibration factors were obtained. These factors were used to adjust the tunnel flow velocity to the expected experimental

condition for the different grids. [Ref. 3] The calibration factors K are 0.8891, 1.5084, 1.6487, 1.6545 and 1.1167 for no grid, and grids 1 through 4 respectively. These values were used in the CONVERT program to calculate the pressure and velocity in the test section.

## 2. Yaw and Pitch Angle Corrections

A test was conducted to find correction factors for yaw and pitch angle. From previous arrow plot data by Lung [Ref. 3], inconsistent crossflow velocity magnitudes and directions were noted toward the outer boundaries of the body-only missile configuration run. These outer boundaries represented the wind tunnel freestream region, where crossflow velocity is expected to reach zero. Therefore, to duplicate just the freestream region, this preliminary test consisted of placing the pressure probe in the tunnel with no VLSAM model and no grid. Thus, the expected pitch and yaw angles should both have been zero. This was not the case however.

Results of the preliminary run (R001A2) are listed in Appendix D (Result 00.DAT File). The yaw angles measured ranged from  $-4.00^\circ$  to  $-7.00^\circ$ , with an average of  $-5.00^\circ$ . The pitch angles ( $\alpha$ ) ranged from approximately  $+17.4^\circ$  to approximately  $+18.4^\circ$ , with the average  $+17.942^\circ$ . Thus, to correct for these errors,  $+5.00^\circ$  was added to the yaw angle and  $-17.942^\circ$  was subtracted from the alpha values in the output file of the CONVERT program (RESULT.DAT).

Though the exact cause for the yaw and pitch angle errors was not known, one possibility might have been a slight bend which was noted in the 5-hole pressure probe. Other causes may have been improper calibration of the probe or a misalignment of the traverser assembly. The corrected errors only effect the velocity vector plots, and should have no effect on the pressure contour plots.

### **III. RESULTS**

The following sections discuss the velocity vector plots and the total and static pressure coefficient contour plots for the VLSAM model configurations A (plus) and C (cross), both with and without turbulence. All plots depict the 3" by 5.5" data acquisition field and the position of the missile model (nose aspect) relative to the field. Vortex sizes and vortex distances from the model surface are referenced to the model base diameter  $d$  (1.75").

#### **A. CONFIGURATION 0A ('PLUS' WITHOUT TURBULENCE)**

For the plus configuration, the swirling patterns of the velocity vector plot (Figure 21) clearly denote the two asymmetric vortices, which form circles that rotate in opposite directions. Although the bottom vortex center is evident, this plot fails to show the center of the top vortex. The vortex strength is a maximum on the outer edges of the vortex cores, denoted by the large vector arrows, where the velocities flow back toward the missile body. Towards the outer boundaries of the data acquisition field, where the vortex strengths are minimal, the vectors plot as points.

The total pressure coefficient ( $C_{PT}$ ) contour plot (Figure 22) shows that the extent of the top vortex is approximately  $0.72d$  at a distance of  $0.33d$  from the missile surface. The bottom vortex is  $0.83d$  at  $0.67d$  from the body. There are more changes in the pressure gradient within a smaller area for the top

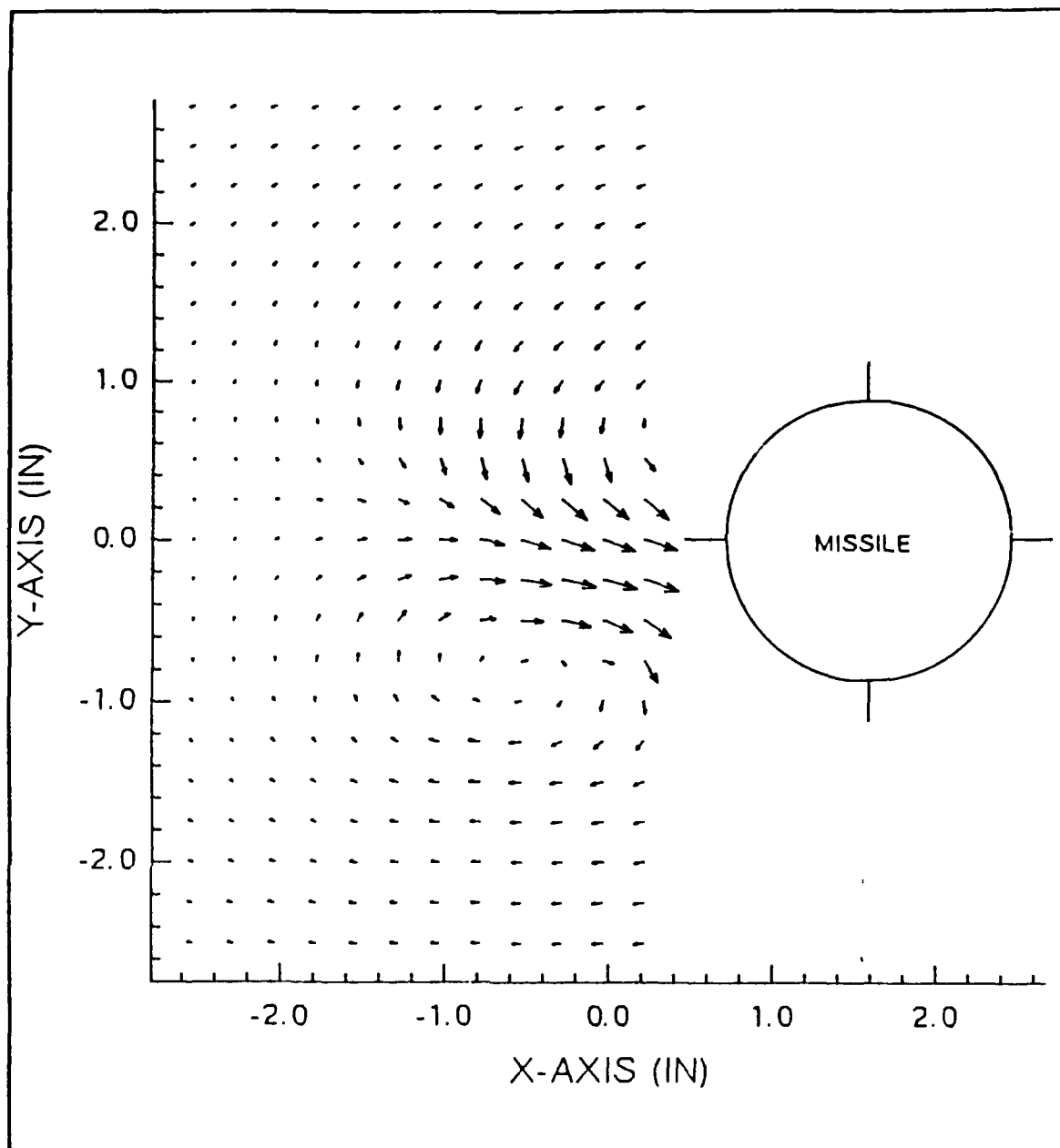


Figure 21. Velocity Vector Plot – Configuration 0A

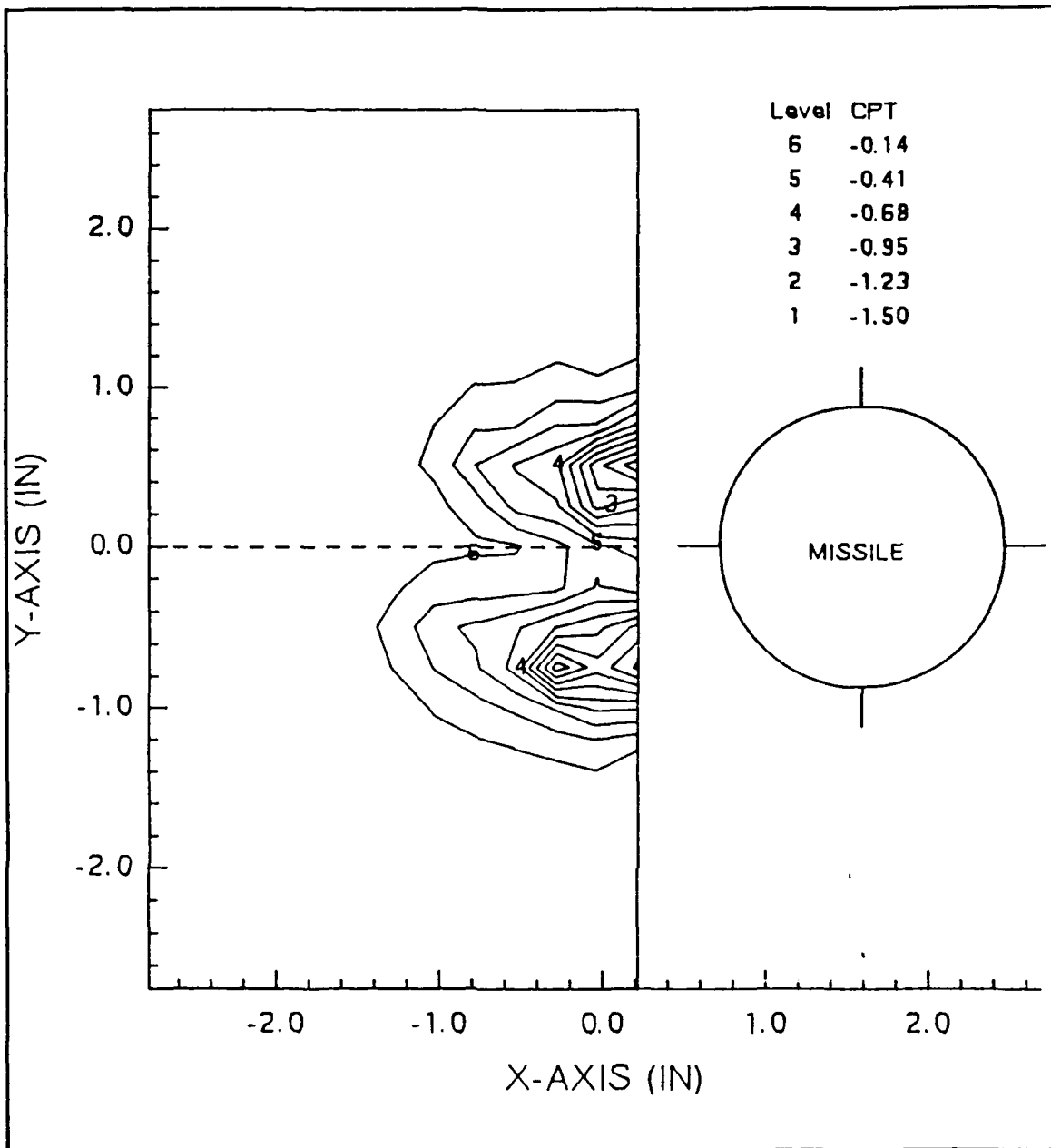


Figure 22. Total Pressure Coefficient – Configuration 0A

vortex, which varies in C<sub>PT</sub> from -0.14 to -1.35 within an inch, indicating greater vortex strength. The bottom vortex is slightly more diffused. The C<sub>PT</sub> plot shows that the distance between the two vortex centers is approximately 0.77d.

The static pressure coefficient (C<sub>ps</sub>) contour plot (Figure 23) shows that the top vortex extends approximately 1.0d at a distance of 0.49d from the body. The bottom vortex extends about the same (1.1d) at a distance of 0.55d. Again, the top vortex appears to be stronger than the bottom vortex. C<sub>ps</sub> for the top vortex varies from -0.55 to -2.70 within 1.2 inches while the bottom vortex varies from -0.55 to about -2.18 in 1.6 inches. The distance between the vortices is approximately 0.70d on the C<sub>ps</sub> plot.

#### B. CONFIGURATION 3A ("PLUS" WITH TURBULENCE)

With added turbulence (grid 3), the velocity vector plot (Figure 24) still indicates vortex asymmetry, but it also indicates that the vortices have less strength (smaller vector arrows) than for the no grid condition. Again the vortex strength is maximized on the outer edges of the vortex cores.

From the C<sub>PT</sub> contour plot (Figure 25), the top vortex extends to approximately 0.72d, centered at about 0.44d from the model. The bottom vortex is slightly larger (0.83d) and is located 0.55d from the model body. The pressure gradient of the top vortex is steeper than for the bottom vortex, indicating greater strength. C<sub>PT</sub> varies from -0.14 to -1.5 within an inch for the top vortex and from -0.14 to -1.35 within 1.4 inches for the bottom vortex. The distance between the two vortices as measured on the C<sub>PT</sub> plot is approximately 0.72d.

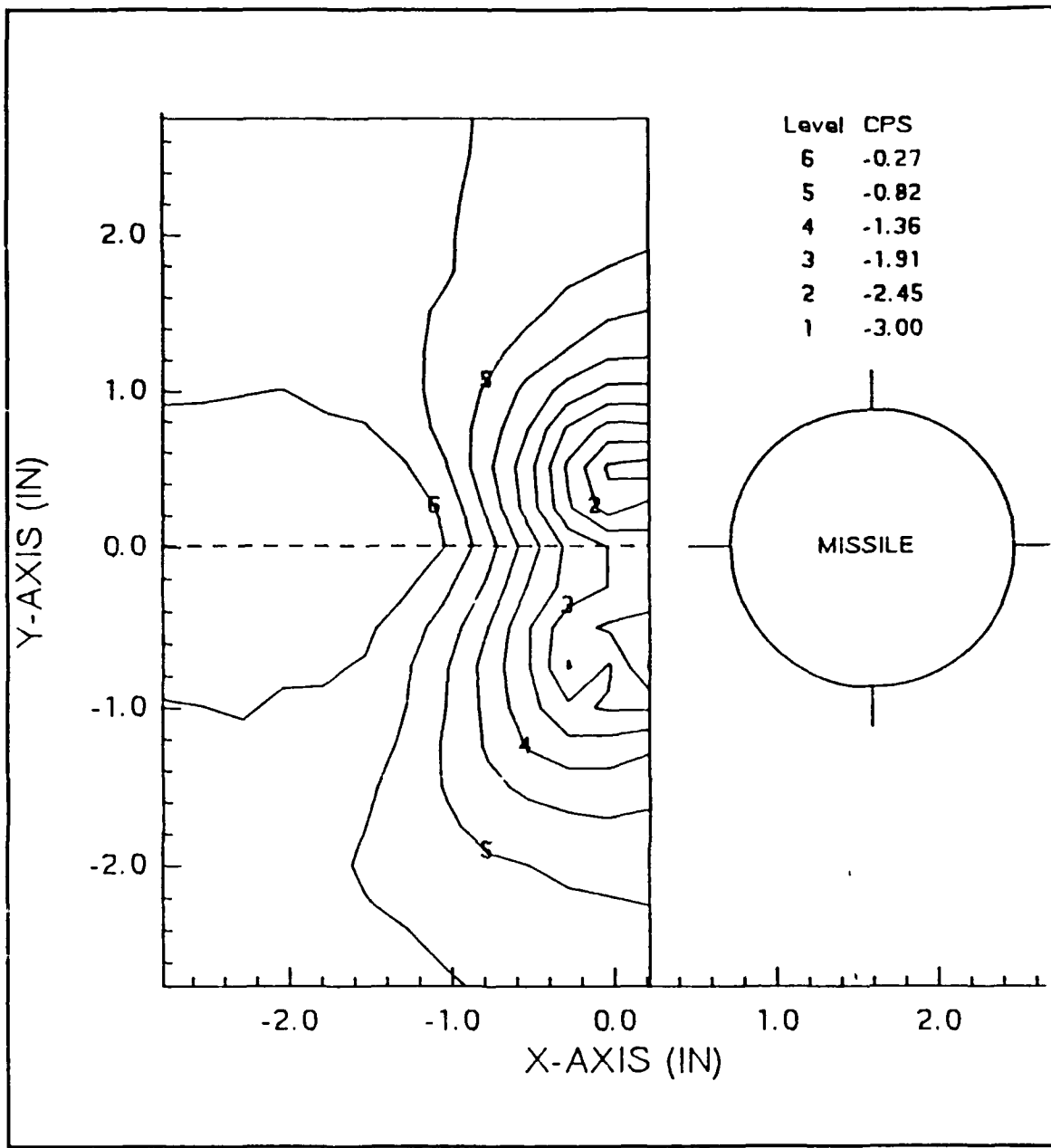


Figure 23. Static Pressure Coefficient – Configuration 0A

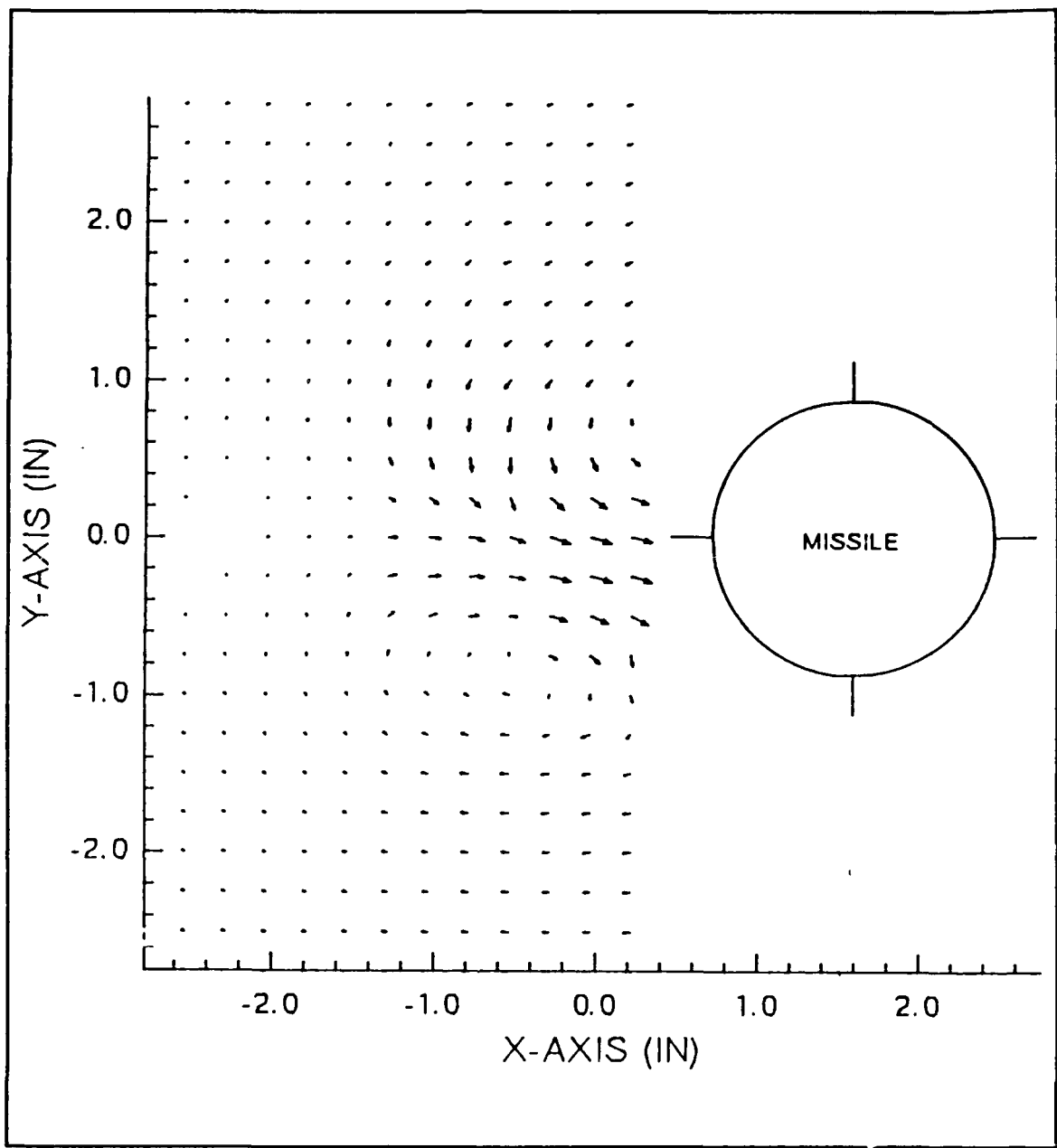


Figure 24. Velocity Vector Plot – Configuration 3A

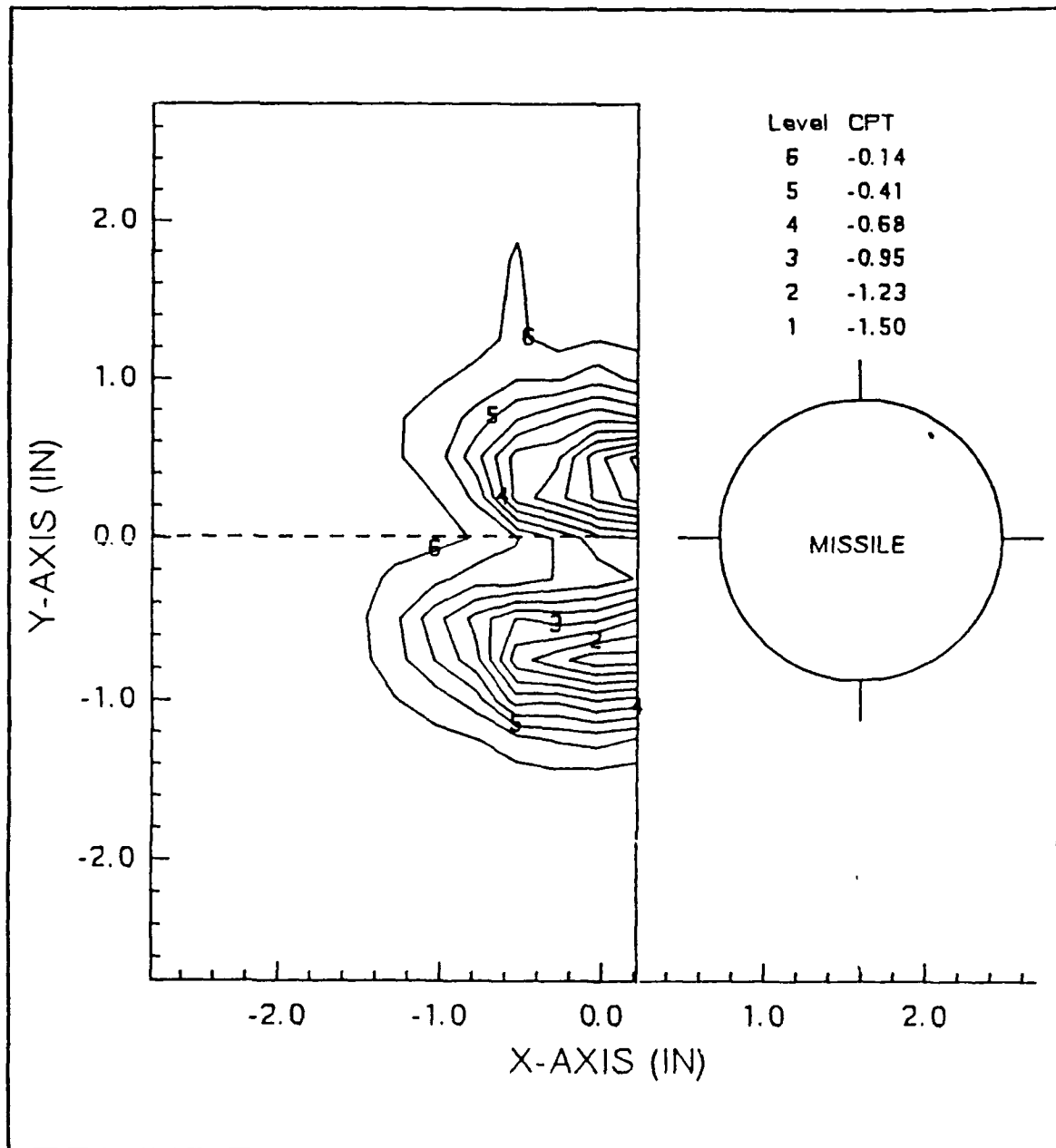


Figure 25. Total Pressure Coefficient – Configuration 3A

Examination of the  $C_{PS}$  contour plot (Figure 26) reveals that both vortices are roughly  $0.83d$  wide. The top vortex is closer to the missile body ( $0.39d$ ) than the bottom vortex ( $0.55d$ ). More contour levels in a smaller area and, consequently, a higher gradient and stronger vortex exists for the top vortex.  $C_{PS}$  for the top vortex varies from -0.27 to -1.60 within 0.8 inch while the bottom vortex  $C_{PS}$  ranges from -0.27 to -1.36 within 1.0 inch. On the  $C_{PS}$  plot, the two vortices are about  $0.66d$  apart.

### C. CONFIGURATION 0C ("CROSS" WITHOUT TURBULENCE)

For the model C configuration (cross), the velocity vector plot (Figure 27) still clearly displays the two asymmetric vortices. As with configuration A, the strengths of the vortices are maximized at the edges of the circular swirls, where the flow is back toward the missile body.

Figure 28, the total pressure coefficient plot, displays a  $0.77d$  wide top vortex located at about  $0.5d$  from the model surface. The bottom vortex extends to approximately  $0.88d$  and is  $0.66d$  from the model. The bottom vortex is more tightly wrapped (i.e., more contour levels per area) closer to its core than is the top vortex. The  $C_{PT}$  range for the bottom vortex (-0.14 to -1.23) is slightly greater than the range for the top vortex (-0.14 to -1.09). The vortex centers are roughly  $0.66d$  apart.

From the static pressure coefficient contour (Figure 29), both vortices extend to  $0.95d$  with the top vortex slightly closer to the model body ( $0.56d$ ) than the bottom vortex ( $0.66d$ ). The relative strengths of the vortices is difficult to interpret from the  $C_{PS}$  plot, but the top vortex appears to be a little less diffused than the bottom vortex and therefore stronger. As with the total pressure coefficient plot, the vortices are  $0.66d$  apart.

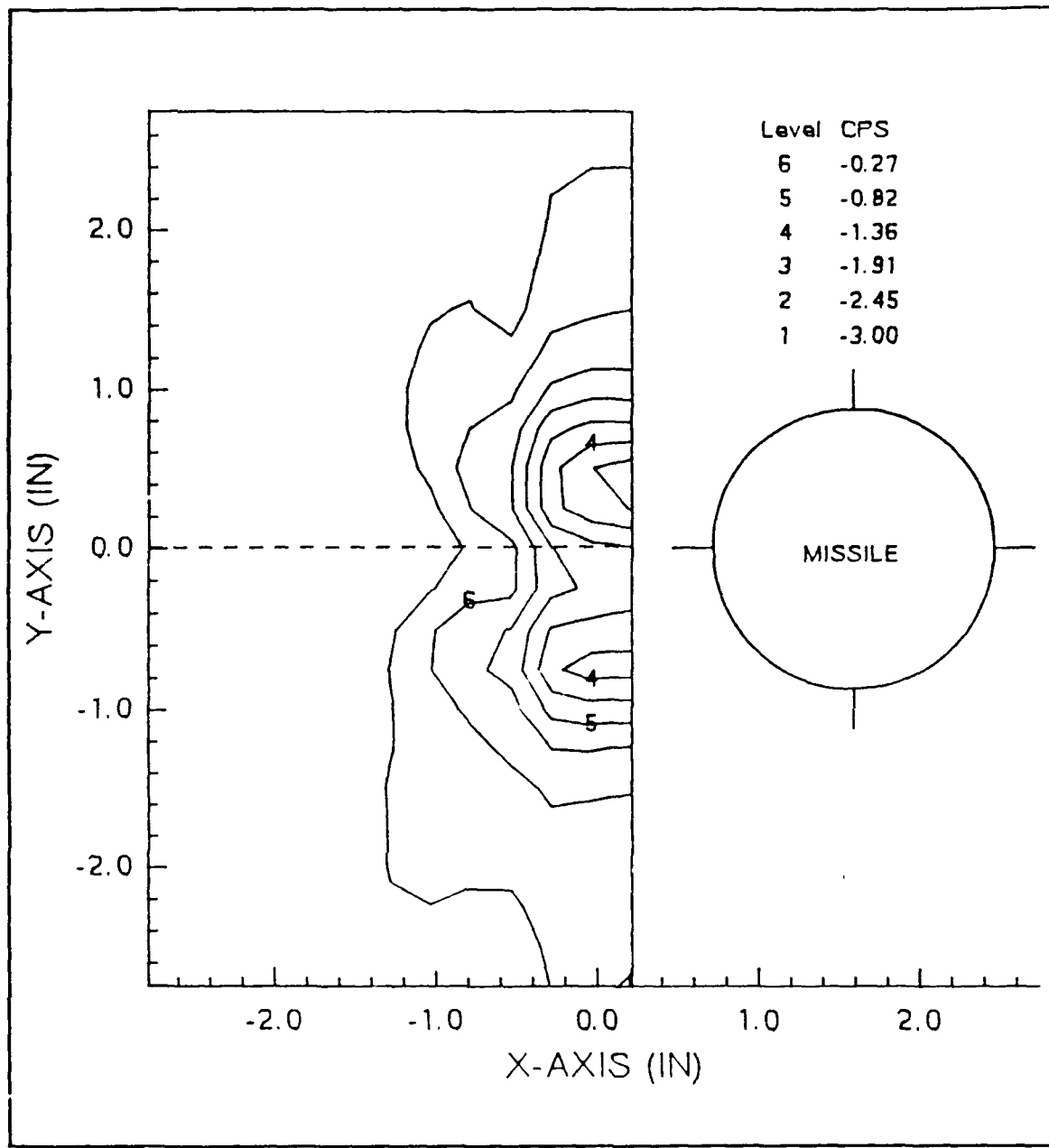


Figure 26. Static Pressure Coefficient – Configuration 3A

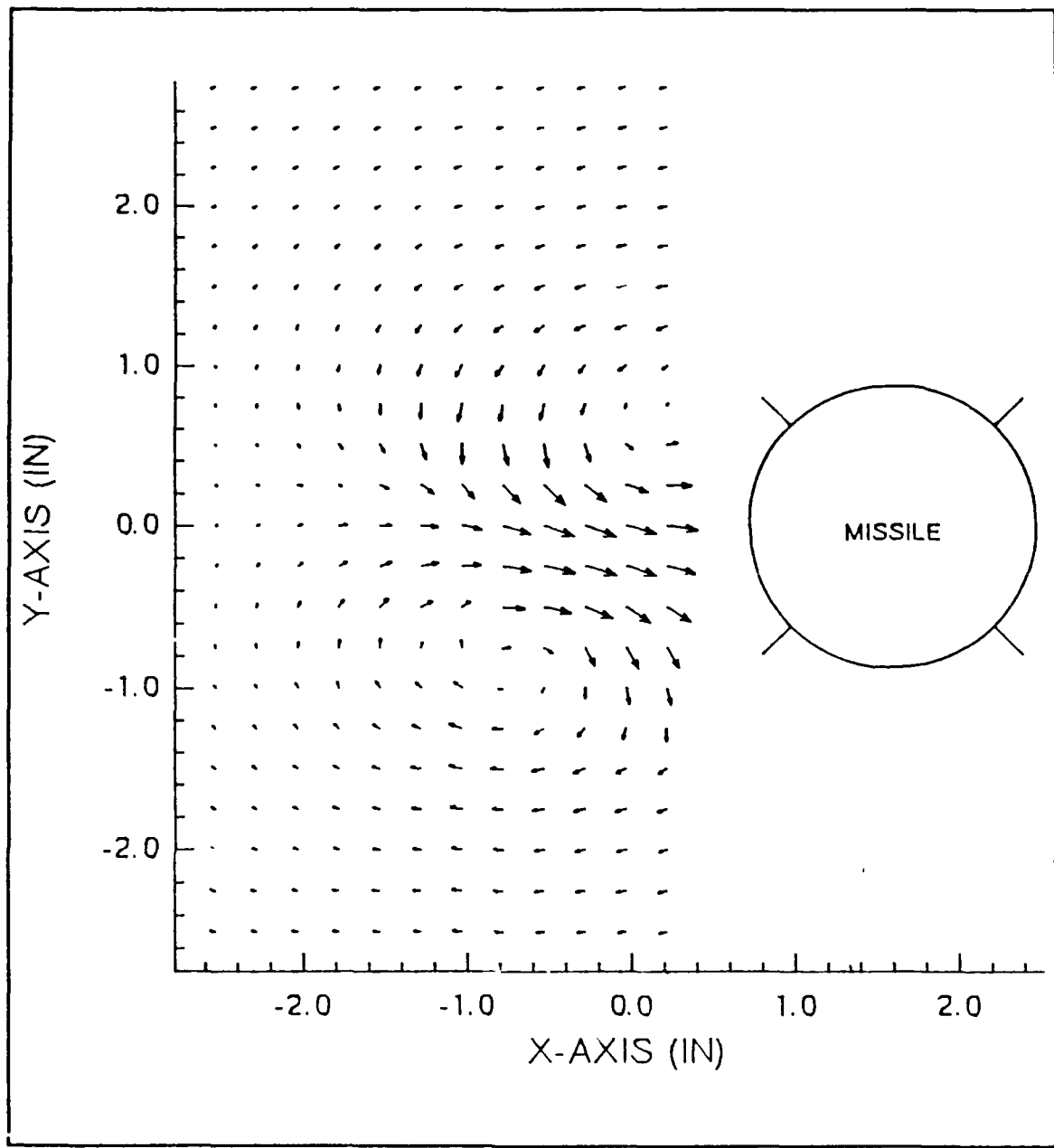


Figure 27. Velocity Vector Plot – Configuration 0C

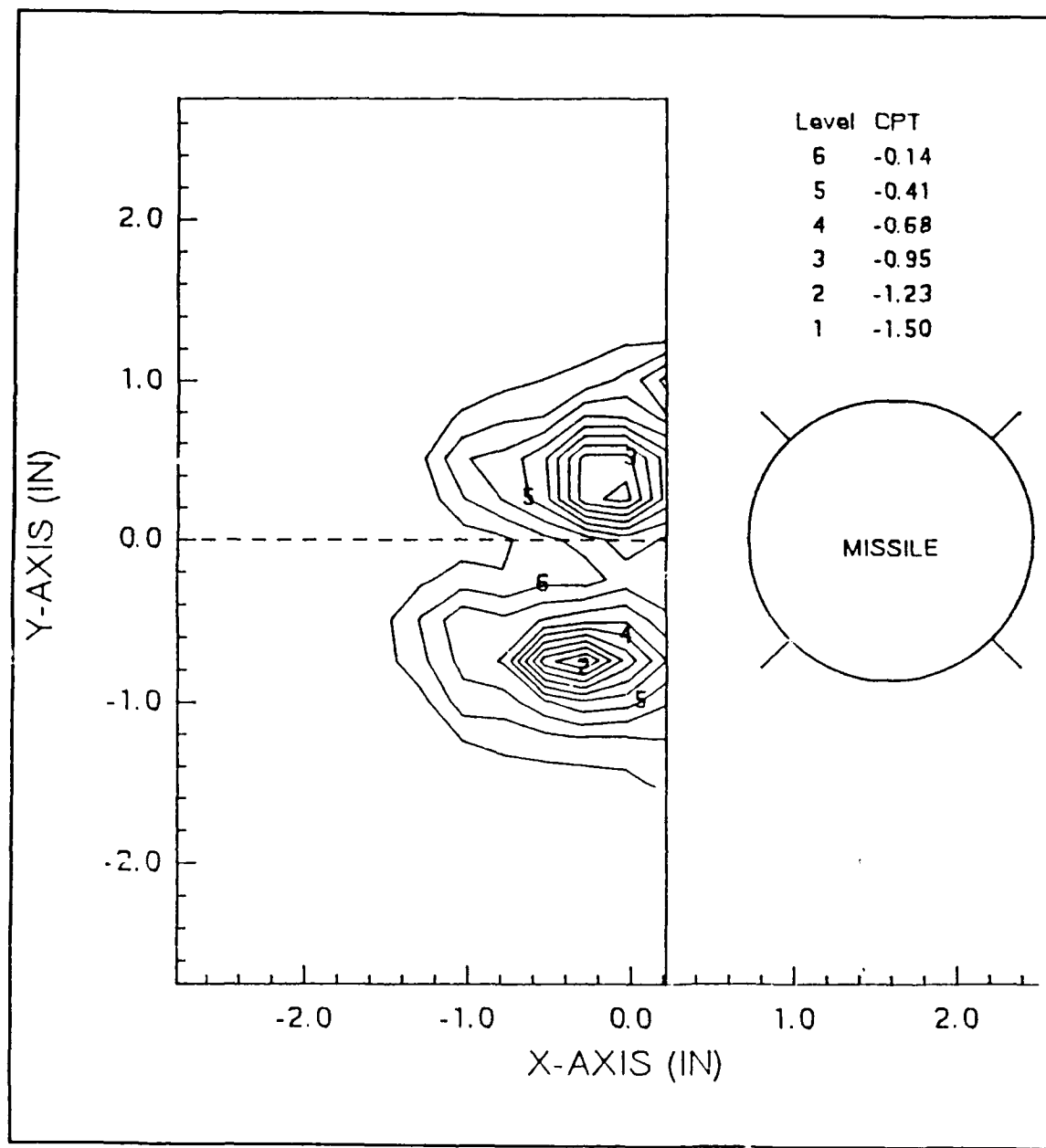


Figure 28. Total Pressure Coefficient – Configuration 0C

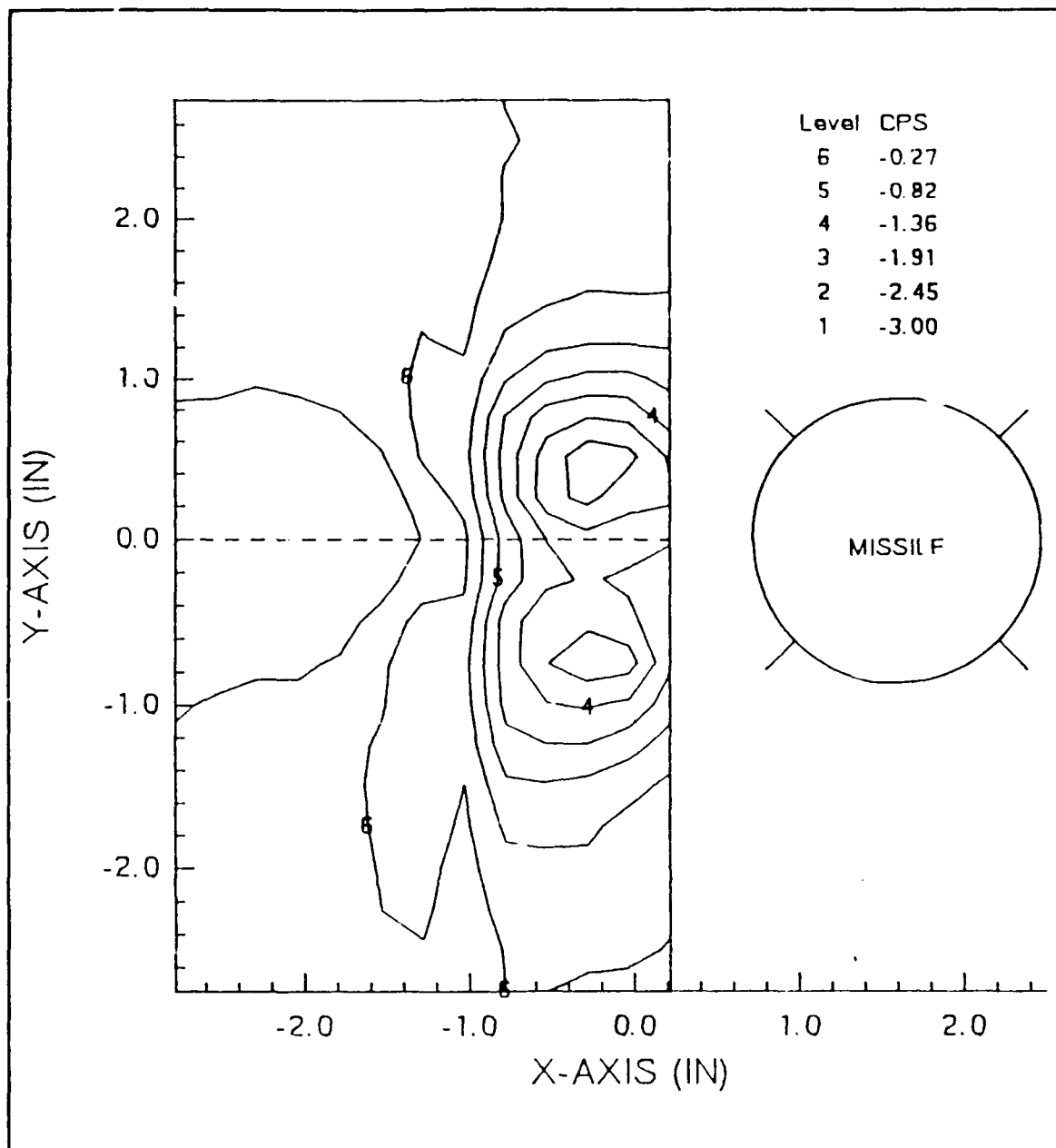


Figure 29. Static Pressure Coefficient – Configuration 0C

#### **D. CONFIGURATION 3C ("CROSS" WITH TURBULENCE)**

The velocity vector plot (Figure 30) shows that the addition of turbulence (grid 3) diffuses the asymmetric vortices for model configuration C. The vector arrows plot smaller for this turbulent case than for the no grid case.

The  $C_{PT}$  contour plot (Figure 31) reveals a  $0.92d$  bottom vortex at a distance of  $0.66d$  from the model body and a  $0.83d$  wide top vortex at  $0.55d$  from the model. The bottom vortex appears to be slightly more tightly wrapped towards the vortex center than the top vortex.  $C_{PT}$  levels for both vortices range from about 0.0 to -1.23. The distance between the vortices is approximately  $0.72d$ .

Figure 32, the static pressure coefficient plot, like the  $C_{PT}$  plot, also shows the distance between the vortices to be  $0.72d$ . The top vortex (extent  $0.77d$ ) is roughly  $0.55d$  from the model's surface while the bottom vortex (extent  $0.88d$ ) is  $0.66d$ . The vortices appear to have the same strength on the  $C_{PS}$  plot, in which the coefficients range from 0.0 to approximately -1.1.

#### **E. COMPARISONS**

##### **1. Between Body Configurations (A and C)**

The following observations were noted when making comparisons between the two missile configurations for both the turbulent (grid 3) and non-turbulent (no grid) runs.

- (1) From the total pressure coefficient ( $C_{PT}$ ) contour plots, the vortices are slightly larger for configuration C. This is more pronounced for the run conducted with added turbulence (grid 3).

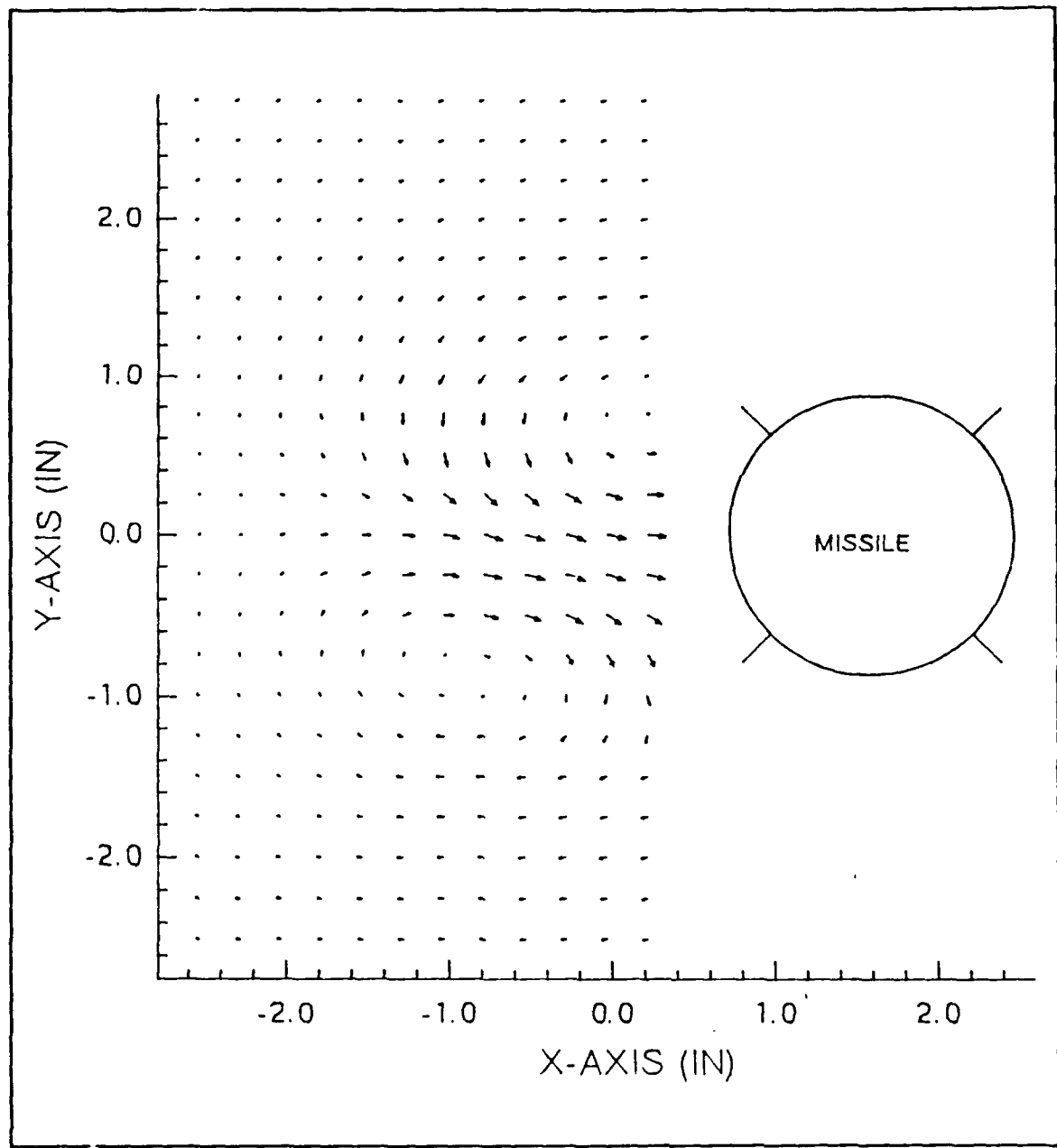


Figure 30. Velocity Vector Plot – Configuration 3C

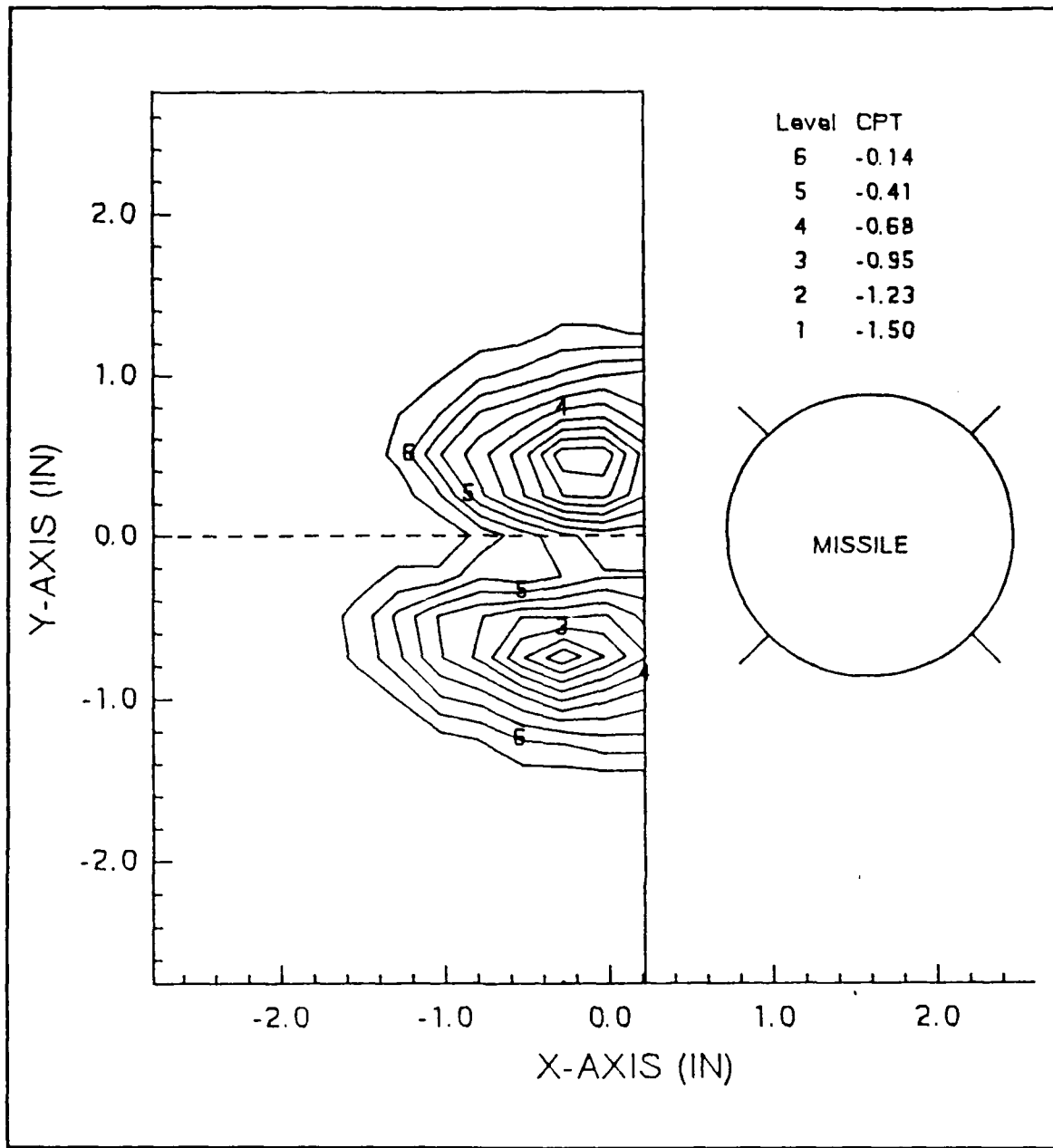


Figure 31. Total Pressure Coefficient – Configuration 3C

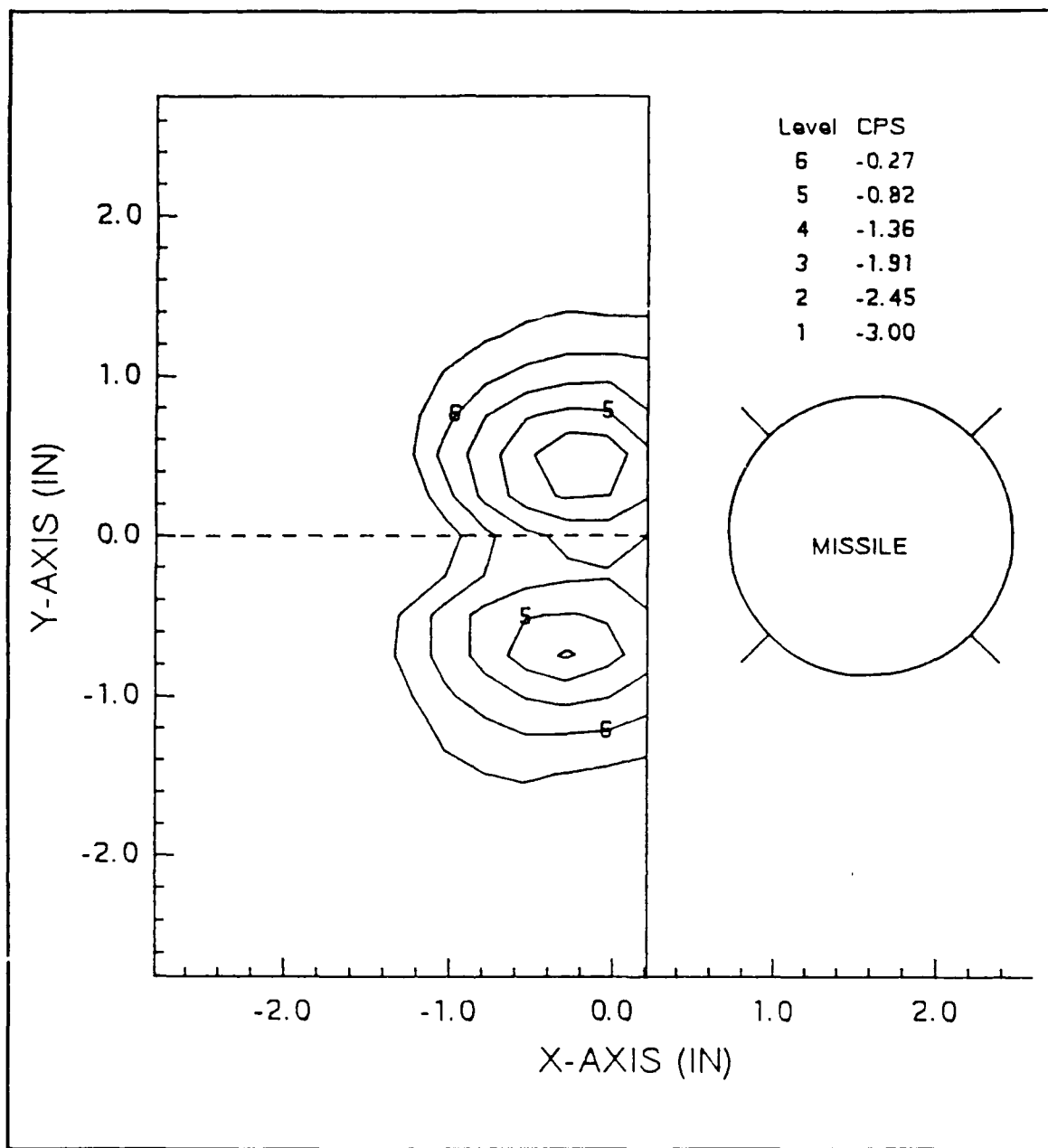


Figure 32. Static Pressure Coefficient – Configuration 3C

- (2) The vortices of the C configuration appear to be centered a little further away from the model surface than do the A configuration vortices. This shift is on the order of 0.2 inches, and is apparent in both the no-grid and grid 3 runs.
- (3) The relative distance between vortex centers does not seem to be affected when the configurations are changed.
- (4) The bottom vortex is more tightly wrapped (stronger) for configuration C based on the CPT plots. This is more noticeable for the run conducted without turbulence.

## 2. Between Turbulence Levels (0 and 3)

The following observations were noted when making comparisons between the two turbulence levels tested for each body configuration. Turbulence level 0 was the no-grid condition and level 3 was the run conducted with a grid inserted.

- (1) The velocity vector plots indicate smaller arrows, therefore weaker vortices (less crossflow), when turbulence is added. This trend holds for both body configurations.
- (2) The two vortices remain in approximately the same positions as indicated on both the vector plots and the static pressure coefficient (C<sub>PS</sub>) plots).
- (3) From the total press coefficient (C<sub>PT</sub>) plots, the center of the bottom vortex for configuration A shifts slightly closer to the model body when the turbulence increases. (-0.2 to 0.0 on the x-axis).
- (4) Also on the C<sub>PT</sub> plots, with added turbulence, the top vortex core for configuration C seems to shift away from the VLSAM body.
- (5) The C<sub>PT</sub> plots for both configurations are slightly more diffused with added turbulence. Specifically, the vortex centers are less tightly wrapped, thus indicating weaker vortices for the more turbulent condition.
- (6) There are no noticeable differences in the static pressure coefficient contours between the turbulent and non-turbulent runs.

### **3. With Body-Only Configuration (B)**

The following observations were made in order to correlate the results of this study with the previous experiment conducted by Lung for a body-only VLSAM model configuration. [Ref. 3] The purpose is to note how the addition of wings and strakes might affect the vortex flow pattern around the missile. The velocity vector, total pressure and static pressure coefficient plots for the body-only run (0B) are displayed in Figures 33, 34, and 35 respectively. These comparisons were made for the nominal ambient (no-grid) flowfield condition.

- (1) From the velocity vector plots, the vortex pattern for configuration B is similar to the one for body C in that the vortex asymmetry is more pronounced for these cases. Body A vortices are closer to the model surface and asymmetry is less pronounced.
- (2) From the total pressure coefficient contours, the vortices appear to be located much closer to the missile body for body A than for either body C or B. Apparently the strake/wing-generated vortices for this configuration act to hold the nose-generated vortices near the body, resulting in the higher induced side forces for this configuration observed by Rabang.
- (3) Also from the CPT plots, the strengths of the bottom vortices appear to be roughly the same for bodies A and B, while the plot for body C seems to be more tightly wrapped (stronger) near its center.
- (4) From the static pressure contours, the body-only vortices are more diffused and larger than either configuration with wings (A and C).
- (5) The relative distances between the top and bottom vortices remains the same on all three plots for all body configurations.

In general, the vortex pattern around the nose of the missile model with wings (in either configuration) resembles the vortex pattern for a body-only configuration. Though there are subtle differences as previously noted, the

relative strengths, sizes and positions of the asymmetric vortices were comparable in all cases.

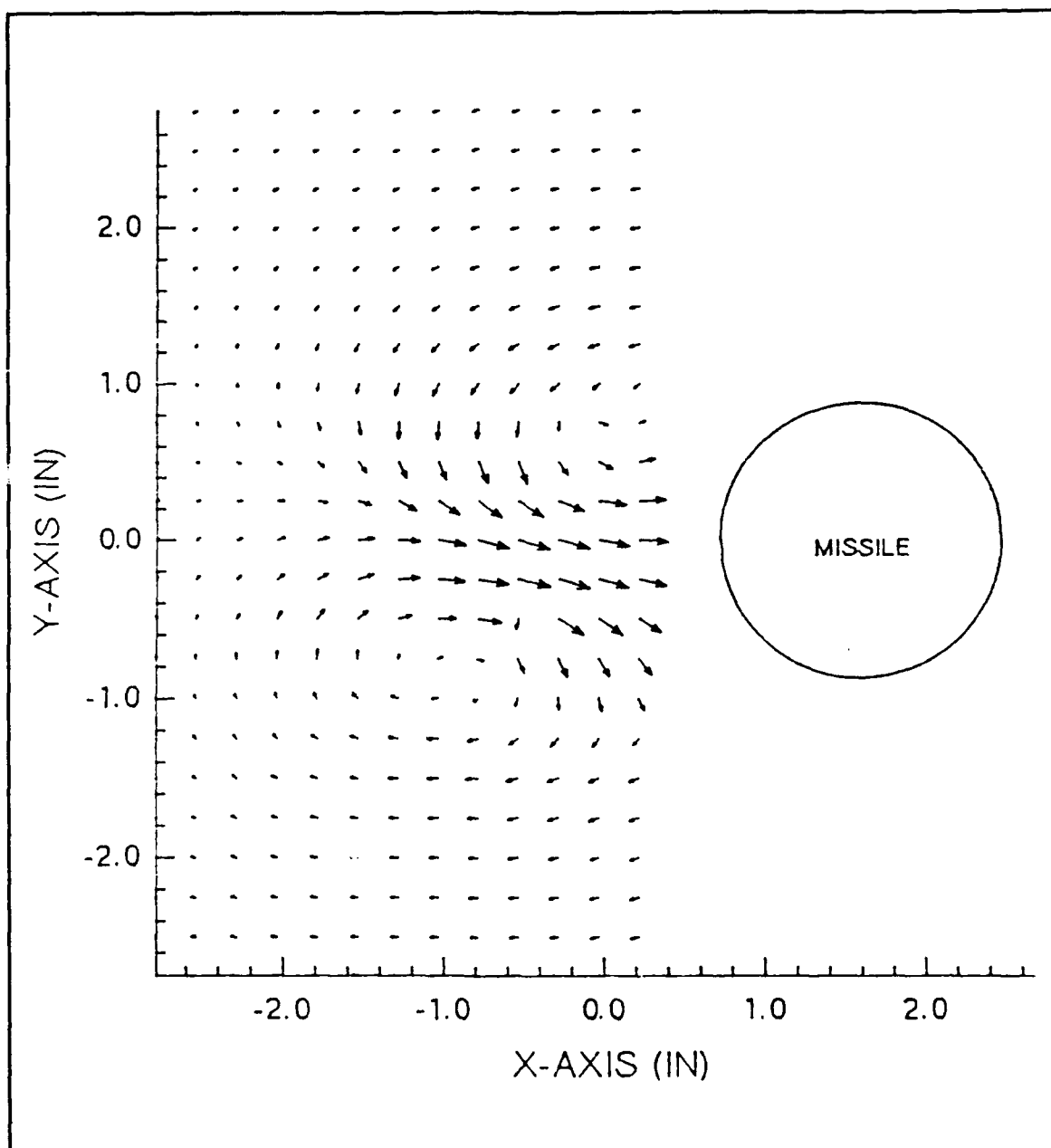


Figure 33. Velocity Vector Plot – Configuration 0B

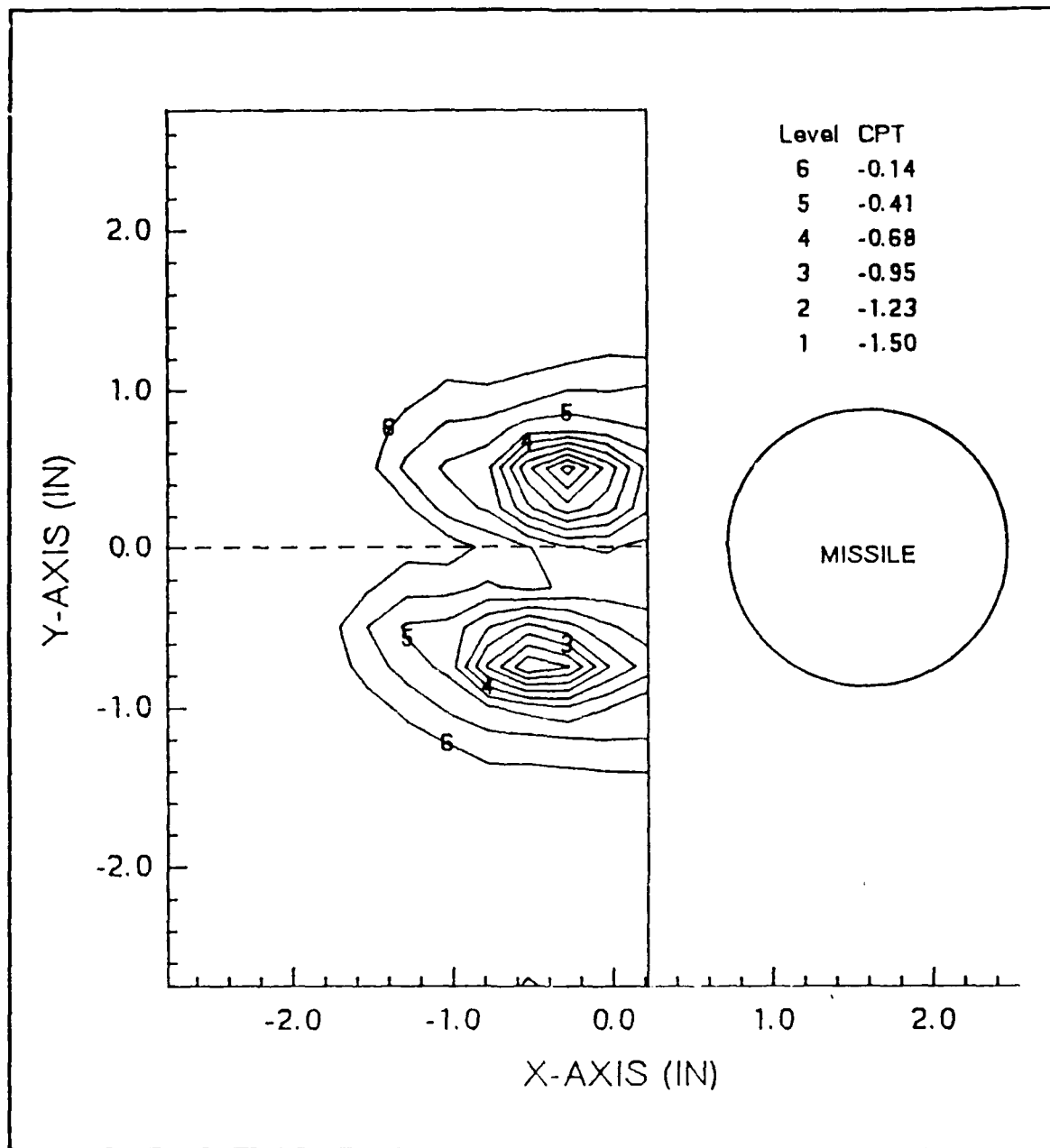


Figure 34. Total Pressure Coefficient – Configuration 0B

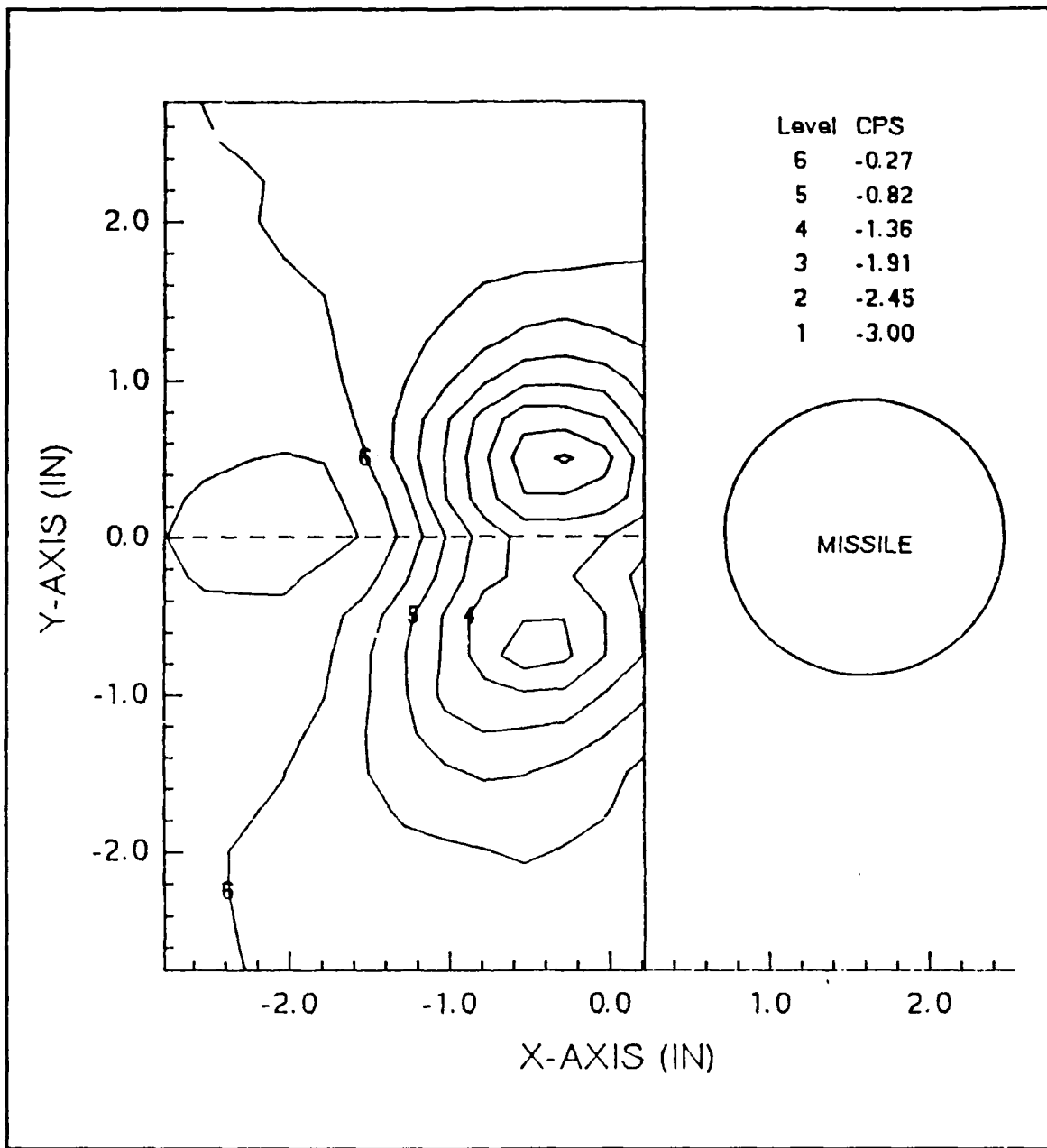


Figure 35. Static Pressure Coefficient – Configuration 0B

#### **IV. CONCLUSIONS AND RECOMMENDATIONS**

The flowfield about a Vertically-Launched Surface-to-Air Missile (VLSAM) model at high angle of attack was investigated in the wind tunnel of the Naval Postgraduate School. Missile "plus" and "cross" body configurations (A and C respectively) were both tested. The angle of attack was set at 50° with a Reynolds number of  $1.1 \times 10^5$  for all data runs. Two flowfield conditions were treated: the nominal ambient wind tunnel condition (no grid) and a condition with a grid-generated turbulence of length scale 1.08 inches and 1.88% turbulence intensity (see Table 2). The following conclusions were reached:

- (1) An increase in turbulence intensity tended to reduce the strength of the asymmetric nose-generated vortices.
- (2) The two asymmetric vortices remained in approximately the same position for an increase in turbulence.
- (3) The top vortex was closer to the model surface and appeared to be stronger for both body configurations. This condition was more pronounced for configuration A.
- (4) The wing/strike arrangement of configuration C caused the vortices to be centered further away from the model surface than those of configuration A, correlating with the differences in induced side forces for those configurations observed by Rabang.
- (5) Configuration C vortices are more diffused and larger. This was more apparent when turbulence was added.
- (6) Crossflow velocity vector plots agreed with the behavior denoted by the total and static pressure coefficient contours for both body configurations and turbulence levels.

- (7) Though subtle differences exist, the addition of wings and tails did not greatly alter the vortex pattern around the nose of the missile model, when compared to the body-only configuration tested by Lung.

Recommendations for a continued study of the behavior of asymmetric vortices under varying flowfield conditions are suggested as follows:

- (1) Examine the vortices at positions further back along the model body, where effects from the wings might better be seen. (Such as at a length/diameter ratio of 9.)
- (2) Investigate asymmetric vortex behavior for just a body-only configuration, at the position described above, to provide comparisons.
- (3) Continue to study vortex behavior at various angles of attack and turbulence with varying intensities and length scales in order to provide a large data base, which can be used to calculate vorticity contours.

## APPENDIX A. PPROBE PROGRAM

```
1 DEF SEG:CLEAR ,&HFE00:GOTO 4 'Begin PCIB Program Shell
2 GOTO 1000 ' User program
3 GOTO 900 ' Error handling
4 I=&HFE00 ' Copyright Hewlett-Packard 1984,1985
5 PCIB.DIR$=ENVIRON$("PCIB")
6 I$=PCIB.DIR$+"\\PCIBILC.BLD"
7 BLOAD I$,I
8 CALL I(FCIB.DIR$,I%,J%):PCIB.SEG=I%
9 IF J%=0 THEN GOTO 13
10 PRINT "Unable to load."
11 PRINT "    (Error #";J%;")"
12 END
13 '
14 DEF SEG=PCIB.SEG:O.S=5:C.S=10:I.V=15
15 I.C=20:L.P=25:LD.FILE=30
16 GET.MEM=35:L.S=40:PANELS=45:DEF.ERR=50
17 PCIB.ERR$=STRING$(64,32) : PCIB.NAME$=STRING$(16,32)
18 CALL DEF.ERR(PCIB.ERR,PCIB.ERR$,PCIB.NAME$,PCIB.GLBERR) : PCIB.BASERR=255
19 ON ERROR GOTO 3
20 J=-1
21 I$=PCIB.DIR$+"\\PCIB.SYN"
22 CALL O.S(I$)
23 IF PCIB.ERR<>0 THEN ERROR PCIB.BASERR
24 I=0
25 CALL I.V(I,READ.REGISTER,READ.SELFID,DEFINE,INITIALIZE.SYSTEM)
26 IF PCIB.ERR<>0 THEN ERROR PCIB.BASERR
27 CALL I.V(I,ENABLE.SYSTEM,DISABLE.SYSTEM,INITIALIZE.POWER.ON)
28 IF FCIB.ERR<>0 THEN ERROR FCIB.BASERR
29 CALL I.V(I,MEASURE.OUTPUT,START,HALT)
30 IF FCIB.ERR<>0 THEN ERROR FCIB.BASEFR
31 CALL I.V(I,ENABLE.INT.TRIGGER,DISABLE.INT.TRIGGER,ENABLE.OUTPUT,DISABLE.OUTPU
T)
32 IF PCIB.ERR<>0 THEN ERROR PCIB.BASERR
33 CALL I.V(I,CHECK.DONE,GET.STATUS,SET.FUNCTION,SET.RANGE)
34 IF PCIB.ERR<>0 THEN ERROR PCIB.BASERR
35 CALL I.V(I,SET.MODE,WRITE.CAL,READ.CAL,STORE.CAL)
36 IF FCIB.EPR<>0 THEN ERROR FCIB.BASERR
37 CALL I.V(I,DELAY,SAVE.SYSTEM,J,J)
38 IF FCIB.ERR<>0 THEN ERROR FCIB.BASERR
39 I=1
40 CALL I.V(I,SET.GATETIME,SET.SAMPLES,SET.SLOPE,SET.SOURCE)
41 IF PCIB.ERR<>0 THEN ERROR PCIB.BASERR
42 CALL I.C(I,FREQUENCY,AUTO.FREQ,PERIOD,AUTO.PER)
43 IF PCIB.ERR<>0 THEN ERROR PCIB.BASERR
44 CALL I.C(I,INTERVAL,RATIO,TOTALIZE,R100MILLI)
45 IF FCIB.ERR<>0 THEN ERROR FCIB.BASERR
46 CALL I.C(I,R1,R10,R100,R1KILO)
47 IF PCIB.ERR<>0 THEN ERROR PCIB.BASERR
48 CALL I.C(I,R10MEGA,R100MEGA,CHAN.A,CHAN.B)
49 IF FCIB.ERR<>0 THEN ERROR FCIB.BASERR
50 CALL I.C(I,POSITIVE,NEGATIVE,COMM,SEPARATE)
51 IF PCIB.ERR<>0 THEN ERROR PCIB.BASERR
52 I=2
53 I=3
```

```

54 CALL I.V(I,ZERO.OHMS,SET.SPEED,J,J)
55 IF PCIB.ERR<>0 THEN ERROR PCIB.BASERR
56 CALL I.C(I,DCVOLTS,ACVOLTS,OHMS,R200MILLI)
57 IF PCIB.ERR<>0 THEN ERROR PCIB.BASERR
58 CALL I.C(I,R2,R20,R200,R2KILO)
59 IF PCIB.ERR<>0 THEN ERROR PCIB.BASERR
60 CALL I.C(I,R20KILO,R200KILO,R2MEGA,R20MEGA)
61 IF PCIB.ERR<>0 THEN ERROR PCIB.BASERR
62 CALL I.C(I,AUTOM,R2.5,R12.5,J)
63 IF PCIB.ERR<>0 THEN ERROR PCIB.BASERR
64 I=4
65 CALL I.V(I,SET.COMPLEMENT,SET.DRIVER,OUTPUT.NO.WAIT,ENABLE.HANDSHAKE)
66 IF PCIB.ERR<>0 THEN ERROR PCIB.BASERR
67 CALL I.V(I,DISABLE.HANDSHAKE,SET.THRESHOLD,SET.START.BIT,SET.NUM.BITS)
68 IF PCIB.ERR<>0 THEN ERROR PCIB.BASERR
69 CALL I.V(I,SET.LOGIC.SENSE,J,J,J)
70 IF PCIB.ERR<>0 THEN ERROR PCIB.BASERR
71 CALL I.C(I,POSITIVE,NEGATIVE,TWOS,UNSIGNED)
72 IF PCIB.ERR<>0 THEN ERROR PCIB.BASERR
73 CALL I.C(I,OC,TTL,R0,R1)
74 IF PCIB.ERR<>0 THEN ERROR PCIB.BASERR
75 CALL I.C(I,R2,R3,R4,R5)
76 IF PCIB.ERR<>0 THEN ERROR PCIB.BASERR
77 CALL I.C(I,R6,R7,R8,R9)
78 IF PCIB.ERR<>0 THEN ERROR PCIB.BASERR
79 CALL I.C(I,R10,R11,R12,R13)
80 IF PCIB.ERR<>0 THEN ERROR PCIB.BASERR
81 CALL I.C(I,R14,R15,R16,J)
82 IF PCIB.ERR<>0 THEN ERROR PCIB.BASERR
83 I=6
84 CALL I.V(I,SET.FREQUENCY,SET.AMPLITUDE,SET.OFFSET,SET.SYMMETRY)
85 IF PCIB.ERR<>0 THEN ERROR PCIB.BASERR
86 CALL I.V(I,SET.BURST.COUNT,J,J,J)
87 IF PCIB.ERR<>0 THEN ERROR PCIB.BASERR
88 CALL I.C(I,SINE,SQUARE,TRIANGLE,CONTINUOUS)
89 IF PCIB.ERR<>0 THEN ERROR PCIB.BASERR
90 CALL I.C(I,GATED,BURST,J,J)
91 IF PCIB.ERR<>0 THEN ERROR PCIB.BASERR
92 I=7
93 CALL I.V(I,AUTOSCALE,CALIBRATE,SET.SENSITIVITY,SET.VERT.OFFSET)
94 IF PCIB.ERR<>0 THEN ERROR PCIB.BASERR
95 CALL I.V(I,SET.COUPLING,SET.POLARITY,SET.SWEEPSPEED,SET.DELAY)
96 IF PCIB.ERR<>0 THEN ERROR PCIB.BASERR
97 CALL I.V(I,SET.TRIG.SOURCE,SET.TRIG.SLOPE,SET.TRIG.LEVEL,SET.TRIG.MODE)
98 IF PCIB.ERR<>0 THEN ERROR PCIB.BASERR
99 CALL I.V(I,GET.SINGLE.WF,GET.TWO.WF,GET.VERT.INFO,GET.TIMERASE.INFO)
100 IF PCIB.ERR<>0 THEN ERROR PCIB.BASERR
101 CALL I.V(I,GET.TRIG.INFO,CALC.WFVOLT,CALC.WFTIME,CALC.WF.STATS)
102 IF PCIB.ERR<>0 THEN ERROR PCIB.BASERR
103 CALL I.V(I,CALC.RISETIME,CALC.FALLTIME,CALC.PERIOD,CALC.FREQUENCY)
104 IF PCIB.ERR<>0 THEN ERROR PCIB.BASERR
105 CALL I.V(I,CALC.PLUSWIDTH,CALC_MINUSWIDTH,CALC_OVERSHOOT,CALC_FRESHOOT)
106 IF PCIB.ERR<>0 THEN ERROR PCIB.BASERR
107 CALL I.V(I,CALC.PK_TO.PK,SET.TIMEOUT,SCOPE.START,MEASURE.SINGLE.WF)
108 IF PCIB.ERR<>0 THEN ERROR PCIB.BASERR
109 CALL I.V(I,MEASURE.TWO.WF,J,J,J)

```

```

110 IF PCIB.ERR<>0 THEN ERROR FCIB.BASERR
111 CALL I.C(I,R10NANO,R100NANO,R1MICRO,R10MICRO)
112 IF PCIB.ERR<>0 THEN ERROR FCIB.BASERR
113 CALL I.C(I,R100MICRO,R1MILLI,R10MILLI,R100MILLI)
114 IF PCIB.ERR<>0 THEN ERROR FCIB.BASERR
115 CALL I.C(I,R1,R10,R20NANO,R200NANO)
116 IF PCIB.ERR<>0 THEN ERROR FCIB.BASERR
117 CALL I.C(I,R2MICRO,R20MICRO,R200MICRO,R2MILLI)
118 IF PCIB.ERR<>0 THEN ERROR FCIB.BASERR
119 CALL I.C(I,R20MILLI,R200MILLI,R2,R20)
120 IF PCIB.ERR<>0 THEN ERROR FCIB.BASERR
121 CALL I.C(I,R50NANO,R500NANO,R5MICRO,R50MICRO)
122 IF PCIB.ERR<>0 THEN ERROR FCIB.BASERR
123 CALL I.C(I,R500MICRO,R5MILLI,R50MILLI,R500MILLI)
124 IF PCIB.ERR<>0 THEN ERROR FCIB.BASERR
125 CALL I.C(I,R5,R50,CHAN.A,CHAN.B)
126 IF PCIB.ERR<>0 THEN ERROR FCIB.BASERR
127 CALL I.C(I,EXTERNAL,POSITIVE,NEGATIVE,AC)
128 IF PCIB.ERR<>0 THEN ERROR FCIB.BASERR
129 CALL I.C(I,DC,TRIGGEPE, AUTO,TRIG,AUTO,LEVEL)
130 IF PCIB.ERR<>0 THEN ERROR FCIB.BASERR
131 CALL I.C(I,X1,X10,STANDARD,AVERAGE)
132 IF PCIB.ERR<>0 THEN ERROR FCIB.BASERR
133 I=8
134 CALL I.V(I,OPEN CHANNEL,CLOSE CHANNEL,J,J)
135 IF PCIB.ERR<>0 THEN ERROR FCIB.BASERR
136 CALL C.S .
137 IF PCIB.ERR<>0 THEN ERROR FCIB.BASERR
138 I$=PCIB.DIR$+"\"PCIB.PID"
139 CALL L.P(I$)
140 IF PCIB.ERR<>0 THEN ERROR FCIB.BASEPR
141 I$="DMM.01":I=3:J=0:K=0:L=1
142 CALL DEFINE(DMM.01,I$,I,J,K,L)
143 IF PCIB.ERR<>0 THEN ERROR FCIB.BASEPR
144 I$="Func.Gen.01":I=6:J=0:K=1:L=1
145 CALL DEFINE(Func.Gen.01,I$,I,J,K,L)
146 IF PCIB.ERR<>0 THEN ERROR FCIB.BASERR
147 I$="Scope.01":I=7:J=0:K=2:L=1
148 CALL DEFINE(Scope.01,I$,I,J,K,L)
149 IF PCIB.ERR<>0 THEN ERROR FCIB.BASEPR
150 I$="Counter.01":J=1:J=0:K=3:L=1
151 CALL DEFINE(Counter.01,I$,I,J,K,L)
152 IF PCIB.ERR<>0 THEN ERROR FCIB.BASERR
153 I$="Dig.In.01":I=4:J=0:K=4:L=1
154 CALL DEFINE(Dig.In.01,I$,I,J,K,L)
155 IF PCIB.ERR<>0 THEN ERROR FCIB.BASEPR
156 I$="Dig.Out.01":I=4:J=1:K=4:L=1
157 CALL DEFINE(Dig.Out.01,I$,I,J,K,L)
158 IF PCIB.ERR<>0 THEN ERROR FCIB.BASERR
159 I$="Relay.Act.01":I=8:J=0:K=5:L=1
160 CALL DEFINE(Relay.Act.01,I$,I,J,K,L)
161 IF PCIB.ERR<>0 THEN ERROR FCIB.PASERR
162 I$="Prelay.Mux.01":I=2:J=0:K=6:L=1
163 CALL DEFINE(Prelay.Mux.01,I$,I,J,K,L)
164 IF PCIB.ERR<>0 THEN ERROR FCIB.PASERR
800 I$=ENVIRON$("FANELS")+"\"PANELS.EXE"
801 CALL L.S(I$)
899 GOTO 2

```





```

1800 INPUT V$
1810 IF V$="Y" THEN 1690
1820 IF V$="N" THEN 1430
1830 PRINT
1840 PRINT
1850 INPUT "ENTER DESIRED VELOCITY OF MOTOR 2";V2
1860 PRINT
1870 GOTO 1780
1880 PRINT
1890 PRINT
1900 INPUT "ENTER DESIRED VELOCITY OF MOTOR #3";V3
1910 PRINT
1920 GOTO 1780
1930 PRINT
1940 PRINT
1950 INPUT "WHICH MOTOR ACCEL RAMP DO YOU WANT TO CHANGE? (1, 2, or 3)";K
1960 ON K GOTO 1970,2060,2120
1970 PRINT
1980 PRINT
1990 INPUT "ENTER DESIRED ACCELERATION RAMP OF MOTOR #1";R1
2000 PRINT
2010 PRINT
2020 PRINT "DO YOU WANT TO CHANGE THE ACCEL RAMP OF ANOTHER MOTOR? (Y or N)?"
2030 INPUT RM$
2040 IF RM$="Y" THEN 1930
2050 IF RM$="N" THEN 1450
2060 PRINT
2070 PRINT
2080 INPUT "ENTER DESIRED ACCELERATION RAMP OF MOTOR #2";R2
2090 PRINT
2100 PRINT
2110 GOTO 2000
2120 PRINT
2130 PRINT
2140 INPUT "ENTER DESIRED ACCELERATION RAMP OF MOTOR #3";R3
2150 PRINT
2160 PRINT
2170 GOTO 2000
2180 REM
2190 REM DEFINE DISTANCE TO MOVE MOTOR
2200 PRINT
2210 PRINT
2220 PRINT
2230 REM INITIALIZE MOTOR INCREMENTS TO ZERO
2240 I1=0
2250 I2=0
2260 I3=0
2270 PRINT
2280 PRINT " ****"
2290 'RI' " **      DEFINE WHICH MOTOR YOU WANT TO MOVE      ***"
2300 'TP' " **      ***"
2310 'RI+I' " **      NOTE!!! A POSITIVE ('+') INCREMENT TO A MOTOR      ***"
2320 PRINT " **      MOVES TRAVERSER AWAY FROM THAT PARTICULAR MOTOR      ***"
2330 PRINT " **      ***"
2340 PRINT " **      -- MOTOR #1 MOVES THE PROBE UPSTREAM AGAINST THE FLOW      ***"
2350 PRINT " **      -- MOTOR #2 MOVES THE PROBE TOWARD THE ACCESS WINDOW      ***"
2360 PRINT " **      -- MOTOR #3 MOVES THE PROBE VERTICALLY DOWNWARD      ***"
2370 PRINT " ****"
2380 PRINT
2390 PRINT
2400 INPUT "WHICH MOTOR DO YOU WANT TO MOVE? (1,2, or 3)";L
2410 ON L GOTO 2420,2680,2970

```

```

2420 PRINT
2430 PRINT
2440 PRINT "HOW FAR DO YOU WANT TO MOVE MOTOR #1?"
2450 PRINT " ***** (ENTER DISTANCE IN INCHES) *****"
2460 INPUT I1
2470 PRINT
2480 PRINT" ****"
2490 PRINT
2500 PRINT "SUMMARY OF OPERATOR INPUTS:"
2510 PRINT " MOTOR #1 VELOCITY = ";V1
2520 PRINT " ACCELERATION RAMP = ";R1
2530 PRINT " INCREMENTAL DISTANCE = ";I1;"INCHES"
2540 PRINT" ****"
2550 PRINT "DO YOU WANT TO CHANGE ANY OF THESE VALUES? (Y or N)"
2560 PRINT
2570 PRINT "ENTER 'N' TO START MOTOR MOVEMENT. ENTER 'Y' TO RETURN"
2580 PRINT "TO VARIABLE SELECTION SUBROUTINE."
2590 INPUT V$
2600 IF V$="Y" THEN 1430
2610 GOSUB 3410
2620 PRINT
2630 PRINT "DO YOU WANT TO MOVE ANOTHER MOTOR ALSO? (Y or N)?"
2640 INPUT C$
2650 IF C$="Y" THEN 2220
2660 IF C$="N" THEN 3260
2670 PRINT
2680 PRINT
2690 PRINT "HOW FAR DO YOU WANT TO MOVE MOTOR #2?"
2700 PRINT " ***** (ENTER DISTANCE IN INCHES) *****"
2710 INPUT I2
2720 PRINT
2730 PRINT
2740 REM DISPLAY OPERATOR SELECTED MOTOR VARIABLES
2750 PRINT" ****"
2760 PRINT
2770 PRINT "SUMMARY OF OPERATOR INPUTS:"
2780 PRINT " MOTOR #2 VELOCITY = ";V2
2790 PRINT " ACCELERATION RAMP = ";R2
2800 PRINT " INCREMENTAL DISTANCE = ";I2;"INCHES"
2810 PRINT" ****"
2820 PRINT
2830 PRINT
2840 PRINT "DO YOU WANT TO CHANGE ANY OF THESE VALUES? (Y or N)"
2850 PRINT
2860 PRINT "ENTER 'N' TO START MOTOR MOVEMENT. ENTER 'Y' TO RETURN"
2870 PRINT "TO VARIABLE SELECTION SUBROUTINE."
2880 INPUT V$
2890 IF V$="Y" THEN 1430
2900 GOSUB 3410
2910 PRINT
2920 PRINT "DO YOU WANT TO MOVE ANOTHER MOTOR ALSO? (Y or N)?"
2930 INPUT C$
2940 IF C$="Y" THEN 2220
2950 IF C$="N" THEN 3260
2960 PRINT
2970 PRINT
2980 PRINT "HOW FAR DO YOU WANT TO MOVE MOTOR #3?"
2990 PRINT " ***** (ENTER DISTANCE IN INCHES) *****"
3000 INPUT I3
3010 PRINT
3020 PRINT
3030 REM DISPLAY OPERATOR SELECTED MOTOR VARIABLES

```

```

3040 PRINT" ****"
3050 PRINT
3060 PRINT "SUMMARY OF OPERATOR INPUTS:"
3070 PRINT"           MOTOR #3 VELOCITY = ";V3
3080 PRINT"           ACCELERATION RAMP = ";R3
3090 PRINT"           INCREMENTAL DISTANCE = ";I3;"INCHES"
3100 PRINT
3110 PRINT" ****"
3120 PRINT
3130 PRINT
3140 PRINT "DO YOU WANT TO CHANGE ANY OF THESE VALUES? (Y or N)"
3150 PRINT
3160 PRINT "ENTER 'N' TO START MOTOR MOVEMENT. ENTER 'Y' TO RETURN"
3170 PRINT "TO VARIABLE SELECTION SUBROUTINE."
3180 INPUT V$
3190 IF V$="Y" THEN 1430
3200 GOSUB 3410
3210 PRINT
3220 PRINT
3230 INPUT "DO YOU WANT TO INPUT ANOTHER MANUAL MOTOR MOVEMENT (Y or N)";MS
3240 IF MS="Y" THEN 2210
3250 PRINT
3260 PRINT "DO YOU WANT TO INPUT COMPUTER CONTROLLED MOTOR MOVEMENT?"
3270 PRINT"      ***** NOTE!!! ***** "
3280 PRINT " ALL PREVIOUS MOTOR INCREMENT INPUTS HAVE BEEN ZEROIZED."
3290 PRINT "PROGRAM WILL LET YOU CHOOSE MANUAL OR CP-CONTROLLED MOVEMENT."
3300 PRINT "***** (IF 'NO', THE PROGRAM WILL END). *****"
3310 PRINT
3320 INPUT "DO YOU WANT COMPUTER CONTROLLED MOTOR MOVEMENT (Y or N)";NS
3330 IF NS="Y" THEN 3500
3340 PRINT
3350 PRINT
3360 PRINT
3370 PRINT" ****"
3380 PRINT"      THE PROGRAM HAS ENDED."
3390 PRINT" ****"
3400 END
3410 REM ***** MOTOR MOVEMENT SUBROUTINE *****
3420 PRINT "#1, "& :PRINT #1, "E";C1=";C1;";C2=";C2;";C3=";C3
3430 PRINT #1, "I1=";I1;"V1=";V1;"R1=";R1;
3440 PRINT #1, ":I2=";I2;"V2=";V2;"R2=";R2
3450 PRINT #1, "I3=";I3;"V3=";V3;"R3=";R3;:@"
3460 RETURN
3470 REM ****
3480 REM ****
3490 PRINT
3500 REM ***** COMPUTER CONTROLLED MOVEMENT *****
3510 PRINT
3520 PRINT "THE PRESSURE DATA WILL BE WRITTEN TO FILES ON DRIVE 'A' "
3530 PRINT
3540 PRINT "YOU WILL BE ASKED TO INPUT FILE NAMES FOR THESE."
3550 PRINT
3560 INPUT "IS A FORMATTED DISK IN DRIVE 'A'? PRESS 'ENTER' TO CONTINUE";D$
3570 PRINT
3580 PRINT
3590 PRINT
3600 PRINT" ****"
3610 PRINT" **      NOTE !!!      **"
3620 PRINT" **  COMPUTER CONTROLLED MOVEMENT  **"
3630 PRINT" **      IS PROGRAMMED WITH A      **"
3640 PRINT" **  DEFULTED NEGATIVE MOTOR INCREMENT **"
3650 PRINT" **  (i.e. MOTOR #3 WILL MOVE UPWARD  **"
3660 PRINT" **      BY ENTERING A (+) DISTANCE).   **"
3670 PRINT" ****"
3680 PRINT
3690 REM SET INITIAL MOVEMENT DISTANCE AND NUMBER OF DATA POINTS TO ZERO
3700 HT=0

```

```

3710 WD=0
3720 DIST=0
3730 XPT=0
3740 YPT=0
3750 N=0
3760 PRINT
3770 PRINT
3780 INPUT "WHAT IS THE DIMENSION ( X , Y ) (IN INCHES) THAT YOU WANT TO MEASURE
." ;WD,HT
3790 PRINT
3800 INPUT "WHAT IS THE STEP (IN INCHES) THAT YOU WANT TO MOVE. ";DIST
3810 YPT=INT(HT /DIST) + 1
3820 XPT=INT(WD /DIST)+ 1
3830 N=XPT*YPT
3840 PRINT
3850 PRINT "THERE ARE " ;XPT; " * " ;YPT; " = " ;N; " POINTS TO BE MEASURED "
3860 PRINT
3870 INPUT "ARE THE NUMBER OF POINTS IS OK.(Y OR N)";C$
3880 IF C$="N" THEN 3780
3890 CLS
3900 N=XPT
3910 IF (N < 1) OR (N > 99) GOTO 3780
3920 REM *** GENERATING STRING STRING SEGMENTS FOR DATA FILE NAMES
3930 BS = MID$(STR$(1), 2): REM ** STRING NUMBER "1"
3940 ES = MID$(STR$(N), 2): REM ** ENDING STRING NUMBER "N"
3950 XS = "XXXXXX"
3960 EX$ = ".DAT"
3970 CLS
3980 PRINT "DATA FILES WILL BE INCREMENTED FROM:"
3990 PRINT
4000 PRINT (XS + BS + EX$); " To " ; (XS + ES + EX$)
4010 PRINT
4020 PRINT
4030 INPUT "ENTER DATA FILE NAME (6 CHARACTERS MAX -- NO EXTENSION)";F2$
4040 PRINT
4050 PRINT
4060 IF LEN(F2$) > 6 OR LEN(F2$) < 1 GOTO 4030
4070 CLS
4080 PRINT N; "DATA FILES WILL BE GENERATED AND INCREMENTED AS FOLLOWS:"
4090 PRINT
4100 PRINT
4110 PRINT (F2$ + BS + EX$); " To " ; (F2$ + ES + EX$)
4120 PRINT
4130 PRINT
4140 INPUT "ARE THE NUMBER OF POINTS AND FILE NAMES OK.(Y OR N)"; C$
4150 IF C$ = "N" GOTO 3780
4160 IF C$ = "Y" GOTO 4180
4170 GOTO 4140
4180 CLS
4190 PRINT
4200 PRINT
4210 REM SET INITIAL POSITION DATA
4220 X(1)=-DIST
4230 Y(1)=-DIST
4240 FOR IX=2 TO XPT+1
4250 X(IX)=0
4260 NEXT IX
4270 FOR JY=2 TO YPT+1
4280 Y(JY)=0
4290 NEXT JY
4300 FOR I=1 TO XPT
4302 I1=0
4304 I2=0
4306 I3=0
4310 FOR J=1 TO YPT
4320 REM MOTOR CP-CONTROLLED MOTOR MOVEMENT

```

```

4330 I1=0
4340 I2=0
4350 I3=0
4360 REM EACH POINT TAKE 10 TIMES READINGS
4370 X(I+1)=X(I)+DIST
4380 XPT(J)=X(I+1)
4390 Y(J+1)=Y(J)+DIST
4400 YPT(J)=Y(J+1)
4405 INPUT " ADJUST THE WHEEL TO MAKE THE P2 =P3, INPUT THE YAW ANGLE";YAW(J)
4408 PRINT
4410 INPUT " PRESS 'ENTER' TO START THE MEASUREMENT";MOVE$
4420 REM
4430 REM READ FIVE CHANNELS AND DISPLAY THE DATA
4440 REM
4450 STEPPER=4
4460 SWITCH = 3
4470 HOMER=8
4480 DELAY1 = .1
4490 DELAY2 = 1
4500 REM SET THE S.V PORT TO #4
4510 FOR IL=1 TO 3
4520 THYME = TIMER
4530 CALL OUTPUT(RELAY.ACT.01,STEPPER)
4540 CHKTIME = TIMER
4550 IF CHKTIME < (THYME + DELAY1) GOTO 4540
4560 CALL OPEN.CHANNEL(RELAY.ACT.01,SWITCH)
4570 CLS
4580 NEXT IL
4590 PRINT
4600 PRINT " NOW IS POINT ";J
4610 REM START MEASURE FROM PORT 4 TO PORT 8
4620 FOR JJ=1 TO 5
4630 CALL OUTPUT(RELAY.ACT.01,STEPPER)
4640 CHKTIME = TIMER
4650 IF CHKTIME < (THYME + DELAY2) GOTO 4640
4660 REM EACH PORT SAMPLE 10 TIMES
4670 FOR II=1 TO 10
4680 ROUT=1
4690 CALL OUTPUT(RELAY.MUX.01,ROUT)
4700 CALL MEASURE(DMM.01,VOLTS)
4710 PA(II,JJ)=VOLTS
4720 NEXT II
4730 CALL OPEN.CHANNEL(RELAY.ACT.01,SWITCH)
4740 IF JJ=5 THEN 4760
4750 NEXT JJ
4760 REM HOME THE S.V PORT TO #48
4770 CALL OUTPUT(PRELAY.ACT.01,HOMER)
4780 CALL OPEN.CHANNEL(RELAY.ACT.01,HOMER)
4790 REM
4800 REM DISPLAY THE SAMPLE DATA
4810 REM
4820 PRINT HEAD1$
4830 FOR IS= 1 TO 10
4840 PRINT USING FORMAT$;IS,XPT(J),YPT(J),PA(IS,1),PA(IS,2),PA(IS,3),PA(IS,4),PA
(IS,5),YAW(J)
4850 NEXT IS
4860 REM
4870 REM AVERAGE THE DATA
4880 REM
4890 FOR JA = 1 TO 5
4900 TOTAL = 0
4910 FOR IA = 1 TO 10
4920 TOTAL = TOTAL + PA(IA,JA)
4930 NEXT IA
4940 AVERAGE = TOTAL /10
4950 F(JA)=AVERAGE
4960 NEXT JA

```

```

4970 PRINT
4980 PRINT "THE AVERAGES ARE: "
5000 PRINT HEAD1$
5010 FOR JD=1 TO 5
5020 PP(J,JD)=P(JD)
5030 NEXT JD
5040 PRINT USING FORMAT$;J,XPT(J),YPT(J),PP(J,1),PP(J,2),PP(J,3),PP(J,4),PP(J,5)
,YAW(J)
5045 PRINT
5048 PRINT USING "THE NULLING ERROR IS +#.#####";PP(J,3)-PP(J,2)
5049 PRINT
5050 PRINT "DO YOU WANT RE-MEASURE AGAIN (Y / N)"
5060 PRINT
5062 PRINT "IF 'Y' WILL RE-SAMPLE AGAIN."
5064 PRINT
5070 INPUT "IF 'N' WILL MOVE THE TRAVERSER STEP UPWARD (WAIT 7 SEC )";C$
5075 PRINT
5080 IF C$="Y" THEN 4405
5082 IF C$="N" THEN 5090
5084 GO TO 5070
5090 IF J=YPT THEN 5160
5100 REM
5110 REM MOVE THE TRAVERSER STEP UPWARD.
5120 REM
5130 I3=-DIST
5140 GOSUB 3410
5150 NEXT J
5160 REM*** STORE DATA BEFORE NEXT SAMPLE***
5170 OPEN "A:\RAW.DAT" FOR OUTPUT AS #2
5180 PRINT #2 ,HEAD1$
5190 FOR ID=1 TO YPT
5200 PRINT #2 ,USING FORMAT$;ID,XPT(ID),YPT(ID),PP(ID,1),PP(ID,2),PP(ID,3),PP(ID
,4),PP(ID,5),YAW(ID)
5210 NEXT ID
5220 CLOSE #2
5230 REM *** GENERATING INCREMENTED DATA FILE NAME
5240 IF (I > 10) OR (I = 10) THEN I$ = MID$(STR$(I), 2)
5250 IF (I < 10) THEN I$ = (MID$(STR$(0), 2) + MID$(STR$(I), 2))
5260 FI2$ = (F2$ + I$ + EX$)
5270 PRINT
5280 PRINT " WRITING DATA FILE "; FI2$
5290 DF2$=RN2$+FI2$
5300 REM ** RENAME DATA FILE
5310 SHELL DF2$
5320 REM
5330 REM MOVE THE TRAVERSER TO THE NEXT SAMPLE POSITION
5340 REM
5350 PRINT
5360 IF I=XPT THEN 5430
5370 INPUT "THEN PRESS 'ENTER' FOR NEXT COLUMN SAMPLE( 90 SEC ) ";MOVE$
5390 I2=-DIST
5400 I3=HT
5410 GOSUB 3410
5420 NEXT I
5430 CLS
5440 PRINT "ALL MOVEMENTS COMPLETE"
5450 PRINT
5460 PRINT
5470 PRINT "YOU WANT TO REPOSITION TRAVERSER FOR ANOTHER MOVEMENT (Y OR N)?"
5480 PRINT
5490 PRINT "IF 'Y', THE PROGRAM WILL TAKE YOU TO MANUAL CONTROL SUBROUTINE."
5500 PRINT "IF 'N', THE PROGRAM WILL END."
5510 PRINT
5520 INPUT "ANOTHER MOVEMENT";R$
5530 IF R$ = "Y" THEN 1370
5540 IF R$ = "N" THEN 3370

```

## APPENDIX B. CALP PROGRAM

```
1 DEF SEG:CLEAR ,&HFE00:GOTO 4 'Begin PCIB Program Shell
2 GOTO 1000 ' User program
3 GOTO 900 ' Error handling
4 I=&HFE00 ' Copyright Hewlett-Packard 1984,1985
5 PCIB.DIR$=ENVIRON$("PCIB")
6 I$=PCIB.DIR$+"\PCIBILC.BLD"
7 BLOAD I$,I
8 CALL I(PCIB.DIR$,I%,J%):PCIB.SEG=I%
9 IF J%=0 THEN GOTO 13
10 PRINT "Unable to load."
11 PRINT " (Error #";J%;")"
12 END
13 '
14 DEF SEG=PCIB.SEG:O.S=5:C.S=10:I.V=15
15 I.C=20:L.P=25:LD.FILE=30
16 GET.MEM=35:L.S=40:PANELS=45:DEF.ERR=50
17 PCIB.ERR$=STRING$(64,32) : PCIB.NAME$=STRING$(16,32)
18 CALL DEF.ERR(PCIB.ERR,PCIB.ERR$,PCIB.NAME$,PCIB.GLBERR) : PCIB.BASERR=255
19 ON ERROR GOTO 3
20 J=-1
21 I$=PCIB.DIR$+"\PCIB.SYN"
22 CALL O.S(I$)
23 IF PCIB.ERR<>0 THEN ERROR PCIB.BASERR
24 I=0
25 CALL I.V(I,READ.REGISTER,READ.SELFID,DEFINE,INITIALIZE.SYSTEM)
26 IF PCIB.ERR<>0 THEN ERROR PCIB.BASERR
27 CALL I.V(I,ENABLE.SYSTEM.DISABLE.SYSTEM,INITIALIZE,POWER.ON)
28 IF PCIB.ERR<>0 THEN ERROR PCIB.BASERR
29 CALL I.V(I,MEASURE.OUTPUT,START,HALT)
30 IF PCIB.ERR<>0 THEN ERROR PCIB.BASERR
31 CALL I ('I,ENABLE.INT.TRIGGER,DISABLE.INT.TRIGGER,ENABLE.OUTPUT,DISABLE.OUTPUT)
32 IF PCIB.ERR<>0 THEN ERROR PCIB.BASERR
33 CALL I.V(I,CHECK.DONE,GET.STATUS,SET.FUNCTION,SET.RANGE)
34 IF PCIB.ERR<>0 THEN ERROR PCIB.BASERR
35 CALL I.V(I,SET.MODE,WRITE.CAL,READ.CAL,STORE.CAL)
36 IF PCIB.ERR<>0 THEN ERROR PCIB.BASERR
37 CALL I.V(I,DELAY,SAVE.SYSTEM,J,J)
38 IF PCIB.ERR<>0 THEN ERROR PCIB.BASERR
39 I=1
40 CALL I.V(I,SET.GATETIME,SET.SAMPLES,SET.SLOPE,SET.SOURCE)
41 IF PCIB.ERR<>0 THEN ERROR PCIB.BASERR
42 CALL I.C(I,FREQUENCY,AUTO.FREQ,PERIOD,AUTO.PER)
43 IF PCIB.ERR<>0 THEN ERROR PCIB.BASERR
44 CALL I.C(I,INTERVAL,RATIO,TOTALIZE,R100MILLI)
45 IF PCIB.ERR<>0 THEN ERROR PCIB.BASERR
46 CALL I.C(I,R1,R10,R100,R1KILO)
47 IF PCIB.ERR<>0 THEN ERROR PCIB.BASERR
48 CALL I.C(I,R10MEGA,R100MEGA,CHAN.A,CHAN.B)
49 IF PCIB.ERR<>0 THEN ERROR PCIB.BASERR
50 CALL I.C(I,POSITIVE,NEGATIVE,COMN,SEPARATE)
51 IF PCIB.ERR<>0 THEN ERROR PCIB.BASERR
52 I=2
53 I=3
```

```

54 CALL I.V(I,ZERO,OHMS,SET.SPEED,J,J)
55 IF PCIB.ERR<>0 THEN ERROR PCIB.BASERR
56 CALL I.C(I,DCVOLTS,ACVOL ),OHMS,R200MILLI)
57 IF PCIB.ERR<>0 THEN ERROR PCIB.BASERR
58 CALL I.C(I,R2,R20,R200,R2KILO)
59 IF PCIB.ERR<>0 THEN ERROR PCIB.BASERR
60 CALL I.C(I,R20KILO,R200KILO,R2MEGA,R20MEGA)
61 IF PCIB.ERR<>0 THEN ERROR PCIB.BASERR
62 CALL I.C(I,AUTOM,R2.5,R12.5,J)
63 IF PCIB.ERR<>0 THEN ERROR PCIB.BASERR
64 I=4
65 CALL I.V(I,SET.COMPLEMENT,SET.DRIVER,OUTPUT.NO.WAIT,ENABLE.HANDSHAKE)
66 IF PCIB.ERR<>0 THEN ERROR PCIB.BASERR
67 CALL I.V(I,DISABLE.HANDSHAKE,SFT.THRESHOLD,SET.START.BIT,SET.NUM.BITS)
68 IF PCIB.ERR<>0 THEN ERROR PCIB.BASERR
69 CALL I.V(I,SET.LOGIC.SENSE,J,J,J)
70 IF PCIB.ERR<>0 THEN ERROR PCIB.BASERR
71 CALL I.C(I,POSITIVE,NEGATIVE,TWOS,UNSIGNED)
72 IF PCIB.ERR<>0 THEN ERROR PCIB.BASERR
73 CALL I.C(I,OC,TTL,R0,R1)
74 IF PCIB.ERR<>0 THEN ERROR PCIB.BASERR
75 CALL I.C(I,R2,P3,R4,R5)
76 IF PCIB.ERR<>0 THEN ERROR PCIB.BASERR
77 CALL I.C(I,R6,P7,R8,R9)
78 IF PCIB.ERR<>0 THEN ERROR PCIB.BASERR
79 CALL I.C(I,P10,R11,R12,R13)
80 IF PCIB.ERR<>0 THEN ERROR PCIB.BASERR
81 CALL I.C(I,R14,R15,R16,J)
82 IF PCIB.ERR<>0 THEN ERROR PCIB.BASERR
83 I=6
84 CALL I.V(I,SET.FREQUENCY,SET.AMPLITUDE,SET.OFFSET,SET.SYMMETRY)
85 IF PCIB.ERR<>0 THEN ERROR PCIB.BASERR
86 CALL I.V(I,SET.BURST.COUNT,J,J,J)
87 IF PCIB.ERR<>0 THEN ERROR PCIB.BASERR
88 CALL I.C(I,SINE,SQUARE,TRIANGLE,CONTINUOUS)
89 IF PCIB.ERR<>0 THEN ERROR PCIB.BASERR
90 CALL I.C(I,GATED,BURST,J,J)
91 IF PCIB.ERR<>0 THEN ERROR PCIB.BASERR
92 I=7
93 CALL I.V(I,AUTOSCALE,CALIBRATE,SET.SENSITIVITY,SET.VERT.OFFSET)
94 IF PCIB.ERR<>0 THEN ERROR PCIB.BASERR
95 CALL I.V(I,SET.COUPLING,SET.POLARITY,SET.SWEEPSPEED,SET.DELAY)
96 IF PCIB.ERR<>0 THEN ERROR PCIB.BASERR
97 CALL I.V(I,SET.TFIG.SOURCE,SET.TRIG.SLOPE,SET.TRIG.LEVEL,SET.TRIG.MODE)
98 IF PCIB.ERR<>0 THEN ERROR PCIB.BASERR
99 CALL I.V(I,GET.SINGLE.WF,GET.TWO.WF,GET.VERT.INFO,GET.TIMEBASE.INFO)
100 IF PCIB.ERR<>0 THEN ERROR PCIB.BASERR
101 CALL I.V(I,GET.TRIG.INFO,CALC.WFVOLT,CALC.WFTIME,CALC.WF STATS)
102 IF PCIB.ERR<>0 THEN ERROR PCIB.PASERR
103 CALL I.V(I,CALC.RISETIME,CALC.FALLTIME,CALC.PERIOD,CALC.FREQUENCY)
104 IF PCIB.ERR<>0 THEN ERROR PCIB.BASERR
105 CALL I.V(I,CALC.PLUSWIDTH,CALC_MINUSWIDTH,CALC.OVERSHOOT,CALC.PRESHOOT)
106 IF PCIB.ERR<>0 THEN ERROR PCIB.BASERR
107 CALL I.V(I,CALC.PK.TO.PK,SET.TIMEOUT,SCOPE.START,MEASURE.SINGLE.WF)
108 IF PCIB.ERR<>0 THEN ERROR PCIB.BASERR
109 CALL I.V(I,MEASURE.TWO.WF,J,J,J)

```

```

110 IF PCIB.ERR<>0 THEN ERROR PCIB.BASERR
111 CALL I.C(I,R10NANO,R100NANO,R1MICRO,R10MICRO)
112 IF PCIB.ERR<>0 THEN ERROR PCIB.BASEPR
113 CALL I.C(I,R100MICRO,R1MILLI,R10MILLI.R100MILLI)
114 IF PCIB.ERR<>0 THEN ERROR PCIB.BASERR
115 CALL I.C(I,R1,R10,R20NANO,R200NANO)
116 IF PCIB.ERR<>0 THEN ERROR PCIB.BASERR
117 CALL I.C(I,R2MICRO,R20MICRO,R200MICRO,R2MILLI)
118 IF PCIB.ERR<>0 THEN ERROR PCIB.BASERR
119 CALL I.C(I,R20MILLI,R200MILLI,R2,R20)
120 IF PCIB.ERR<>0 THEN ERROR PCIB.BASERR
121 CALL I.C(I,R50NANO,R500NANO,R5MICRO,R50MICRO)
122 IF PCIB.ERR<>0 THEN ERROR PCIB.BASERR
123 CALL I.C(I,R500MICRO,R5MILLI,R50MILLI.R500MILLI)
124 IF PCIB.ERR<>0 THEN ERROR PCIB.BASERR
125 CALL I.C(I,R5,R50,CHAN.A.CHAN.B)
126 IF PCIB.ERR<>0 THEN ERROR PCIB.BASERR
127 CALL I.C(I,EXTERNAL,POSITIVE,NEGATIVE.AC)
128 IF PCIB.ERR<>0 THEN ERROR PCIB.BASERR
129 CALL I.C(I,DC,TRIGGERED,AUTO.TRIG,AUTO.LEVEL)
130 IF PCIB.ERR<>0 THEN ERROR PCIB.BASERR
131 CALL I.C(I,X1,X10,STANDARD,AVERAGE)
132 IF PCIB.ERR<>0 THEN ERROR PCIB.BASERR
133 I=8
134 CALL I.V(I,OPEN.CHANNEL,CLOSE.CHANNEL,J,J)
135 IF PCIB.ERR<>0 THEN ERROR PCIB.BASERR
136 CALL C.S
137 IF PCIB.ERR<>0 THEN ERROR PCIB.BASERR
138 I$=PCIB.DIR$+"\"PCIB.PLD"
139 CALL L.P(I$)
140 IF PCIB.ERR<>0 THEN ERROR PCIB.BASERR
141 I$="DMM.01":I=3:J=0:K=0:L=1
142 CALL DEFINE(DMM1.01,I$,I,J,K,L)
143 IF PCIB.ERR<>0 THEN ERROR PCIB.BASERR
144 I$="Func.Gen.01":I=6:J=0:K=1:L=1
145 CALL DEFINE(FUNC.GEN.01,I$,I,J,K,L)
146 IF PCIB.ERR<>0 THEN ERROR PCIB.BASERR
147 I$="Scope.01":I=7:J=0:K=2:L=1
148 CALL DEFINE(SCOPE.01,I$,I,J,K,L)
149 IF PCIB.ERR<>0 THEN ERROR PCIB.BASERR
150 I$="Counter.01":I=1:J=0:K=3:L=1
151 CALL DEFINE(COUNTER.01,I$,I,J,K,L)
152 IF PCIB.ERR<>0 THEN ERROR PCIB.BASERR
153 I$="Dig.In.01":I=4:J=0:K=4:L=1
154 CALL DEFINE(DIG.IN.01,I$,I,J,K,L)
155 IF PCIB.ERR<>0 THEN ERROR PCIB.BASERR
156 I$="Dig.Out.01":I=4:J=1:K=4:L=1
157 CALL DEFINE(DIG.OUT.01,I$,I,J,K,L)
158 IF PCIB.ERR<>0 THEN ERROR PCIB.BASERR
159 I$="Relay.Act.01":I=8:J=0:K=5:L=1
160 CALL DEFINE(RELAY.ACT.01,I$,I,J,K,L)
161 IF PCIB.ERR<>0 THEN ERROR PCIB.BASERR
162 I$="Relay.Mux.01":I=2:J=0:K=6:L=1
163 CALL DEFINE(RELAY.MUX.01,I$,I,J,K,L)
164 IF PCIB.ERR<>0 THEN ERROR PCIB.BASERR
800 I$=ENVIRON$("PANELS")+"\"PANELS.EXE"
801 CALL L.S(I$)
899 GOTO 2

```

```

900 IF ERR=PCIB.BASERR THEN GOTO 903
901 PRINT "BASIC error #";ERR;" occurred in line ";ERL
902 STOP
903 TMPERR=PC.B.ERR:IF TMPERR=0 THEN TMPERR=PCIB.GLBERR
904 PRINT "PC Instrument error #";TMPERR;" detected at line ";ERL
905 PRINT "Error: ";PCIB.ERR$
906 IF LEFT$(PCIB.NAME$,1)<>CHR$(32) THEN PRINT "Instrument: ";PCIB.NAME$
907 STOP
908 COMMON PCIB.DIR$,PCIB.SEG
909 COMMON LD.FILE,GET.MEM,PANELS,DEF.ERR
910 COMMON PCIB.BASERR,PCIB.ERR,PCIB.ERR$,PCIB.NAME$,PCIB.GLBERR
911 COMMON READ.REGISTER,READ.SELFID,DEFINE,INITIALIZE.SYSTEM,ENABLE.SYSTEM,DISA
BLE.SYSTEM,INITIALIZE,POWER.ON,MEASURE,OUTPUT,START,HALT,ENABLE.INT.TRIGGER,DISA
BLE.INT.TRIGGER,ENABLE.OUTPUT,DISABLE.OUTPUT,CHECK.DONE,GET.STATUS
912 COMMON SET.FUNCTION,SET.RANGE,SET.MODE,WRITE.CAL,READ.CAL,STORE.CAL,DELAY.SA
VE.SYSTEM,SET.GATETIME,SET.SAMPLES,SET.SLOPE,SET.SOURCE,ZERO.OHMS,SET.SPEED,SET.
COMPLEMENT,SET.DRIVER,OUTPUT.NO.WAIT,ENABLE.HANDSHAKE,DISABLE.HANDSHAKE
913 COMMON SET.THRESHOLD,SET.START.BIT,SET.NUMBITS,SET.LOGIC.SENSE,SET.FREQUENC
Y,SET.AMPLITUDE,SET.OFFSET,SET.SYMMETRY,SET.BURST.COUNT,AUTOSCALE,CALIBRATE,SET.
SENSITIVITY,SET.VERT.OFFSET,SET.COUPLING,SET.POLARITY,SET.SWEEPSPEED
914 COMMON SET.DELAY,SET.TRIG.SOURCE,SET.TRIG.SLOPE,SET.TRIG.LEVEL,SET.TRIG.MODE
,GET.SINGLE.WF,GET.TWO.WF,GET.VERT.INFO,GET.TIMEBASE.INFO,GET.TRIG.INFO,CALC.WFV
OLT,CALC.WFTIME,CALC.WF STATS,CALC.RISETIME,CALC.FALLTIME,CALC.PERIOD
915 COMMON CALC.FREQUENCY,CALC.PLUSWIDTH,CALC_MINUSWIDTH,CALC.OVERSHOOT,CALC.PRE
SHOOT,CALC.PK.TO.PK,SET.TIMEOUT,SCOPE.START,MEASURE.SINGLE.WF,MEASURE.TWO.WF,OPE
N.CHANNEL,CLOSE.CHANNEL
916 COMMON FREQUENCY,AUTO.FREQ,PERIOD,AUTO.PER,INTERVAL,RATIO,TOTALIZE,R100MILLI
,R1,R10,R100,R1KILO,R10MEGA,R100MEGA,CHAN.A,CHAN.B,POSITIVE,NEGATIVE,COMM,SEPARA
TE,DCVOLTS,ACVOLTS,OHMS,R200MILLI,R2,R20,R200,R2KILO,R200KILO
917 COMMON R2MEGA,R20MEGA,AUTOM,R2.5,R12.5,POSITIVE,NEGATIVE,TWOS.UNSIGNED,OC,TT
L,R0,R1,R2,R3,R4,R5,R6,R7,R8,R9,R10,R11,R12,R13,R14,R15,R16,SINE,SQUARE,TRIANGLE
,CONTINUOUS,GATED,BURST,R10NANO,R100NANO,R1MICRO,R10MICRO,R100MICRO
918 COMMON R1MILLI,R10MILLI,R100MILLI,P1,R10,R20NANO,R200NANO,R2MICRO,R20MICRO,R
200MICRO,R2MILLI,R20MILLI,R200MILLI,P2,R20,R50NANO,R500NANO,R5MICRO,R50MICRO,R50
0MICRO,R5MILLI,R50MILLI,R500MILLI,P5,R50,CHAN.A,CHAN.B,EXTERNAL.POSITIVE
919 COMMON NEGATIVE.AC,DC,TRIGGERED,AUTO.TRIG,AUTO.LEVEL,X1,X10,STANDARD,AVERAGE
920 COMMON DMM.01,FUNC.GEN.01,SCOPE.01,COUNTER.01,DIG.IN.01,DIG.OUT.01,RELAY.ACT
.01,RELAY MUX.01
999 'End PCIB Program Shell
1000 REM
1010 REM This step initializes the HP system
1020 CLS
1030 OPTION BASE 1
1040 DIM P(10),PA(50,6),PP(50,6),XPT(40),CAL(40)
1050 CALL INITIALIZE.SYSTEM(PGMSHEL.HPC)
1060 REM
1070 REM All PC devices now have an initial state
1080 REM Set function on the DMM and Relay MUX
1090 REM
1100 CALL SET.FUNCTION(DMM.01,DCVOLTS)
1110 CALL SET.RANGE(DMM.01,AUTOM)
1120 CALL DISABLE.INT.TRIGGER(DMM.01)
1130 CALL ENABLE.OUTPUT(RELAY.MUX.01)
1140 FORMAT$="## ##.#### ##.#### ##.#### ##.#### ##.#### ##.####"
1200 FOR I=1 TO 10
1210 CAL(I)=0.0

```

```

1220 NEXT I
1510 REM
1520 REM READ THE VOLTAGE OF 48TH CHANNEL AND DISPLAY THE DATA
1530 REM
1540 PRINT " CHOOSE 6 POINTS"
1550 PRINT
1550 PRINT "THE CALIBRATION WILL BE STORES IN 'CAL.DAT'"
1560 REM
1570 REM Begin sampling loop
1580 REM
1600 FOR J=1 TO 1
1610 PRINT
1630 FOR JJ=1 TO 6
1631 INPUT "INPUT THE CALIBRATION PRESSURE";CAL(JJ)
1632 INPUT "PRESS 'ENTER' TO START MEASUREMENT";MOVE$
1640 FOR JI=1 TO 10
1650 ROUT=1
1660 CALL OUTPUT(RELAY.MUX.01,ROUT)
1670 CALL MEASURE(DMM.01,VOLTS)
1680 PA(II,JJ) VOLTS
1690 NEXT II
1700 IF JJ=6 THEN 1740
1730 NEXT JJ
1740 REM
1750 REM DISPLAY THE SAMPLE DATA
1760 REM
1780 FOR IS= 1 TO 10
1790 PRINT USING FORMAT$;IS,PA(IS,1),PA(IS,2),PA(IS,3),PA(IS,4),PA(IS,5),PA(IS,6)
)
1800 NEXT IS
1810 REM
1820 REM AVERAGE THE DATA
1830 REM
1840 FOR JA = 1 TO 6
1850 TOTAL = 0
1860 FOR IA = 1 TO 10
1870 TOTAL = TOTAL + PA(IA,JA)
1880 NEXT IA
1890 AVERAGE = TOTAL /10
1900 P(JA)=AVERAGE
1920 NEXT JA
1930 PRINT
1940 PRINT "THE AVERAGE ARE: "
2000 FOR JD=1 TO 6
2010 FP(J,JD)=P(JD)
2020 NEXT JD
2055 PRINT USING FORMAT$;J,FP(J,1),FP(J,2),FP(J,3),FP(J,4),FP(J,5),FP(J,6)
2070 PRINT
2080 INPUT "DO YOU WANT RE-MEASURE AGAIN ? (Y / N)";C$
2090 IF C$="Y" THEN 1580
2101 REM*** STORE DATA BEFORE NEXT SAMPLE***
2102 OPEN "A:\CAL.DAT" FOR OUTPUT AS #2
2106 FOR ID=1 TO 6
2107 PRINT #2,USING FORMAT$;ID,FP(J,ID),CAL(ID)
2108 NEXT ID
2109 CLOSE #2
2210 NEXT J

```

## APPENDIX C. CONVERT PROGRAM

```

*****  

* THIS PROGRAM CONVERTS THE VOLTAGE OF TRANSDUCER INTO PHYSICAL *  

* PRESSURE, VELOCITY, YAW ANGLE AND PITCH ANGLE. THOSE DATA ARE *  

* USED FOR PLOT PROGRAM LATER.  

*****  

CHARACTER*12 FNAME  

CHARACTER*12 NAME  

CHARACTER*2 A(50)  

CHARACTER*80 ST  

REAL K,INTR  

INTEGER COLS,RWS,DTPTS  

DATA A/'01','02','03','04','05','06','07','08','09',  

*      '10','11','12','13','14','15','16','17','18',  

*      '19','20','21','22','23','24','25','26','27',  

*      '28','29','30','31','32','33','34','35','36',  

*      '37','38','39','40','41','42','43','44','45',  

*      '46','47','48','49','50'/  

WRITE (*,'(A\')') ' # OF COLS (AWAY FROM MSL) = '  

READ (*,'(I5)') COLS  

WRITE (*,'(A\')') ' # OF DATA PTS IN A COL (UP/DOWN) = '  

READ (*,'(I5)') RWS  

WRITE (*,'(A\')') ' DATA FILE NAME? (IE R001A2XX.DAT) '  

READ (*,'(A12)') NAME  

WRITE (*,'(A\')') ' PI (F4.2) = '  

READ (*,'(F4.2)') PI  

WRITE (*,'(A\')') ' PF (F4.2) = '  

READ (*,'(F4.2)') PF  

WRITE (*,'(A\')') ' TI (F3.1) = '  

READ (*,'(F3.1)') TI  

WRITE (*,'(A\')') ' TF (F3.1) = '  

READ (*,'(F3.1)') TF  

WRITE (*,'(A\')') ' K (F6.4) = '  

READ (*,'(F6.4)') K  

WRITE (*,'(A\')') ' SLOPE FOR DELTAP (F9.6) = '  

READ (*,'(F9.6)') SLOPE  

WRITE (*,'(A\')') ' INTERCEPT FOR DELTAP (F9.6) = '  

READ (*,'(F9.6)') INTR  

WRITE (*,'(A\')') ' QM1 FACTOR (F4.2) = '  

READ (*,'(F4.2)') QM1FAC  

WRITE (*,'(A\')') ' X OFFSET = '  

READ (*,'(F5.2)') XOFF  

WRITE (*,'(A\')') ' Y OFFSET = '  

READ (*,'(F5.2)') YOFF  

* CONVERT THE PRESSURE UNIT FROM inHg TO psf  

PATM=(PI+PF)*35.3631  

R=1716.5  

E=0.0123  

T=(TI+TF)/2.+460  

RO=PATM/(R*T)  

DTPTS=RWS*COLS

```

```

* OPEN A NEW FILE TO STORE THE REDUCED DATA
OPEN(2,FILE='RESULT.DAT',STATUS='OLD')
WRITE(2,222) DTPTS
222 FORMAT (15)
* OPEN A SEQUENTIAL OF DATA FILE
DO 20 I=1,COLS
    NAME(7:8)=A(I)
    FNAME=NAME
    OPEN(1,FILE=FNAME)
    READ(1,100,END=20)ST
100   FORMAT(A65)
15     READ(1,1000,END=30)NO,X,Y,V1,V2,V3,V4,V5,BETA
1000  FORMAT(I2,F7.2,F6.2,F9.3,F8.2)
* CONVERT THE VOLTAGE TO PRESSURE IN LBF/FT**2
    P1=DELTAP(V1,SLOPE,INTR)*2.0475+PATM
    P2=DELTAP(V2,SLOPE,INTR)*2.0475+PATM
    P3=DELTAP(V3,SLOPE,INTR)*2.0475+PATM
    P4=DELTAP(V4,SLOPE,INTR)*2.0475+PATM
    P5=DELTAP(V5,SLOPE,INTR)*2.0475+PATM
* CALCULATE THE PITCH ANGLE IN DEGREES
    P=(P4-P5)/(P1-P2)
    ALPHA=FPITCH(P)
* CALCULATE THE VELOCITY IN FT/SEC
    YSLOP=FYSLOP(ALPHA)
    VELM=SQRT((2*YSLOP*(P1-P2))/(RO*K))
    VEL=VELM*(1+E)
* CALCULATE THE LOCAL DYNAMIC PRESSURE
    QM1=QM1FAC*2.0475/K
    QM=RO*VEL**2/2.
    Q1=QM1*(1+2*E)
    Q=QM*(1+2*E)
* CALCULATE THE YAW ANGLE IN DEGREES
    YAW=FYAW(BETA+5.0)
* CALCULATE THE VELOCITY COMPONENTS
    BETAR=YAW*.017453
    ALPHAR=(ALPHA-17.942)*.017453
    VELY=VEL*SIN(ALPHAR)
    VELX=VEL*COS(ALPHAR)*SIN(BETAR)
* CALCULATE THE TOTAL PRESSURE IN LBF/IN**2
    FTC=FFT(ALPHA)
    PT1=P1-Q*FTC
    PT=PT1/144.
    CPT=(PT1-PATM-Q1)/Q1
* CALCULATE THE STATIC PRESSURE IN LBF/IN**2
    PS1=PT1-Q
    PS=PS1/144
    CPS=(PS1-PATM)/Q1
* WRITE ZERO VALUES IF VELOCITY IS TOO HIGH (BAD)
    IF(VEL.GT.200.0) THEN
        Z=0.0
        WRITE(2,2000)-X+XOFF,Y+YOFF,Z,Z,Z,Z,Z,Z,Z,Z
        ELSE
        WRITE(2,2000)-X+XOFF,Y+YOFF,VEL,VELX,VELY,YAW,
        C   ALPHA-17.942,FT,CPT,PS,CPS

```

```

2000      FORMAT(11F10.3)
          ENDIF
          GO TO 15
30      CLOSE(1)
20      CONTINUE
          CLOSE(2)
          STOP
          END
*****
* THIS FUNCTION CONVERTS THE VOLTAGE TO PHYSICAL PRESSURE
FUNCTION DELTAP(X,SLOPE,INTR)
REAL INTR
DELTAP=X*SLOPE+INTR
END
*****
* THIS FUNCTION CALCULATES THE PITCH ANGLE
FUNCTION FPITCH(X)
FPITCH=3.759+53.7568*X-1.3085*X**2-1.6583*X**3
*           -0.8061*X**4+16.5115*X**5
END
*****
* THIS FUNCTION CALCULATES THE VELOCITY PRESSURE COEFFICIENT
FUNCTION FYSLOP(X)
IF(X.LT.-10)THEN
  FYSLOP=0.981-0.0102*X-3.000E-4*X**2-2.500E-6*X**3
ELSE IF((X.GE.-10).AND.(X.LE.10))THEN
  FYSLOP=0.98-0.006*X+2.000E-4*X**2
ELSE
  FYSLOP=0.9801-0.0035*X-1.143E-4*X**2+5.833E-6*X**3
END IF
END
*****
* THIS FUNCTION CALCULATES THE YAW ANGLE
FUNCTION FYAW(X)
IF((X.GE.0).AND.(X.LE.180)) THEN
  FYAW=-X
ELSE
  FYAW=360-X
END IF
END
*****
* THIS FUNCTION CALCULATES THE TOTAL PRESSURE COEFFICIENT
FUNCTION FFT(X)
IF(X.LE.-30) THEN
  FFT=-0.01
ELSE IF((X.GT.-30).AND.(X.LT.-20)) THEN
  FFT=0.02+1.00E-3*X
ELSE IF((X.GE.-20).AND.(X.LE.30)) THEN
  FFT=0
ELSE
  FFT=0.03-1.00E-3*X
END IF
END

```

## APPENDIX D. RESULT 00.DAT

84									
1	.000	.000	122.209	-7.000	18.214	15.002	.017	1	
4.875	-.060		122.155	-7.000	18.388	15.002	.015	1	
2	.000	.500	122.267	-7.000	18.254	15.002	.017	1	
4.875	-.061		1.000	122.199	-7.000	18.297	15.002	.016	1
3	.000		122.310	-7.000	18.433	15.002	.018	1	
4.875	-.062		1.500	122.155	-7.000	18.388	15.002	.016	1
4	.000		122.293	-7.000	18.302	15.002	.018	1	
4.875	-.061		2.000	122.359	-7.000	18.287	15.002	.018	1
5	.000		122.287	-7.000	18.357	15.002	.017	1	
4.875	-.061		3.000	125.471	-5.000	17.651	15.002	.017	1
6	.000		125.733	-5.000	17.773	15.002	.018	1	
4.875	-.062		4.000	125.881	-5.000	17.614	15.002	.019	1
7	.000		125.918	-5.000	17.784	15.002	.017	1	
4.875	-.062		4.500	126.131	-5.000	17.814	15.002	.015	1
10	.000		125.773	-5.000	17.773	15.002	.018	1	
4.868	-.118		1.000	125.015	-5.000	17.764	15.002	.015	1
11	.000		125.944	-5.000	17.669	15.001	.012	1	
4.868	-.122		1.500	125.812	-5.000	17.570	15.002	.015	1
12	.000		125.731	-5.000	17.688	15.002	.014	1	
4.867	-.124		2.000	125.777	-5.000	17.688	15.002	.013	1
1	.500		125.918	-5.000	17.714	15.002	.016	1	
4.867	-.127		2.500	126.524	-5.000	17.655	15.002	.012	1
2	.500		125.624	-5.000	17.570	15.002	.015	1	
4.868	-.122		3.000	125.944	-5.000	17.570	15.002	.013	1
3	.500		125.881	-5.000	17.669	15.001	.012	1	
4.866	-.132		3.500	126.015	-5.000	17.669	15.002	.015	1
4	.500		125.773	-5.000	17.570	15.002	.015	1	
4.867	-.125		4.000	125.812	-5.000	17.688	15.002	.013	1
5	.500		125.731	-5.000	17.688	15.002	.014	1	
4.867	-.131		4.500	125.777	-5.000	17.688	15.002	.013	1
6	.500		125.918	-5.000	17.714	15.002	.014	1	
4.867	-.128		5.000	125.881	-5.000	17.669	15.001	.012	1
7	.500		125.812	-5.000	17.570	15.002	.015	1	
4.867	-.126		5.500	126.015	-5.000	17.669	15.001	.013	1
8	.500		125.773	-5.000	17.570	15.002	.015	1	
4.867	-.126		6.000	125.881	-5.000	17.669	15.001	.012	1
9	.500		125.944	-5.000	17.714	15.002	.014	1	
4.867	-.127		6.500	126.015	-5.000	17.669	15.001	.013	1
10	.500		125.812	-5.000	17.570	15.002	.013	1	
4.867	-.131		7.000	125.731	-5.000	17.688	15.002	.015	1
11	.500		125.773	-5.000	17.688	15.002	.014	1	
4.865	-.140		7.500	125.918	-5.000	17.714	15.002	.015	1
12	.500		125.881	-5.000	17.669	15.002	.015	1	
4.867	-.129		8.000	126.015	-5.000	17.669	15.001	.013	1

1	1.000	.000	126.500	-5.000	17.408	15.001	.012	1
4.865	-.142							
2	1.000	.500	126.304	-5.000	17.474	15.002	.015	1
4.866	-.136							
3	1.000	1.000	126.169	-5.000	17.625	15.002	.015	1
4.866	-.134							
4	1.000	1.500	125.976	-5.000	17.822	15.001	.011	1
4.866	-.134							
5	1.000	2.000	125.656	-5.000	17.662	15.001	.012	1
4.867	-.126							
6	1.000	2.500	125.659	-5.000	17.636	15.001	.012	1
4.867	-.127							
7	1.000	3.000	125.571	-5.000	17.604	15.001	.011	1
4.867	-.126							
8	1.000	3.500	125.821	-5.000	17.602	15.001	.011	1
4.867	-.131							
9	1.000	4.000	125.881	-5.000	17.614	15.001	.013	1
4.867	-.130							
10	1.000	4.500	125.617	-5.000	17.722	15.001	.009	1
4.867	-.129							
11	1.000	5.000	125.492	-5.000	17.723	15.001	.010	1
4.867	-.125							
12	1.000	5.500	126.317	-5.000	17.396	15.002	.014	1
4.866	-.137							
1	1.500	.000	126.253	-5.000	17.611	15.001	.011	1
4.866	-.138							
2	1.500	.500	125.896	-5.000	17.509	15.001	.012	1
4.867	-.131							
3	1.500	1.000	125.926	-5.000	17.732	15.001	.011	1
4.866	-.133							
4	1.500	1.500	125.860	-5.000	17.543	15.001	.011	1
4.866	-.132							
5	1.500	2.000	125.405	-5.000	17.895	15.001	.008	1
4.867	-.126							
6	1.500	2.500	125.941	-5.000	17.627	15.001	.009	1
4.866	-.135							
7	1.500	3.000	126.016	-5.000	17.536	15.001	.007	1
4.866	-.139							
8	1.500	3.500	126.063	-5.000	17.424	15.001	.010	1
4.866	-.136							
9	1.500	4.000	125.824	-5.000	17.576	15.001	.007	1
4.866	-.135							
10	1.500	4.500	125.881	-5.000	17.614	15.001	.010	1
4.866	-.133							
11	1.500	5.000	125.853	-5.000	17.594	15.001	.008	1
4.866	-.134							
12	1.500	5.500	125.784	-5.000	17.635	15.001	.008	1
4.866	-.133							
1	2.000	.000	125.709	-5.000	17.727	15.001	.007	1
4.866	-.133							
2	2.000	.500	125.242	-5.000	17.725	15.001	.007	1
4.867	-.125							
3	2.000	1.000	125.934	-5.000	17.679	15.001	.006	1
4.866	-.138							
4	2.000	1.500	125.925	-5.000	17.529	15.001	.006	1
4.866	-.137							
5	2.000	2.000	125.833	-5.000	17.726	15.001	.006	1
4.866	-.136							
6	2.000	2.500	125.844	-5.000	17.876	15.001	.006	1
4.866	-.136							

7	2.000	3.000	125.890	-5.000	17.765	15.001	.008	1
4.866	-.135							
8	2.000	3.500	126.253	-5.000	17.611	15.001	.009	1
4.865	-.141							
9	2.000	4.000	125.720	-5.000	17.649	15.001	.008	1
4.866	-.132							
10	2.000	4.500	125.289	-5.000	17.613	15.001	.006	1
4.867	-.127							
11	2.000	5.000	125.982	-5.000	17.770	15.001	.009	1
4.866	-.136							
12	2.000	5.500	125.549	-5.000	17.762	15.001	.007	1
4.867	-.130							
1	2.500	.000	125.971	-5.000	17.848	15.001	.005	1
4.866	-.139							
2	2.500	.500	125.873	-5.000	17.667	15.001	.006	1
4.866	-.137							
3	2.500	1.000	125.760	-5.000	17.589	15.001	.005	1
4.866	-.136							
4	2.500	1.500	125.886	-5.000	17.791	15.001	.006	1
4.866	-.137							
5	2.500	2.000	125.235	-4.000	17.778	15.000	.005	1
4.867	-.127							
6	2.500	2.500	125.696	-4.000	17.603	15.000	.005	1
4.866	-.135							
7	2.500	3.000	125.117	-4.000	17.726	15.000	.005	1
4.867	-.124							
8	2.500	3.500	125.394	-4.000	17.539	15.000	.004	1
4.867	-.130							
9	2.500	4.000	125.169	-4.000	17.793	15.001	.006	1
4.867	-.124							
10	2.500	4.500	125.871	-4.000	17.464	15.001	.007	1
4.866	-.135							
11	2.500	5.000	124.912	-4.000	17.848	15.001	.006	1
4.868	-.119							
12	2.500	5.500	124.873	-4.000	17.676	15.001	.007	1
4.868	-.118							
1	3.000	.000	125.254	-4.000	17.646	15.001	.006	1
4.867	-.125							
2	3.000	.500	125.013	-4.000	17.800	15.000	.002	1
4.867	-.125							
3	3.000	1.000	125.231	-4.000	17.804	15.000	.002	1
4.867	-.129							
4	3.000	1.500	125.775	-4.000	17.484	15.000	.004	1
4.866	-.137							
5	3.000	2.000	125.213	-4.000	17.706	15.001	.007	1
4.867	-.124							
6	3.000	2.500	125.353	-4.000	17.599	15.001	.005	1
4.867	-.128							
7	3.000	3.000	125.550	-4.000	17.532	15.001	.007	1
4.867	-.130							
8	3.000	3.500	124.923	-4.000	17.768	15.000	.005	1
4.868	-.121							
9	3.000	4.000	125.558	-4.000	17.479	15.000	.002	1
4.866	-.135							
10	3.000	4.500	125.077	-4.000	17.787	15.001	.006	1
4.867	-.123							
11	3.000	5.000	124.878	-4.000	17.649	15.001	.006	1
4.868	-.119							
12	3.000	5.500	125.433	-4.000	17.480	15.001	.005	1
4.867	-.130							

## APPENDIX E. RESULT 0A.DAT

299								
1	.000	.000	150.248	-16.000	15.148	14.700	-.041	1
4.516	-.604		155.911	-15.000	14.475	14.701	-.039	1
2	.000	.250	160.315	-15.000	13.866	14.701	-.037	1
4.502	-.722							
3	.000	.500	164.509	-14.000	13.393	14.701	-.037	1
4.491	-.817							
4	.000	.750	169.716	-14.000	12.697	14.701	-.039	1
4.480	-.911							
5	.000	1.000	175.393	-13.000	10.631	14.700	-.047	1
4.465	-1.033							
6	.000	1.250	180.980	-8.000	2.980	14.688	-.147	1
4.448	-1.177							
7	.000	1.500	185.168	9.000	-5.242	14.637	-.581	1
4.420	-1.414							
8	.000	1.750	190.544	39.000	-23.961	14.556	-1.262	1
4.357	-1.955							
9	.000	2.000	199.011	84.000	-1.061	14.673	-.274	1
4.293	-2.493							
10	.000	2.250	181.551	73.000	-13.886	14.587	-.999	1
4.318	-2.281							
11	.000	2.500	190.920	61.000	-17.689	14.604	-.856	1
4.349	-2.016							
12	.000	2.750	192.122	81.000	-.585	14.649	-.480	1
4.347	-2.035							
13	.000	3.000	190.574	4.000	3.291	14.621	-.713	1
4.307	-2.379							
14	.000	3.250	186.191	24.000	-3.723	14.533	-1.456	1
4.250	-2.857							
15	.000	3.500	180.810	-8.000	4.141	14.679	-.219	1
4.325	-2.227							
16	.000	3.750	178.573	-11.000	3.863	14.693	-.102	1
4.388	-1.687							
17	.000	4.000	171.008	-13.000	4.608	14.696	-.077	1
4.433	-1.310							
18	.000	4.250	162.822	-13.000	6.181	14.696	-.075	1
4.457	-1.101							
19	.000	4.500	155.653	-13.000	8.050	14.697	-.074	1
4.480	-.911							
20	.000	4.750	151.143	-12.000	9.417	14.696	-.075	1
4.499	-.752							
21	.000	5.000	151.143	-12.000	10.473	14.697	-.073	1
4.510	-.656							
22	.000	5.250	150.027	-12.000	11.461	14.697	-.073	1
4.513	-.631							
23	.000	5.500	147.773	-12.000	16.164	14.692	-.112	1
4.518	-.585							
1	.250	.000	147.058	-12.000	15.207	14.696	-.077	1
4.515	-.609							
2	.250	.250	152.564	-16.000	14.221	14.696	-.076	1
4.506	-.688							
3	.250	.500	157.323	-16.000	14.424	14.690	-.131	1
4.494	-.789							
4	.250	.750	159.896	-17.000	12.905	14.696	-.078	1
4.481	-.901							
5	.250	1.000	169.024	-16.000				
4.463	-1.056							

6	.250	1.250	176.146	-16.000	11.158	14.695	-.087	1
4.442	-1.235							
7	.250	1.500	183.110	-10.000	5.264	14.681	-.206	1
4.407	-1.527							
8	.250	1.750	184.142	2.000	1.110	14.636	-.589	1
4.359	-1.936							
9	.250	2.000	164.120	25.000	12.257	14.586	-1.009	1
4.366	-1.874							
10	.250	2.250	187.888	68.000	-2.918	14.613	-.779	1
4.325	-2.223							
11	.250	2.500	189.832	84.000	1.471	14.656	-.418	1
4.362	-1.913							
12	.250	2.750	191.492	81.000	-3.333	14.661	-.376	1
4.361	-1.915							
13	.250	3.000	192.988	63.000	-16.674	14.586	-1.014	1
4.281	-2.592							
14	.250	3.250	193.453	22.000	-23.030	14.565	-1.189	1
4.259	-2.780							
15	.250	3.500	203.195	1.000	-5.046	14.655	-.426	1
4.318	-2.285							
16	.250	3.750	192.065	-9.000	.336	14.686	-.159	1
4.385	-1.713							
17	.250	4.000	178.709	-11.000	3.538	14.596	-.075	1
4.436	-1.286							
18	.250	4.250	169.131	-11.000	4.692	14.698	-.064	1
4.464	-1.045							
19	.250	4.500	159.931	-12.000	6.521	14.697	-.071	1
4.488	-.842							
20	.250	4.750	153.467	-12.000	7.862	14.698	-.065	1
4.505	-.696							
21	.250	5.000	151.014	-12.000	9.189	14.698	-.063	1
4.512	-.642							
22	.250	5.250	149.874	-12.000	10.150	14.698	-.063	1
4.514	-.619							
23	.250	5.500	149.154	-12.000	11.166	14.698	-.061	1
4.516	-.602							
1	.500	.000	150.077	-14.000	16.013	14.696	-.078	1
4.512	-.637							
2	.500	.250	152.885	-13.000	15.585	14.697	-.067	1
4.506	-.685							
3	.500	.500	156.663	-14.000	15.429	14.698	-.065	1
4.497	-.764							
4	.500	.750	161.989	-14.000	14.704	14.698	-.063	1
4.483	-.880							
5	.500	1.000	168.212	-15.000	14.154	14.697	-.069	1
4.466	-1.028							
6	.500	1.250	175.219	-16.000	13.498	14.696	-.078	1
4.445	-1.204							
7	.500	1.500	185.504	-12.000	9.860	14.686	-.164	1
4.405	-1.546							
8	.500	1.750	187.433	-1.000	9.338	14.655	-.428	1
4.368	-1.860							
9	.500	2.000	165.116	12.000	8.913	14.550	-1.312	1
4.328	-2.200							
10	.500	2.250	186.450	60.000	6.790	14.624	-.688	1
4.340	-2.095							
11	.500	2.500	189.835	78.000	5.301	14.678	-.234	1
4.383	-1.729							
12	.500	2.750	188.824	80.000	-1.206	14.678	-.229	1
4.387	-1.697							

13	.500	3.000	194.616	60.000	-17.478	14.643	-.524	1
4.334	-2.146	3.250	193.223	25.000	-27.707	14.628	-.651	1
14	.500							
4.324	-2.236	3.500	191.035	.000	-14.391	14.656	-.415	1
15	.500							
4.358	-1.941	3.750	181.406	-10.000	-4.021	14.683	-.191	1
16	.500							
4.414	-1.470	4.000	170.055	-12.000	2.001	14.693	-.103	1
17	.500							
4.457	-1.105	4.250	163.175	-11.000	4.393	14.696	-.076	1
18	.500							
4.479	-.919	4.500	156.143	-11.000	6.655	14.697	-.073	1
19	.500							
4.497	-.761	4.750	151.731	-10.000	7.797	14.697	-.074	1
20	.500							
4.509	-.667	5.000	150.462	-10.000	8.948	14.697	-.070	1
21	.500							
4.512	-.638	5.250	149.237	-10.000	10.084	14.697	-.070	1
22	.500							
4.515	-.612	5.500	147.595	-10.000	10.912	14.697	-.070	1
23	.500							
4.519	-.578	.000	145.274	-12.000	17.251	14.691	-.121	1
1	.750							
4.519	-.582	.250	152.155	-12.000	16.399	14.697	-.074	1
2	.750							
4.507	-.677	.500	153.989	-12.000	16.382	14.697	-.069	1
3	.750							
4.503	-.711	.750	158.660	-14.000	16.088	14.697	-.071	1
4	.750							
4.491	-.814	1.000	164.981	-15.000	15.845	14.697	-.074	1
5	.750							
4.474	-.959	1.250	172.719	-16.000	15.866	14.695	-.087	1
6	.750							
4.451	-1.152	1.500	179.926	-15.000	15.086	14.689	-.139	1
7	.750							
4.424	-1.380	1.750	179.845	-4.000	16.331	14.670	-.299	1
8	.750							
4.406	-1.538	2.000	170.797	17.000	20.555	14.635	-.597	1
9	.750							
4.396	-1.617	2.250	173.431	47.000	16.014	14.643	-.525	1
10	.750							
4.398	-1.608	2.500	176.462	71.000	8.908	14.680	-.214	1
11	.750							
4.426	-1.370	2.750	173.657	75.000	.888	14.691	-.120	1
12	.750							
4.445	-1.208	3.000	170.957	60.000	-18.135	14.651	-.457	1
13	.750							
4.413	-1.480	3.250	168.242	23.000	-28.507	14.639	-.559	1
14	.750							
4.408	-1.519	3.500	173.179	.000	-20.551	14.674	-.266	1
15	.750							
4.429	-1.343	3.750	170.676	-10.000	-8.831	14.688	-.143	1
16	.750							
4.450	-1.160	4.000	162.930	-11.000	-.383	14.694	-.097	1
17	.750							
4.477	-.934	4.250	155.194	-11.000	3.759	14.696	-.080	1
18	.750							
4.499	-.748	4.500	151.792	-11.000	6.123	14.696	-.077	1
19	.750							
4.508	-.673							

20	.50	4.750	148.596	-11.000	7.698	14.696	-.076	1	
4.516	.605	5.000	147.997	-11.000	8.892	14.697	-.073	1	
21	.750	5.250	146.891	-11.000	10.095	14.697	-.073	1	
4.518	-.589	5.500	146.590	-11.000	10.781	14.696	-.075	1	
22	.750	1.000	146.890	-12.000	17.324	14.696	-.079	1	
4.520	-.567	1.000	.250	147.914	-12.000	17.458	14.697	-.074	1
23	.750	1.000	.500	151.406	-12.000	17.417	14.697	-.073	1
4.521	-.562	1.000	.750	156.556	-13.000	17.266	14.696	-.075	1
1		1.000	1.000	162.577	-14.000	17.246	14.696	-.078	1
4.520	-.573	1.000	1.250	167.675	-15.000	17.796	14.696	-.077	1
2		1.000	1.500	170.656	-15.000	19.734	14.693	-.106	1
4.496	-.772	1.000	1.750	167.455	-7.000	22.512	14.679	-.222	1
5		1.000	2.000	161.789	11.000	24.818	14.659	-.389	1
4.480	-.908	1.000	2.250	153.979	38.000	22.243	14.654	-.434	1
6		1.000	3.000	156.105	54.000	-12.188	14.682	-.198	1
4.466	-1.024	1.000	3.250	152.532	24.000	-30.428	14.657	-.409	1
7		1.000	3.500	155.504	2.000	-25.690	14.675	-.254	1
4.455	-1.123	1.000	3.750	156.984	-6.000	-11.813	14.689	-.139	1
8		1.000	4.000	153.365	-7.000	-2.027	14.694	-.092	1
4.450	-1.164	1.000	4.250	152.086	-8.000	2.982	14.696	-.082	1
9		1.000	4.500	149.479	-9.000	5.555	14.696	-.080	1
4.446	-1.202	1.000	4.750	147.604	-9.000	7.457	14.696	-.080	1
10		1.000	5.000	147.178	-9.000	8.759	14.696	-.080	1
4.460	-1.075	1.000	5.250	146.303	-9.000	9.897	14.696	-.077	1
11		1.000	5.500	146.112	-9.000	10.535	14.696	-.076	1
4.487	-.853	1.250	.000	143.934	-11.000	18.032	14.695	-.086	1
12		1.250	.250	147.049	-10.000	17.891	14.695	-.083	1
4.507	-.683	1.250	.500	150.805	-11.000	18.032	14.696	-.079	1
13		1.250	.654						

4	1.250	.750	152.581	-11.000	18.451	14.696	-.062	1
4.505	-.694							
5	1.250	1.000	156.293	-14.000	18.681	14.695	-.085	1
4.496	-.776							
6	1.250	1.250	159.465	-14.000	19.636	14.695	-.085	1
4.488	-.845							
7	1.250	1.500	159.374	-14.000	23.039	14.693	-.107	1
4.485	-.865							
8	1.250	1.750	155.497	-10.000	28.847	14.688	-.144	1
4.491	-.818							
9	1.250	2.000	148.004	6.000	32.505	14.672	-.281	1
4.493	-.798							
10	1.250	2.250	136.553	30.000	32.222	14.661	-.376	1
4.509	-.667							
11	1.250	2.500	137.451	50.000	23.529	14.684	-.181	1
4.530	-.489							
12	1.250	2.750	130.058	52.000	15.444	14.693	-.106	1
4.555	-.277							
13	1.250	3.000	132.861	42.000	-3.035	14.693	-.105	1
4.549	-.327							
14	1.250	3.250	140.729	23.000	-20.497	14.687	-.158	1
4.525	-.530							
15	1.250	3.500	146.995	6.000	-18.677	14.689	-.136	1
4.513	-.632							
16	1.250	3.750	148.910	-2.000	-9.649	14.694	-.097	1
4.513	-.632							
17	1.250	4.000	147.630	-7.000	-1.620	14.695	-.089	1
4.517	-.597							
18	1.250	4.250	146.738	-8.000	2.969	14.695	-.086	1
4.519	-.577							
19	1.250	4.500	144.477	-8.000	5.902	14.696	-.082	1
4.525	-.527							
20	1.250	4.750	144.758	-9.000	7.645	14.696	-.082	1
4.524	-.532							
21	1.250	5.000	144.212	10.000	9.007	14.695	-.085	1
4.525	-.525							
22	1.250	5.250	144.362	-8.000	10.099	14.695	-.084	1
4.525	-.527							
23	1.250	5.500	144.482	-8.000	10.769	14.696	-.083	1
4.525	-.528							
1	1.500	.000	144.399	-11.000	18.211	14.694	-.098	1
4.523	-.541							
2	1.500	.250	143.875	-11.000	18.874	14.695	-.086	1
4.526	-.520							
3	1.500	.500	146.765	-10.000	18.882	14.695	-.085	1
4.519	-.577							
4	1.500	.750	149.098	-11.000	19.123	14.696	-.082	1
4.514	-.621							
5	1.500	1.000	149.425	-12.000	19.987	14.695	-.087	1
4.513	-.633							
6	1.500	1.250	150.554	-12.000	21.497	14.695	-.088	1
4.510	-.657							
7	1.500	1.500	146.989	-9.000	25.643	14.695	-.091	1
4.518	-.587							
8	1.500	1.750	144.651	-5.000	31.710	14.694	-.096	1
4.523	-.544							
9	1.500	2.000	140.980	6.000	39.948	14.689	-.140	1
4.526	-.516							
10	1.500	2.250	134.535	24.000	39.304	14.685	-.168	1
4.538	-.421							

11	1.500	2.500	126.672	18.000	28.349	14.691	-.119	1
4.560	-.230							
12	1.500	2.750	121.238	40.000	19.736	14.695	-.089	1
4.575	-.107							
13	1.500	3.000	122.646	31.000	5.343	14.695	-.090	1
4.572	-.131							
14	1.500	3.250	129.062	21.000	~5.348	14.694	-.098	1
4.558	-.251							
15	1.500	3.500	137.188	9.000	~8.529	14.694	-.098	1
4.540	-.401							
16	1.500	3.750	141.477	.000	~4.700	14.694	-.093	1
4.531	-.479							
17	1.500	4.000	142.942	-4.000	.016	14.695	-.087	1
4.528	-.502							
18	1.500	4.250	142.681	-6.000	3.828	14.695	-.090	1
4.528	-.499							
19	1.500	4.500	142.203	-7.000	6.380	14.695	-.087	1
4.530	-.487							
20	1.500	4.750	142.386	-8.000	8.066	14.695	-.087	1
4.529	-.491							
21	1.500	5.000	144.617	-8.000	9.066	14.695	-.085	1
4.524	-.533							
22	1.500	5.250	143.124	-8.000	10.249	14.695	-.085	1
4.528	-.504							
23	1.500	5.500	142.683	-8.000	10.919	14.695	-.086	1
4.529	-.496							
1	1.750	.000	141.506	-9.000	18.702	14.694	-.091	1
4.531	-.478							
2	1.750	.250	143.781	-10.000	18.934	14.695	-.090	1
4.526	-.521							
3	1.750	.500	144.629	-10.000	19.340	14.695	-.087	1
4.524	-.536							
4	1.750	.750	146.268	-11.000	19.788	14.695	-.086	1
4.520	-.567							
5	1.750	1.000	144.476	-9.000	20.866	14.693	-.100	1
4.523	-.545							
6	1.750	1.250	142.575	-8.000	22.820	14.694	-.092	1
4.528	-.499							
7	1.750	1.500	139.562	-6.000	26.376	14.695	-.090	1
4.536	-.439							
8	1.750	1.750	134.757	-1.000	31.806	14.694	-.092	1
4.546	-.349							
9	1.750	2.000	132.375	8.000	36.357	14.695	-.087	1
4.552	-.300							
10	1.750	2.250	127.296	18.000	35.297	14.694	-.092	1
4.562	-.214							
11	1.750	2.500	123.417	26.000	27.562	14.694	-.092	1
4.570	-.147							
12	1.750	2.750	119.050	29.000	21.176	14.695	-.084	1
4.580	-.065							
13	1.750	3.000	121.768	24.000	11.504	14.695	-.088	1
4.574	-.115							
14	1.750	3.250	124.045	16.000	3.943	14.694	-.094	1
4.568	-.160							
15	1.750	3.500	129.513	9.000	.237	14.694	-.094	1
4.557	-.255							
16	1.750	3.750	135.102	2.000	.421	14.694	-.098	1
4.545	-.362							
17	1.750	4.000	138.314	-1.000	2.993	14.694	-.092	1
4.538	-.417							

19	1.750	4.250	141.095	-4.000	5.168	14.695	-.088	1
4.532	-.466							
19	1.750	4.500	141.603	-6.000	6.952	14.695	-.090	1
4.531	-.478							
20	1.750	4.750	141.016	-6.000	8.538	14.695	-.090	1
4.532	-.466							
21	1.750	5.000	141.857	-7.000	9.607	14.694	-.091	1
4.530	-.484							
22	1.750	5.250	141.262	-7.000	10.438	14.695	-.089	1
4.532	-.470							
23	1.750	5.500	141.679	-8.000	11.172	14.695	-.089	1
4.531	-.478							
1	2.000	.000	140.603	-8.000	18.846	14.694	-.091	1
4.533	-.460							
2	2.000	.250	141.762	-8.000	19.271	14.695	-.087	1
4.531	-.479							
3	2.000	.500	141.204	-8.000	19.868	14.694	-.092	1
4.532	-.472							
4	2.000	.750	142.729	-7.000	20.171	14.694	-.091	1
4.528	-.502							
5	2.000	1.000	142.057	-6.000	21.208	14.695	-.089	1
4.530	-.486							
6	2.000	1.250	137.202	-6.000	23.387	14.695	-.090	1
4.541	-.393							
7	2.000	1.500	135.449	-3.000	25.579	14.695	-.090	1
4.545	-.360							
8	2.000	1.750	132.664	1.000	28.438	14.694	-.092	1
4.551	-.311							
9	2.000	2.000	129.110	8.000	30.712	14.695	-.089	1
4.559	-.243							
10	2.000	2.250	125.656	14.000	29.880	14.694	-.091	1
4.566	-.184							
11	2.000	2.500	121.723	19.000	26.464	14.694	-.091	1
4.573	-.117							
12	2.000	2.750	120.114	20.000	21.600	14.695	-.088	1
4.577	-.087							
13	2.000	3.000	120.962	19.000	15.284	14.695	-.087	1
4.575	-.100							
14	2.000	3.250	124.213	12.000	8.984	14.694	-.091	1
4.568	-.159							
15	2.000	3.500	129.190	7.000	5.797	14.694	-.092	1
4.558	-.248							
16	2.000	3.750	132.360	3.000	4.641	14.695	-.091	1
4.551	-.304							
17	2.000	4.000	135.840	.000	5.429	14.694	-.092	1
4.544	-.370							
18	2.000	4.250	136.641	-2.000	6.915	14.694	-.096	1
4.541	-.389							
19	2.000	4.500	138.622	-5.000	8.039	14.695	-.090	1
4.538	-.421							
20	2.000	4.750	140.363	-6.000	9.088	14.695	-.091	1
4.534	-.455							
21	2.000	5.000	140.388	-7.000	10.113	14.694	-.093	1
4.533	-.458							
22	2.000	5.250	140.115	-7.000	10.725	14.694	-.091	1
4.534	-.450							
23	2.000	5.500	139.474	-7.000	11.784	14.695	-.088	1
4.536	-.435							
1	2.250	.000	139.150	-8.000	19.331	14.694	-.097	1
4.536	-.437							

	.250	.250	139.879	-8.000	19.482	14.694	-.094	1
4.534	-.449							
3	2.250	.500	140.493	-8.000	19.896	14.694	-.091	1
4.533	-.458							
4	2.250	.750	139.515	-7.000	20.720	14.694	-.092	1
4.535	-.439							
5	2.250	1.000	139.098	-6.000	21.430	14.694	-.092	1
4.536	-.432							
6	2.250	1.250	136.812	-5.000	22.758	14.694	-.094	1
4.541	-.390							
7	2.250	1.500	134.041	-3.000	24.479	14.694	-.093	1
4.547	-.337							
8	2.250	1.750	131.625	.000	25.857	14.694	-.094	1
4.553	-.293							
9	2.250	2.000	129.434	4.000	26.472	14.694	-.093	1
4.557	-.253							
10	2.250	2.250	125.858	8.000	26.214	14.694	-.092	1
4.565	-.189							
11	2.250	2.500	123.005	12.000	24.345	14.694	-.093	1
4.571	-.141							
12	2.250	2.750	121.787	14.000	20.795	14.694	-.093	1
4.573	-.120							
13	2.250	3.000	123.064	13.000	16.584	14.694	-.092	1
4.571	-.140							
14	2.250	3.250	126.007	10.000	12.254	14.694	-.092	1
4.565	-.192							
15	2.250	3.500	128.818	6.000	9.059	14.694	-.092	1
4.559	-.241							
16	2.250	3.750	130.406	3.000	8.319	14.694	-.094	1
4.555	-.271							
17	2.250	4.000	133.263	.000	7.898	14.694	-.094	1
4.549	-.324							
18	2.250	4.250	136.828	-2.000	8.247	14.694	-.093	1
4.541	-.390							
19	2.250	4.500	138.581	-4.000	8.893	14.694	-.092	1
4.538	-.421							
20	2.250	4.750	138.972	-5.000	9.896	14.694	-.093	1
4.536	-.430							
21	2.250	5.000	139.883	-6.000	10.476	14.694	-.093	1
4.534	-.448							
22	2.250	5.250	140.954	-7.000	11.068	14.695	-.091	1
4.532	-.466							
23	2.250	5.500	139.195	-7.000	12.018	14.695	-.091	1
4.536	-.432							
1	2.500	.000	139.106	-8.000	19.184	14.693	-.101	1
4.535	-.441							
2	2.500	.250	138.050	-7.000	19.868	14.694	-.094	1
4.539	-.413							
3	2.500	.500	139.275	-7.000	19.905	14.694	-.092	1
4.536	-.435							
4	2.500	.750	137.681	-6.000	20.869	14.694	-.091	1
4.540	-.404							
5	2.500	1.000	136.138	-5.000	21.704	14.694	-.092	1
4.543	-.375							
6	2.500	1.250	134.820	-3.000	22.396	14.694	-.095	1
4.546	-.353							
7	2.500	1.500	131.967	-2.000	23.529	14.694	-.093	1
4.552	-.299							
8	2.500	1.750	129.894	.000	24.565	14.694	-.093	1
4.556	-.261							

9	2.500	2.000	128.533	3.000	24.775	14.694	-.095	1
4.559	-.239							
10	2.500	2.250	126.605	6.000	24.010	14.694	-.094	1
4.563	-.204							
11	2.500	2.500	124.167	9.000	23.041	14.694	-.092	1
4.569	-.159							
12	2.500	2.750	124.178	10.000	20.269	14.694	-.092	1
4.568	-.159							
13	2.500	3.000	123.766	10.000	17.285	14.694	-.091	1
4.569	-.152							
14	2.500	3.250	125.674	8.000	14.250	14.694	-.094	1
4.565	-.187							
15	2.500	3.500	128.244	5.000	11.864	14.694	-.093	1
4.560	-.231							
16	2.500	3.750	130.984	2.000	10.355	14.694	-.092	1
4.554	-.280							
17	2.500	4.000	133.260	.000	9.763	14.694	-.092	1
4.549	-.322							
18	2.500	4.250	134.352	-1.000	9.967	14.694	-.095	1
4.547	-.345							
19	2.500	4.500	137.272	-3.000	9.854	14.695	-.091	1
4.541	-.395							
20	2.500	4.750	138.307	-4.000	10.717	14.694	-.095	1
4.538	-.419							
21	2.500	5.000	138.018	-5.000	11.186	14.694	-.097	1
4.538	-.416							
22	2.500	5.250	140.275	-6.000	11.427	14.694	-.092	1
4.534	-.454							
23	2.500	5.500	139.403	-6.000	12.040	14.694	-.092	1
4.536	-.437							
1	2.750	.000	136.503	-6.000	19.577	14.694	-.095	1
4.542	-.385							
2	2.750	.250	138.039	-6.000	19.644	14.694	-.093	1
4.539	-.413							
3	2.750	.500	136.966	-5.000	20.210	14.694	-.092	1
4.541	-.391							
4	2.750	.750	135.667	-5.000	21.090	14.694	-.099	1
4.543	-.374							
5	2.750	1.000	135.751	-4.000	21.306	14.694	-.096	1
4.543	-.372							
6	2.750	1.250	133.520	-2.000	22.140	14.694	-.097	1
4.548	-.331							
7	2.750	1.500	132.715	-1.000	22.617	14.694	-.094	1
4.550	-.314							
8	2.750	1.750	130.405	.000	23.326	14.694	-.097	1
4.555	-.274							
9	2.750	2.000	128.451	2.000	23.336	14.694	-.094	1
4.559	-.237							
10	2.750	2.250	126.067	5.000	23.275	14.694	-.094	1
4.564	-.195							
11	2.750	2.500	125.547	6.000	21.968	14.694	-.095	1
4.565	-.187							
12	2.750	2.750	124.766	8.000	19.978	14.694	-.095	1
4.567	-.173							
13	2.750	3.000	125.708	7.000	17.726	14.694	-.095	1
4.565	-.189							
14	2.750	3.250	127.202	6.000	15.210	14.694	-.094	1
4.562	-.214							
15	2.750	3.500	128.912	4.000	13.281	14.694	-.094	1
4.558	-.245							

16	2.750	3.750	131.082	2.000	11.912	14.694	-.096	1
4.554	-.286							
17	2.750	4.000	133.010	.000	11.213	14.694	-.098	1
4.549	-.322							
18	2.750	4.250	134.364	-2.000	11.045	14.694	-.097	1
4.546	-.346							
19	2.750	4.500	135.631	-2.000	11.369	14.694	-.097	1
4.544	-.371							
20	2.750	4.750	135.879	-4.000	11.604	14.694	-.094	1
4.543	-.372							
21	2.750	5.000	136.300	-4.000	12.006	14.694	-.097	1
4.542	-.383							
22	2.750	5.250	137.662	-5.000	12.127	14.694	-.094	1
4.539	-.406							
23	2.750	5.500	137.966	-6.000	12.482	14.694	-.096	1
4.538	-.414							
1	3.000	.000	137.666	-7.000	19.159	14.694	-.099	1
4.539	-.411							
2	3.000	.250	136.269	-6.000	19.793	14.694	-.094	1
4.543	-.380							
3	3.000	.500	136.121	-6.000	20.107	14.694	-.097	1
4.542	-.380							
4	3.000	.750	135.758	-5.000	20.499	14.694	-.097	1
4.543	-.373							
5	3.000	1.000	135.100	-3.000	20.755	14.694	-.097	1
4.545	-.360							
6	3.000	1.250	132.869	-2.000	21.721	14.694	-.097	1
4.550	-.319							
7	3.000	1.500	132.240	-1.000	21.942	14.694	-.096	1
4.551	-.307							
8	3.000	1.750	130.758	.000	22.124	14.694	-.097	1
4.554	-.281							
9	3.000	2.000	128.425	2.000	22.556	14.694	-.098	1
4.559	-.240							
10	3.000	2.250	127.872	4.000	21.826	14.694	-.097	1
4.560	-.229							
11	3.000	2.500	125.955	5.000	21.269	14.693	-.101	1
4.564	-.200							
12	3.000	2.750	126.365	5.000	19.824	14.694	-.096	1
4.564	-.202							
13	3.000	3.000	127.438	5.000	17.839	14.694	-.097	1
4.561	-.221							
14	3.000	3.250	128.762	4.000	15.775	14.694	-.097	1
4.558	-.245							
15	3.000	3.500	129.447	2.000	14.213	14.694	-.097	1
4.557	-.257							
16	3.000	3.750	131.016	1.000	13.191	14.694	-.095	1
4.554	-.283							
17	3.000	4.000	131.773	.000	12.485	14.694	-.096	1
4.552	-.298							
18	3.000	4.250	134.443	-1.000	11.912	14.694	-.094	1
4.547	-.345							
19	3.000	4.500	135.208	-3.000	12.111	14.694	-.098	1
4.544	-.364							
20	3.000	4.750	135.578	-4.000	12.020	14.694	-.095	1
4.544	-.368							
21	3.000	5.000	137.068	-5.000	12.267	14.694	-.096	1
4.540	-.397							
22	3.000	5.250	137.214	-4.000	12.644	14.694	-.097	1
4.540	-.400							
23	3.000	5.500	138.068	-6.000	12.904	14.694	-.097	1
4.538	-.416							

## APPENDIX F. RESULT 3A.DAT

						299		
1	.000	.000	102.457	-14.000	15.145	14.699	-.016	1
4.613	.018							
2	.000	.250	105.302	-15.000	14.925	14.699	-.013	1
4.609	-.034							
3	.000	.500	108.193	-16.000	14.512	14.699	-.015	1
4.604	-.092							
4	.000	.750	111.256	-16.000	14.187	14.699	-.012	1
4.598	-.152							
5	.000	1.000	112.435	-15.000	13.569	14.698	-.016	1
4.596	-.180							
6	.000	1.250	116.266	-12.000	12.188	14.696	-.044	1
4.586	-.288							
7	.000	1.500	116.796	-5.000	6.146	14.676	-.266	1
4.566	-.522							
8	.000	1.750	113.592	12.000	-2.410	14.631	-.783	1
4.526	-.970							
9	.000	2.000	105.727	15.000	-18.450	14.577	-1.436	1
4.483	-1.465							
10	.000	2.250	112.650	72.000	-10.308	14.604	-1.090	1
4.501	-1.258							
11	.000	2.500	121.443	80.000	.145	14.651	-.555	1
4.531	-.913							
12	.000	2.750	122.507	76.000	2.894	14.641	-.674	1
4.519	-1.055							
13	.000	3.000	114.758	62.000	-.907	14.573	-1.436	1
4.467	-1.649							
14	.000	3.250	115.506	29.000	-3.502	14.564	-1.543	1
4.456	-1.771							
15	.000	3.500	127.261	7.000	2.973	14.639	-.689	1
4.508	-1.179							
16	.000	3.750	124.883	-6.000	4.305	14.680	-.227	1
4.553	-.663							
17	.000	4.000	119.450	-11.000	5.371	14.692	-.095	1
4.576	-.409							
18	.000	4.250	114.584	-12.000	5.783	14.694	-.063	1
4.588	-.272							
19	.000	4.500	109.382	-13.000	7.370	14.695	-.059	1
4.598	-.161							
20	.000	4.750	104.913	-13.000	8.771	14.695	-.061	1
4.605	-.074							
21	.000	5.000	102.151	-13.000	10.026	14.695	-.060	1
4.610	-.021							
22	.000	5.250	99.973	-12.000	10.983	14.694	-.067	1
4.613	.013							
23	.000	5.500	99.244	-12.000	11.734	14.694	-.070	1
4.614	.024							
1	.250	.000	99.007	-13.000	16.599	14.689	.128	1
4.609	-.030							
2	.250	.250	102.225	-14.000	15.663	14.694	-.064	1
4.610	-.026							
3	.250	.500	105.584	-13.000	15.208	14.696	-.049	1
4.605	-.075							
4	.250	.750	109.947	-15.000	14.537	14.695	-.051	1
4.597	-.164							
5	.250	1.000	111.917	-15.000	13.818	14.696	-.046	1
4.594	-.199							

6	.250	1.250	116.050	-15.000	12.554	14.694	-.068	1
4.585	-.308							
7	.250	1.500	115.894	-18.000	8.020	14.671	-.325	1
4.562	-.562							
8	.250	1.750	111.691	6.000	4.110	14.626	-.837	1
4.525	-.985							
9	.250	2.000	106.136	38.000	-8.086	14.571	-1.462	1
4.480	-1.499							
10	.250	2.250	116.315	68.000	-4.916	14.618	-.932	1
4.508	-1.177							
11	.250	2.500	123.638	80.000	1.103	14.659	-.460	1
4.536	-.867							
12	.250	2.750	121.840	78.000	-1.236	14.644	-.632	1
4.524	-.999							
13	.250	3.000	117.905	61.000	-13.427	14.589	-1.260	1
4.476	-1.540							
14	.250	3.250	119.056	25.000	-17.151	14.583	-1.327	1
4.468	-1.632							
15	.250	3.500	122.576	3.000	-5.042	14.631	-.788	1
4.509	-1.171							
16	.250	3.750	121.202	-9.000	1.027	14.669	-.356	1
4.550	-.708							
17	.250	4.000	117.119	-12.000	4.538	14.689	-.127	1
4.577	-.390							
18	.250	4.250	111.865	-12.000	6.053	14.692	-.087	1
4.591	-.239							
19	.250	4.500	106.677	-12.000	7.574	14.693	-.077	1
4.601	-.125							
20	.250	4.750	102.973	-12.000	8.538	14.693	-.077	1
4.607	-.053							
21	.250	5.000	100.629	-11.000	9.803	14.693	-.083	1
4.611	-.015							
22	.250	5.250	99.034	-10.000	10.696	14.692	-.086	1
4.613	.011							
23	.250	5.500	98.167	-10.000	11.313	14.692	-.088	1
4.614	.025							
1	.500	.000	98.413	-13.000	16.611	14.690	-.112	1
4.612	-.004							
2	.500	.250	101.564	-14.000	16.245	14.694	-.072	1
4.610	-.022							
3	.500	.500	105.061	-14.000	15.761	14.695	-.055	1
4.606	-.071							
4	.500	.750	107.600	-15.000	15.474	14.695	-.059	1
4.601	-.125							
5	.500	1.000	112.692	-16.000	14.832	14.695	-.057	1
4.592	-.226							
6	.500	1.250	115.654	-16.000	14.043	14.693	-.083	1
4.584	-.314							
7	.500	1.500	116.735	-11.000	11.956	14.675	-.284	1
4.564	-.539							
8	.500	1.750	113.647	2.000	10.109	14.638	-.708	1
4.533	-.897							
9	.500	2.000	103.777	30.000	4.818	14.584	-1.321	1
4.496	-1.312							
10	.500	2.250	115.338	61.000	2.243	14.622	-.885	1
4.514	-1.109							
11	.500	2.500	119.358	77.000	2.778	14.663	-.418	1
4.548	-.729							
12	.500	2.750	122.453	76.000	-2.076	14.662	-.430	1
4.541	-.810							

13	.500	3.000	116.265	\$6.000	-18.045	14.608	-.1.048	1
4.498	-1.293							
14	.500	3.250	122.111	22.000	-21.903	14.619	-.923	1
4.498	-1.296							
15	.500	3.500	121.160	.000	-13.009	14.641	-.665	1
4.522	-1.016							
16	.500	3.750	120.284	-10.000	-3.352	14.677	-.255	1
4.560	-.587							
17	.500	4.000	116.651	-13.000	2.459	14.693	-.083	1
4.582	-.336							
18	.500	4.250	110.173	-12.000	5.354	14.694	-.068	1
4.595	-.186							
19	.500	4.500	105.546	-12.000	7.166	14.694	-.068	1
4.604	-.093							
20	.500	4.750	102.194	-11.000	8.362	14.694	-.067	1
4.609	-.028							
21	.500	5.000	100.392	-11.000	9.737	14.694	-.069	1
4.612	.003							
22	.500	5.250	99.530	-10.000	10.559	14.693	-.074	1
4.613	.014							
23	.500	5.500	98.634	-10.000	11.221	14.693	-.077	1
4.614	.028							
1	.750	.000	95.558	-15.000	18.163	14.693	-.076	1
4.619	.084							
2	.750	.250	98.128	-17.000	17.883	14.695	-.058	1
4.617	.056							
3	.750	.500	99.621	-17.000	18.016	14.695	-.057	1
4.614	.030							
4	.750	.750	103.641	-17.000	17.445	14.696	-.050	1
4.606	-.039							
5	.750	1.000	106.934	-18.000	17.074	14.695	-.053	1
4.603	-.106							
6	.750	1.250	109.850	-19.000	17.213	14.693	-.077	1
4.595	-.187							
7	.750	1.500	110.546	-17.000	17.596	14.682	-.207	1
4.583	-.332							
8	.750	1.750	85.529	-16.000	25.840	14.633	-.763	1
4.573	-.436							
9	.750	2.000	71.067	5.000	28.441	14.597	-1.169	1
4.556	-.634							
10	.750	2.250	80.319	37.000	14.872	14.615	-.959	1
4.563	-.553							
11	.750	2.500	97.719	63.000	7.230	14.672	-.319	1
4.594	-.198							
12	.750	2.750	100.959	63.000	-1.452	14.677	-.263	1
4.594	-.201							
13	.750	3.000	84.073	39.000	-37.227	14.622	-.882	1
4.565	-.532							
14	.750	3.250	83.792	7.000	-58.694	14.622	-.884	1
4.565	-.531							
15	.750	3.500	96.421	-5.000	-29.768	14.653	-.531	1
4.578	-.387							
16	.750	3.750	101.893	-18.000	-10.090	14.676	-.268	1
4.592	-.224							
17	.750	4.000	98.526	-18.000	.273	14.686	-.159	1
4.607	-.052							
18	.750	4.250	89.234	-21.000	4.126	14.686	-.154	1
4.622	.113							
19	.750	4.500	87.949	-20.000	7.847	14.687	-.145	1
4.624	.143							

20	.750	4.750	87.887	-18.000	9.952	14.689	-.125	1
4.626	.164							
21	.750	5.000	87.645	-18.000	11.298	14.689	-.118	1
4.627	.175							
22	.750	5.250	87.342	-16.000	12.154	14.690	-.114	1
4.628	.183							
23	.750	5.500	87.415	-16.000	12.911	14.690	-.111	1
4.628	.186							
1	1.000	.000	96.264	-13.000	18.081	14.693	-.079	1
4.618	.068							
2	1.000	.250	97.677	-14.000	18.196	14.693	-.075	1
4.616	.047							
3	1.000	.500	99.431	-15.000	18.181	14.694	-.071	1
4.613	.019							
4	1.000	.750	101.525	-16.000	18.281	14.694	-.072	1
4.610	-.021							
5	1.000	1.000	104.078	-17.000	18.567	14.694	-.072	1
4.606	-.069							
6	1.000	1.250	107.156	-18.000	19.289	14.693	-.077	1
4.600	-.134							
7	1.000	1.500	107.180	-16.000	21.635	14.688	-.131	1
4.595	-.188							
8	1.000	1.750	103.297	-8.000	23.270	14.670	-.338	1
4.584	-.321							
9	1.000	2.000	95.999	11.000	24.132	14.644	-.637	1
4.569	-.486							
10	1.000	2.250	90.685	40.000	18.752	14.636	-.730	1
4.569	-.487							
11	1.000	2.500	94.632	61.000	14.185	14.670	-.339	1
4.597	-.163							
12	1.000	2.750	98.709	62.000	4.109	14.687	-.147	1
4.608	-.044							
13	1.000	3.000	102.864	46.000	-16.235	14.673	-.302	1
4.588	-.276							
14	1.000	3.250	98.566	17.000	-32.752	14.656	-.501	1
4.577	-.396							
15	1.000	3.500	101.731	-1.000	-24.308	14.671	-.323	1
4.588	-.275							
16	1.000	3.750	104.921	-8.000	-9.762	14.686	-.162	1
4.596	-.176							
17	1.000	4.000	102.181	-10.000	-.777	14.691	-.105	1
4.606	-.067							
18	1.000	4.250	99.692	-10.000	4.004	14.692	-.093	1
4.611	-.008							
19	1.000	4.500	97.560	-10.000	6.666	14.692	-.092	1
4.615	.032							
20	1.000	4.750	96.394	-10.000	8.416	14.692	-.092	1
4.616	.052							
21	1.000	5.000	97.039	-9.000	9.728	14.691	-.098	1
4.615	.035							
22	1.000	5.250	96.773	-9.000	10.474	14.691	-.097	1
4.615	.041							
23	1.000	5.500	96.661	-9.000	11.250	14.691	-.098	1
4.616	.042							
1	1.250	.000	97.770	-12.000	17.727	14.692	-.088	1
4.615	.032							
2	1.250	.250	98.844	-12.000	17.960	14.693	-.081	1
4.614	.020							
3	1.250	.500	99.910	-11.000	18.359	14.693	-.079	1
4.612	.002							

4	1.250	.750	101.885	-12.000	18.504	14.693	-.079	1
4.609	-.034							
5	1.250	1.000	104.621	-13.000	18.724	14.693	-.077	1
4.604	-.085							
6	1.250	1.250	105.257	-13.000	20.428	14.693	-.083	1
4.603	-.103							
7	1.250	1.500	103.937	-11.000	24.025	14.691	-.101	1
4.603	-.095							
8	1.250	1.750	101.837	-6.000	27.631	14.683	-.197	1
4.598	-.152							
9	1.250	2.000	96.149	10.000	28.491	14.663	-.416	1
4.588	-.267							
10	1.250	2.250	89.410	35.000	26.651	14.656	-.497	1
4.591	-.233							
11	1.250	2.500	90.132	51.000	20.337	14.680	-.230	1
4.614	.022							
12	1.250	2.750	89.270	50.000	10.748	14.692	-.094	1
4.627	.172							
13	1.250	3.000	93.274	40.000	-6.844	14.688	-.136	1
4.617	.063							
14	1.250	3.250	96.970	20.000	-19.226	14.682	-.200	1
4.606	-.066							
15	1.250	3.500	99.719	4.000	-16.445	14.684	-.177	1
4.604	-.092							
16	1.250	3.750	100.666	-3.000	-7.599	14.689	-.122	1
4.607	-.055							
17	1.250	4.000	99.493	-6.000	-.590	14.691	-.103	1
4.611	-.015							
18	1.250	4.250	98.444	-8.000	3.859	14.691	-.098	1
4.613	.009							
19	1.250	4.500	97.239	-9.000	6.660	14.691	-.100	1
4.614	.030							
20	1.250	4.750	96.095	-9.000	8.573	14.691	-.101	1
4.616	.049							
21	1.250	5.000	96.536	-10.000	9.714	14.691	-.103	1
4.615	.039							
22	1.250	5.250	96.393	-8.000	10.427	14.691	-.105	1
4.615	.039							
23	1.250	5.500	96.164	-8.000	11.102	14.691	-.101	1
4.616	.048							
1	1.500	.000	96.080	-10.000	18.857	14.691	-.102	1
4.616	.048							
2	1.500	.250	97.668	-11.000	18.759	14.692	-.090	1
4.615	.032							
3	1.500	.500	98.462	-10.000	19.261	14.692	-.092	1
4.613	.016							
4	1.500	.750	99.912	-11.000	19.633	14.692	-.090	1
4.611	-.009							
5	1.500	1.000	99.959	-11.000	20.766	14.692	-.090	1
4.611	-.010							
6	1.500	1.250	100.299	-11.000	22.280	14.692	-.090	1
4.610	-.016							
7	1.500	1.500	98.345	-9.000	26.126	14.691	-.098	1
4.613	.011							
8	1.500	1.750	96.469	-5.000	30.741	14.688	-.131	1
4.613	.013							
9	1.500	2.000	92.707	8.000	35.146	14.681	-.217	1
4.611	-.008							
10	1.500	2.250	87.781	27.000	32.588	14.679	-.242	1
4.616	.049							

11	1.500	2.500	84.424	38.000	24.848	14.686	-.157	1
4.628	.186							
12	1.500	2.750	83.900	38.000	15.662	14.692	-.092	1
4.635	.260							
13	1.500	3.000	85.581	30.000	2.586	14.691	-.105	1
4.631	.220							
14	1.500	3.250	89.913	18.000	-7.235	14.689	-.123	1
4.624	.133							
15	1.500	3.500	93.919	6.000	-7.982	14.689	-.124	1
4.617	.064							
16	1.500	3.750	95.981	.000	-3.717	14.690	-.114	1
4.615	.038							
17	1.500	4.000	96.097	-4.000	.804	14.690	-.112	1
4.615	.038							
18	1.500	4.250	96.161	-6.000	4.285	14.690	-.113	1
4.615	.036							
19	1.500	4.500	95.900	-7.000	6.483	14.690	-.116	1
4.615	.038							
20	1.500	4.750	96.113	-7.000	7.933	14.690	-.117	1
4.615	.033							
21	1.500	5.000	95.992	-8.000	9.017	14.689	-.120	1
4.615	.032							
22	1.500	5.250	96.413	.000	9.779	14.689	-.120	1
4.614	.025							
23	1.500	5.500	96.016	-9.000	10.352	14.689	-.121	1
4.614	.030							
1	1.750	.000	94.009	-9.000	18.398	14.693	-.074	1
4.622	.113							
2	1.750	.250	94.237	-9.000	18.682	14.693	-.077	1
4.621	.105							
3	1.750	.500	94.814	-9.000	19.152	14.693	-.075	1
4.620	.097							
4	1.750	.750	94.484	-8.000	20.009	14.694	-.072	1
4.621	.106							
5	1.750	1.000	93.920	-7.000	20.890	14.694	-.072	1
4.622	.116							
6	1.750	1.250	93.212	-6.000	22.355	14.694	-.068	1
4.623	.132							
7	1.750	1.500	90.777	-4.000	24.931	14.693	-.079	1
4.626	.163							
8	1.750	1.750	88.902	-1.000	27.004	14.693	-.080	1
4.629	.192							
9	1.750	2.000	86.939	4.000	28.381	14.693	-.082	1
4.631	.222							
10	1.750	2.250	83.861	11.000	27.685	14.692	-.092	1
4.635	.260							
11	1.750	2.500	82.564	16.000	23.956	14.692	-.090	1
4.637	.283							
12	1.750	2.750	82.981	18.000	18.856	14.694	-.065	1
4.638	.301							
13	1.750	3.000	83.399	15.000	13.646	14.693	-.082	1
4.636	.278							
14	1.750	3.250	84.960	11.000	8.886	14.691	-.096	1
4.633	.239							
15	1.750	3.500	86.841	6.000	6.315	14.691	-.098	1
4.630	.208							
16	1.750	3.750	89.393	2.000	5.694	14.691	-.099	1
4.626	.165							
17	1.750	4.000	91.298	-1.000	6.332	14.691	-.098	1
4.624	.135							

18	1.750	4.250	92.271	-3.000	7.284	14.691	-.098	1
4.622	.118							
19	1.750	4.500	93.531	-5.000	8.406	14.691	-.101	1
4.620	.094							
20	1.750	.750	94.118	-6.000	9.225	14.691	-.099	1
4.619	.085							
21	1.750	5.000	93.920	-7.000	10.093	14.691	-.101	1
4.619	.087							
22	1.750	5.250	93.930	-7.000	10.640	14.691	-.104	1
4.619	.084							
23	1.750	5.500	93.847	-7.000	11.300	14.691	-.104	1
4.619	.085							
1	2.000	.000	91.870	-8.000	19.014	14.690	-.109	1
4.622	.114							
2	2.000	.250	91.914	-8.000	19.370	14.692	-.094	1
4.623	.129							
3	2.000	.500	92.790	-7.000	19.526	14.692	-.089	1
4.622	.118							
4	2.000	.750	91.851	-6.000	20.507	14.692	-.087	1
4.624	.137							
5	2.000	1.000	91.450	-5.000	21.328	14.692	-.087	1
4.624	.143							
6	2.000	1.250	89.835	-4.000	22.789	14.692	-.094	1
4.626	.163							
7	2.000	1.500	88.170	-2.000	24.131	14.691	-.097	1
4.628	.187							
8	2.000	1.750	86.432	.000	25.580	14.692	-.094	1
4.631	.219							
9	2.000	2.000	84.670	5.000	27.429	14.692	-.085	1
4.634	.255							
10	2.000	2.250	82.338	.000	25.561	14.691	-.098	1
4.636	.277							
11	2.000	2.500	81.975	12.000	23.624	14.693	-.073	1
4.639	.308							
12	2.000	2.750	83.162	14.000	19.664	14.696	-.046	1
4.640	.318							
13	2.000	3.000	83.903	12.000	15.440	14.695	-.056	1
4.638	.296							
14	2.000	3.250	84.740	9.000	12.121	14.694	-.068	1
4.636	.271							
15	2.000	3.500	87.154	1.000	9.655	14.694	-.064	1
4.633	.237							
16	2.000	3.750	88.830	2.000	8.664	14.694	-.069	1
4.630	.205							
17	2.000	4.000	90.335	.000	8.563	14.694	-.070	1
4.628	.178							
18	2.000	4.250	91.765	-2.000	9.086	14.693	-.073	1
4.625	.152							
19	2.000	4.500	92.619	-4.000	9.646	14.693	-.073	1
4.624	.137							
20	2.000	4.750	92.560	-4.000	10.355	14.694	-.072	1
4.624	.139							
21	2.000	5.000	93.276	-5.000	10.838	14.694	-.071	1
4.623	.128							
22	2.000	5.250	93.131	-6.000	11.466	14.694	-.071	1
4.623	.130							
23	2.000	5.500	93.224	-7.000	11.975	14.694	-.072	1
4.623	.128							
1	2.250	.000	92.923	-7.000	18.964	14.695	-.061	1
4.625	.144							

2	2.250	.250	92.939	-7.000	19.373	14.695	-.059	1
4.625	.146							
3	2.250	.500	92.104	-6.000	20.099	14.695	-.059	1
4.626	.160							
4	2.250	.750	91.778	-5.000	20.561	14.694	-.066	1
4.626	.159							
5	2.250	1.000	90.785	-5.000	21.612	14.694	-.064	1
4.627	.177							
6	2.250	1.250	89.973	-4.000	22.387	14.694	-.065	1
4.629	.190							
7	2.250	1.500	88.498	-2.000	23.316	14.694	-.066	1
4.631	.213							
8	2.250	1.750	87.297	1.000	23.870	14.694	-.066	1
4.632	.233							
9	2.250	2.000	85.229	3.000	24.368	14.694	-.068	1
4.635	.263							
10	2.250	2.250	83.489	6.000	24.278	14.693	-.073	1
4.637	.285							
11	2.250	2.500	82.547	9.000	22.324	14.693	-.077	1
4.638	.296							
12	2.250	2.750	83.658	10.000	19.162	14.694	-.061	1
4.638	.294							
13	2.250	3.000	83.333	9.000	16.490	14.693	-.079	1
4.637	.281							
14	2.250	3.250	84.599	7.000	13.975	14.693	-.081	1
4.635	.260							
15	2.250	3.500	86.013	4.000	11.915	14.693	-.083	1
4.633	.236							
16	2.250	3.750	87.663	2.000	10.789	14.693	-.083	1
4.630	.210							
17	2.250	4.000	88.991	.000	10.384	14.693	-.080	1
4.629	.191							
18	2.250	4.250	90.110	-2.000	10.481	14.693	-.083	1
4.627	.169							
19	2.250	4.500	91.566	-4.000	10.769	14.693	-.083	1
4.625	.145							
20	2.250	4.750	91.610	-4.000	11.171	14.692	-.086	1
4.624	.141							
21	2.250	5.000	91.555	-5.000	11.587	14.692	-.084	1
4.625	.144							
22	2.250	5.250	92.289	-6.000	12.029	14.692	-.085	1
4.623	.130							
23	2.250	5.500	91.893	-6.000	12.500	14.692	-.088	1
4.624	.134							
1	2.500	.000	91.560	-7.000	19.061	14.693	-.077	1
4.625	.152							
2	2.500	.250	92.009	-6.000	19.338	14.694	-.072	1
4.625	.148							
3	2.500	.500	91.723	-6.000	19.779	14.693	-.075	1
4.625	.150							
4	2.500	.750	91.319	-5.000	20.322	14.693	-.073	1
4.626	.159							
5	2.500	1.000	90.127	-4.000	21.200	14.693	-.076	1
4.627	.176							
6	2.500	1.250	89.567	-3.000	21.728	14.693	-.076	1
4.628	.186							
7	2.500	1.500	88.310	-2.000	22.420	14.693	-.079	1
4.630	.203							
8	2.500	1.750	86.670	.000	22.892	14.693	-.077	1
4.632	.231							

9	2.500	2.000	85.969	2.000	22.707	14.693	-.080	1
4.633	.240							
10	2.500	2.250	84.224	4.000	22.530	14.692	-.085	1
4.635	.262							
11	2.500	2.500	84.007	5.000	21.010	14.692	-.086	1
4.635	.264							
12	2.500	2.750	84.061	6.000	19.271	14.693	-.079	1
4.636	.271							
13	2.500	3.000	84.715	5.000	16.808	14.692	-.088	1
4.634	.251							
14	2.500	3.250	84.589	4.000	15.321	14.692	-.095	1
4.634	.246							
15	2.500	3.500	86.336	2.000	13.493	14.692	-.094	1
4.631	.219							
16	2.500	3.750	87.139	1.000	12.460	14.691	-.096	1
4.630	.205							
17	2.500	4.000	88.613	.000	12.040	14.692	-.095	1
4.628	.182							
18	2.500	4.250	89.726	-2.000	11.616	14.692	-.094	1
4.626	.164							
19	2.500	4.500	90.245	-3.000	11.725	14.692	-.090	1
4.626	.160							
20	2.500	4.750	90.971	-4.000	12.015	14.692	-.093	1
4.625	.145							
21	2.500	5.000	91.511	-5.000	12.219	14.692	-.094	1
4.624	.135							
22	2.500	5.250	91.362	-6.000	12.652	14.692	-.095	1
4.624	.137							
23	2.500	5.500	91.328	-6.000	12.983	14.691	-.096	1
4.624	.136							
1	2.750	.000	91.392	-7.300	19.116	14.693	-.077	1
4.625	.155							
2	2.750	.250	91.334	-6.000	19.617	14.693	-.075	1
4.626	.158							
3	2.750	.500	91.078	-6.000	19.948	14.693	-.073	1
4.626	.163							
4	2.750	.750	89.948	-4.000	20.765	14.694	-.070	1
4.628	.185							
5	2.750	1.000	90.279	-3.000	20.865	14.694	-.069	1
4.628	.181							
6	2.750	1.250	89.358	-2.000	21.300	14.694	-.071	1
4.629	.194							
7	2.750	1.500	88.115	-2.000	21.736	14.693	-.077	1
4.630	.209							
8	2.750	1.750	87.428	-1.000	21.959	14.693	-.077	1
4.631	.219							
9	2.750	2.000	86.165	1.000	21.878	14.693	-.078	1
4.633	.239							
10	2.750	2.250	85.369	4.000	21.404	14.693	-.081	1
4.634	.248							
11	2.750	2.500	85.128	5.000	20.256	14.693	-.080	1
4.634	.253							
12	2.750	2.750	85.040	5.000	18.772	14.693	-.079	1
4.634	.255							
13	2.750	3.000	85.167	3.000	17.104	14.692	-.090	1
4.633	.242							
14	2.750	3.250	85.256	2.000	15.700	14.692	-.095	1
4.633	.236							
15	2.750	3.500	86.455	2.000	14.368	14.691	-.096	1
4.631	.216							

16	2.750	3.750	87.240	.000	13.360	14.693	-.091	1
4.630	.208							
17	2.750	4.000	88.755	-1.000	12.647	14.692	-.095	1
4.628	.180							
18	2.750	4.250	88.990	-2.000	12.573	14.691	-.096	1
4.627	.175							
19	2.750	4.500	89.990	-3.000	12.328	14.692	-.094	1
4.626	.161							
20	2.750	4.750	90.463	-4.000	12.409	14.592	-.094	1
4.625	.152							
21	2.750	5.000	90.749	-5.000	12.439	14.692	-.095	1
4.625	.147							
22	2.750	5.250	91.233	-5.000	12.568	14.691	-.098	1
4.624	.136							
23	2.750	5.500	90.735	-5.000	13.073	14.691	-.101	1
4.624	.142							
1	3.000	.000	91.045	-6.000	19.015	14.693	-.078	1
4.626	.159							
2	3.000	.250	90.844	-5.000	19.513	14.694	-.071	1
4.627	.169							
3	3.000	.500	90.071	-5.000	20.110	14.693	-.077	1
4.627	.177							
4	3.000	.750	89.285	-4.000	20.535	14.693	-.075	1
4.629	.191							
5	3.000	1.000	89.378	-3.000	20.613	14.694	-.071	1
4.629	.194							
6	3.000	1.250	88.641	-2.000	20.975	14.693	-.075	1
4.630	.201							
7	3.000	1.500	87.780	-1.000	21.311	14.693	-.076	1
4.631	.215							
8	3.000	1.750	86.667	.000	21.519	14.693	-.081	1
4.632	.227							
9	3.000	2.000	86.102	1.000	21.138	14.693	-.079	1
4.633	.238							
10	3.000	2.250	85.416	3.000	20.609	14.693	-.079	1
4.634	.250							
11	3.000	2.500	85.428	2.000	19.804	14.693	-.079	1
4.634	.249							
12	3.000	2.750	85.133	3.000	18.556	14.693	-.083	1
4.634	.250							
13	3.000	3.000	85.059	2.000	17.413	14.692	-.092	1
4.633	.242							
14	3.000	3.250	85.748	1.000	16.023	14.692	-.094	1
4.632	.229							
15	3.000	3.500	85.929	1.000	15.219	14.691	-.099	1
4.631	.221							
16	3.000	3.750	87.250	.000	14.095	14.692	-.094	1
4.630	.205							
17	3.000	4.000	88.061	.000	13.537	14.692	-.093	1
4.629	.193							
18	3.000	4.250	88.435	-2.000	13.227	14.691	-.097	1
4.628	.183							
19	3.000	4.500	89.064	-2.000	13.298	14.691	-.097	1
4.627	.173							
20	3.000	4.750	88.967	-3.000	13.290	14.691	-.101	1
4.627	.171							
21	3.000	5.000	89.440	-3.000	13.249	14.691	-.099	1
4.626	.164							
22	3.000	5.250	89.756	-4.000	13.409	14.691	-.101	1
4.626	.157							
23	3.000	5.500	89.789	-4.000	13.653	14.691	-.101	1
4.626	.157							

## APPENDIX G. RESULT 0C.DAT

299									
1	.000	.000	135.701	-12.000	14.346	14.737	.063	1	
4.585	-.225								
2	.000	.250	140.986	-13.000	12.734	14.745	.128	1	
4.581	-.262								
3	.000	.500	143.144	-14.000	12.003	14.745	.132	1	
4.576	-.301								
4	.000	.750	143.325	-15.000	10.993	14.745	.132	1	
4.576	-.304								
5	.000	1.000	145.356	-17.000	9.953	14.745	.127	1	
4.570	-.351								
6	.000	1.250	143.712	-15.000	4.871	14.725	-.043	1	
4.554	-.488								
7	.000	1.500	149.850	4.000	-11.861	14.715	-.128	1	
4.529	-.699								
8	.000	1.750	153.629	15.000	-19.567	14.695	-.291	1	
4.501	-.942								
9	.000	2.000	151.278	44.000	-29.743	14.665	-.547	1	
4.476	-1.148								
10	.000	2.250	162.101	70.000	-12.751	14.694	-.307	1	
4.477	-1.145								
11	.000	2.500	167.065	77.000	2.944	14.711	-.160	1	
4.481	-1.112								
12	.000	2.750	175.726	73.000	9.831	14.699	-.258	1	
4.445	-1.418								
13	.000	3.000	172.112	55.000	16.570	14.656	-.627	1	
4.411	-1.699								
14	.000	3.250	168.349	26.000	21.499	14.657	-.615	1	
4.423	-1.597								
15	.000	3.500	168.201	8.000	21.068	14.701	-.241	1	
4.468	-1.220								
16	.000	3.750	149.545	-6.000	8.895	14.675	-.462	1	
4.491	-1.026								
17	.000	4.000	157.828	-17.000	8.079	14.731	.007	1	
4.525	-.736								
18	.000	4.250	154.562	-16.000	12.284	14.742	.107	1	
4.545	-.564								
19	.000	4.500	149.529	-14.000	12.413	14.743	.112	1	
4.558	-.452								
20	.000	4.750	148.561	-14.000	12.446	14.744	.116	1	
4.561	-.427								
21	.000	5.000	146.364	-12.000	12.679	14.743	.114	1	
4.567	-.384								
22	.000	5.250	143.843	-11.000	12.963	14.743	.111	1	
4.572	-.336								
23	.000	5.500	143.081	-11.000	13.261	14.743	.111	1	
4.574	-.321								
1	.250	.000	132.867	-12.000	15.605	14.731	.007	1	
4.585	-.228								
2	.250	.250	142.775	-13.000	13.341	14.744	.121	1	
4.576	-.305								
3	.250	.500	145.758	-15.000	12.454	14.745	.131	1	
4.570	-.355								
4	.250	.750	148.977	-16.000	11.239	14.745	.128	1	
4.562	-.424								
5	.250	1.000	150.799	-18.000	9.884	14.745	.128	1	
4.557	-.462								

6	.250	1.250	154.569	-16.000	6.363	14.734	.038	1
4.537	-.633							
7	.250	1.500	162.436	-2.000	-5.137	14.720	-.084	1
4.502	-.930							
8	.250	1.750	162.148	12.000	-16.843	14.673	-.483	1
4.456	-1.321							
9	.250	2.000	162.590	42.000	-27.952	14.622	-.911	1
4.404	-1.760							
10	.250	2.250	164.872	74.000	-13.870	14.667	-.533	1
4.443	-1.435							
11	.250	2.500	173.461	82.000	.397	14.706	-.201	1
4.458	-1.306							
12	.250	2.750	175.977	76.000	2.980	14.688	-.355	1
4.432	-1.521							
13	.250	3.000	149.982	60.000	2.154	14.594	-1.149	1
4.409	-1.722							
14	.250	3.250	168.175	19.000	7.057	14.611	-1.011	1
4.377	-1.989							
15	.250	3.500	175.525	3.000	10.704	14.681	-.410	1
4.427	-1.565							
16	.250	3.750	167.877	-10.000	6.064	14.709	-.172	1
4.477	-1.143							
17	.250	4.000	159.261	-17.000	9.054	14.732	.023	1
4.523	-.751							
18	.250	4.250	154.163	-16.000	11.100	14.742	.106	1
4.546	-.556							
19	.250	4.500	148.675	-15.000	11.766	14.744	.118	1
4.561	-.428							
20	.250	4.750	146.031	-14.000	12.087	14.744	.118	1
4.568	-.373							
21	.250	5.000	145.914	-12.000	12.199	14.744	.121	1
4.568	-.368							
22	.250	5.250	143.882	-11.000	12.613	14.744	.118	1
4.573	-.330							
23	.250	5.500	142.481	-10.000	12.946	14.744	.118	1
4.576	-.302							
1	.500	.000	139.198	-12.000	14.892	14.742	.103	1
4.582	-.252							
2	.500	.250	142.098	-13.000	13.863	14.743	.115	1
4.577	-.297							
3	.500	.500	145.454	-14.000	13.243	14.744	.119	1
4.569	-.361							
4	.500	.750	151.754	-16.000	12.043	14.744	.120	1
4.554	-.491							
5	.500	1.000	156.454	-18.000	10.963	14.744	.117	1
4.542	-.595							
6	.500	1.250	160.952	-18.000	7.847	14.738	.072	1
4.524	-.740							
7	.500	1.500	168.533	-9.000	1.301	14.718	-.098	1
4.484	-1.085							
8	.500	1.750	163.098	5.000	-3.847	14.667	-.534	1
4.447	-1.395							
9	.500	2.000	143.480	35.000	-26.721	14.566	-1.387	1
4.396	-1.826							
10	.500	2.250	171.707	72.000	-4.380	14.669	-.513	1
4.426	-1.575							
11	.500	2.500	182.794	80.000	1.619	14.723	-.060	1
4.447	-1.397							
12	.500	2.750	183.419	78.000	-2.722	14.706	-.198	1
4.429	-1.551							

13	.500	3.000	167.126	60.000	-15.922	14.607	-1.045	1
4.376	-1.998							
14	.500	3.250	172.456	17.000	-16.400	14.611	-1.011	1
4.365	-2.091							
15	.500	3.500	176.695	-2.000	-.589	14.678	-.442	1
4.420	-1.626							
16	.500	3.750	173.935	-7.000	3.007	14.725	-.044	1
4.475	-1.160							
17	.500	4.000	161.446	-16.000	7.520	14.737	.059	1
4.522	-.764							
18	.500	4.250	155.708	-15.000	9.528	14.744	.120	1
4.544	-.576							
19	.500	4.500	146.914	-13.000	10.912	14.742	.101	1
4.564	-.408							
20	.500	4.750	143.760	-12.000	11.546	14.743	.109	1
4.572	-.336							
21	.500	5.000	144.642	-11.000	11.070	14.743	.115	1
4.571	-.349							
22	.500	5.250	145.209	-11.000	12.019	14.743	.112	1
4.569	-.363							
23	.500	5.500	142.775	-10.000	12.499	14.743	.113	1
4.575	-.313							
1	.750	.000	140.591	-11.000	14.871	14.743	.109	1
4.580	-.273							
2	.750	.250	143.323	-12.000	14.649	14.743	.111	1
4.573	-.326							
3	.750	.500	145.531	-14.000	14.119	14.743	.112	1
4.568	-.370							
4	.750	.750	150.600	-16.000	13.515	14.743	.108	1
4.555	-.478							
5	.750	1.000	157.465	-19.000	12.714	14.743	.108	1
4.538	-.626							
6	.750	1.250	163.323	-19.000	11.520	14.738	.069	1
4.518	-.796							
7	.750	1.500	169.848	-12.000	6.396	14.722	-.064	1
4.484	-1.082							
8	.750	1.750	167.730	.000	8.944	14.685	-.381	1
4.453	-1.349							
9	.750	2.000	144.568	25.000	4.923	14.592	-1.167	1
4.420	-1.628							
10	.750	2.250	175.792	61.000	7.052	14.680	-.425	1
4.425	-1.586							
11	.750	2.500	177.358	78.000	5.303	14.719	-.094	1
4.459	-1.294							
12	.750	2.750	180.378	76.000	-1.937	14.719	-.095	1
4.450	-1.371							
13	.750	3.000	182.138	56.000	-19.087	14.672	-.487	1
4.399	-1.807							
14	.750	3.250	178.197	16.000	-27.991	14.668	-.527	1
4.406	-1.748							
15	.750	3.500	183.748	-3.000	-9.988	14.713	-.148	1
4.434	-1.509							
16	.750	3.750	170.629	-7.000	-1.229	14.730	-.002	1
4.489	-1.039							
17	.750	4.000	160.593	-15.000	4.599	14.741	.092	1
4.528	-.711							
18	.750	4.250	151.566	-14.000	7.923	14.742	.101	1
4.552	-.506							
19	.750	4.500	144.754	-13.000	9.982	14.742	.102	1
4.569	-.363							

20	.750	4.750	142.311	-12.000	11.115	14.742	.104	1
4.575	-.312							
21	.750	5.000	142.236	-11.000	11.374	14.742	.102	1
4.575	-.313							
22	.750	5.250	141.997	-10.000	11.797	14.742	.104	1
4.576	-.306							
23	.750	5.500	140.999	-9.000	12.268	14.742	.105	1
4.578	-.286							
1	1.000	.000	139.824	-12.000	15.877	14.741	.094	1
4.580	-.274							
2	1.000	.250	141.010	-13.000	15.974	14.742	.102	1
4.578	-.288							
3	1.000	.500	145.331	-15.000	15.286	14.742	.104	1
4.568	-.373							
4	1.000	.750	149.707	-16.000	15.314	14.742	.103	1
4.557	-.465							
5	1.000	1.000	155.589	-17.000	14.970	14.742	.103	1
4.542	-.590							
6	1.000	1.250	162.647	-19.000	14.998	14.741	.091	1
4.522	-.759							
7	1.000	1.500	167.301	-15.000	14.658	14.725	-.043	1
4.494	-.1000							
8	1.000	1.750	167.898	-14.000	16.258	14.706	-.203	1
4.473	-.1175							
9	1.000	2.000	160.472	20.000	19.773	14.680	-.425	1
4.467	-.1226							
10	1.000	2.250	165.125	50.000	14.600	14.694	-.302	1
4.469	-.1209							
11	1.000	2.500	166.154	72.000	8.456	14.729	-.009	1
4.501	-.940							
12	1.000	2.750	167.262	72.000	1.246	14.733	.029	1
4.502	-.927							
13	1.000	3.000	164.428	51.000	-19.543	14.696	-.283	1
4.473	-.1174							
14	1.000	3.250	164.282	20.000	-25.503	14.693	-.316	1
4.470	-.1204							
15	1.000	3.500	168.203	-3.000	-15.672	14.715	-.123	1
4.482	-.1102							
16	1.000	3.750	162.036	-12.000	-5.622	14.735	.046	1
4.519	-.791							
17	1.000	4.000	154.477	-14.000	2.555	14.741	.095	1
4.544	-.574							
18	1.000	4.250	148.954	-13.000	6.621	14.743	.114	1
4.560	-.438							
19	1.000	4.500	144.130	-12.000	8.945	14.744	.119	1
4.572	-.334							
20	1.000	4.750	141.491	-11.000	10.368	14.744	.119	1
4.579	-.281							
21	1.000	5.000	141.625	-10.000	11.289	14.744	.118	1
4.578	-.285							
22	1.000	5.250	139.809	-9.000	11.967	14.743	.115	1
4.582	-.254							
23	1.000	5.500	141.326	-9.000	12.335	14.744	.119	1
4.579	-.278							
1	1.250	.000	130.251	-16.000	18.744	14.740	.087	1
4.600	-.099							
2	1.250	.250	132.031	-17.000	18.427	14.743	.109	1
4.599	-.110							
3	1.250	.500	133.449	-18.000	19.196	14.743	.113	1
4.596	-.132							

4	1.250	.750	135.252	-20.000	19.980	14.742	.107	1
4.592	-.172							
5	1.250	1.000	137.600	-23.000	20.789	14.742	.104	1
4.586	-.220							
6	1.250	1.250	138.908	-25.000	22.934	14.739	.079	1
4.580	-.271							
7	1.250	1.500	139.116	-26.000	26.961	14.730	.003	1
4.571	-.350							
8	1.250	1.750	131.898	-17.000	31.812	14.705	-.210	1
4.562	-.426							
9	1.250	2.000	127.652	2.000	38.120	14.692	-.321	1
4.557	-.461							
10	1.250	2.250	117.633	29.000	31.219	14.685	-.378	1
4.571	-.346							
11	1.250	2.500	129.667	56.000	20.458	14.723	-.059	1
4.584	-.235							
12	1.250	2.750	134.967	58.000	6.096	14.738	.074	1
4.588	-.200							
13	1.250	3.000	133.208	43.000	-18.586	14.715	-.127	1
4.568	-.368							
14	1.250	3.250	130.398	8.000	-39.174	14.699	-.264	1
4.558	-.454							
15	1.250	3.500	139.705	-8.000	-26.762	14.728	-.018	1
4.567	-.383							
16	1.250	3.750	141.158	-12.000	-10.015	14.737	.061	1
4.573	-.333							
17	1.250	4.000	138.039	-14.000	.859	14.742	.106	1
4.585	-.226							
18	1.250	4.250	.135.955	-13.000	6.206	14.743	.110	1
4.590	-.183							
19	1.250	4.500	133.573	-13.000	8.855	14.743	.111	1
4.596	-.137							
20	1.250	4.750	133.391	-13.000	10.640	14.743	.113	1
4.596	-.132							
21	1.250	5.000	133.472	-13.000	11.799	14.743	.115	1
4.596	-.131							
22	1.250	5.250	132.834	-12.000	12.232	14.743	.113	1
4.597	-.122							
23	1.250	5.500	132.974	-12.000	12.880	14.743	.115	1
4.597	-.122							
1	1.500	.000	134.633	-10.000	18.295	14.735	.042	1
4.585	-.226							
2	1.500	.250	139.641	-11.000	17.475	14.742	.107	1
4.582	-.257							
3	1.500	.500	142.828	-12.000	17.458	14.743	.112	1
4.575	-.315							
4	1.500	.750	144.611	-13.000	18.004	14.743	.113	1
4.571	-.350							
5	1.500	1.000	148.444	-14.000	18.541	14.744	.116	1
4.562	-.425							
6	1.500	1.250	153.197	-15.000	20.159	14.743	.113	1
4.549	-.528							
7	1.500	1.500	152.768	-13.000	24.145	14.742	.103	1
4.549	-.529							
8	1.500	1.750	149.813	-7.000	29.800	14.735	.045	1
4.550	-.525							
9	1.500	2.000	140.858	10.000	33.559	14.717	-.108	1
4.553	-.496							
10	1.500	2.250	132.801	35.000	30.724	14.712	-.154	1
4.566	-.388							

11	1.500	2.500	128.548	53.000	25.001	14.733	.024	1
4.596	-.132							
12	1.500	2.750	125.862	51.000	13.554	14.742	.100	1
4.611	-.008							
13	1.500	3.000	130.583	41.000	-5.156	14.740	.089	1
4.600	-.104							
14	1.500	3.250	137.768	21.000	-20.669	14.732	.022	1
4.576	-.306							
15	1.500	3.500	141.283	3.000	-17.513	14.736	.055	1
4.572	-.341							
16	1.500	3.750	143.024	-5.000	-7.419	14.741	.099	1
4.573	-.332							
17	1.500	4.000	141.164	-8.000	.351	14.743	.114	1
4.579	-.280							
18	1.500	4.250	139.051	-9.000	4.993	14.743	.114	1
4.584	-.239							
19	1.500	4.500	138.066	-8.000	7.706	14.743	.114	1
4.586	-.220							
20	1.500	4.750	138.196	-9.000	9.576	14.743	.116	1
4.586	-.220							
21	1.500	5.000	139.079	-8.000	11.097	14.745	.132	1
4.586	-.221							
22	1.500	5.250	139.367	-9.000	11.635	14.743	.115	1
4.583	-.243							
23	1.500	5.500	139.201	-8.000	11.915	14.743	.114	1
4.583	-.242							
1	1.750	.000	136.003	-10.000	18.036	14.741	.095	1
4.588	-.199							
2	1.750	.250	138.038	-10.000	18.130	14.743	.111	1
4.586	-.222							
3	1.750	.500	140.745	-11.000	18.312	14.743	.112	1
4.580	-.274							
4	1.750	.750	141.745	-11.000	18.896	14.743	.116	1
4.578	-.290							
5	1.750	1.000	142.073	-11.000	20.125	14.743	.113	1
4.577	-.299							
6	1.750	1.250	144.335	-12.000	22.251	14.743	.112	1
4.571	-.345							
7	1.750	1.500	142.761	-10.000	26.418	14.743	.108	1
4.574	-.318							
8	1.750	1.750	138.788	-6.000	33.601	14.742	.102	1
4.583	-.245							
9	1.750	2.000	135.251	7.000	39.858	14.737	.063	1
4.586	-.217							
10	1.750	2.250	126.872	28.000	38.345	14.735	.048	1
4.603	-.078							
11	1.750	2.500	119.810	38.000	28.628	14.741	.095	1
4.623	.091							
12	1.750	2.750	114.731	38.000	19.354	14.743	.113	1
4.634	.192							
13	1.750	3.000	118.630	30.000	5.704	14.743	.111	1
4.627	.127							
14	1.750	3.250	124.230	19.000	-5.190	14.742	.102	1
4.615	.023							
15	1.750	3.500	131.934	6.000	-7.685	14.742	.104	1
4.598	-.114							
16	1.750	3.750	134.980	-1.000	-3.566	14.743	.110	1
4.592	-.164							
17	1.750	4.000	135.951	-4.000	1.752	14.744	.117	1
4.591	-.175							

18	1.750	4.250	136.167	-6.000	5.624	14.743	.113	1
4.590	-.184							
19	1.750	4.500	137.488	-7.000	7.878	14.743	.115	1
4.587	-.207							
20	1.750	4.750	138.808	-7.000	9.622	14.743	.113	1
4.589	-.196							
21	1.750	5.000	138.312	-8.000	10.576	14.743	.113	1
4.585	-.225							
22	1.750	5.250	138.281	-8.000	11.512	14.743	.115	1
4.586	-.222							
23	1.750	5.500	137.170	-8.000	12.306	14.743	.113	1
4.588	-.203							
1	2.000	.000	135.553	-9.000	17.879	14.742	.105	1
4.591	-.180							
2	2.000	.250	135.580	-8.000	18.774	14.743	.113	1
4.591	-.173							
3	2.000	.500	137.043	-9.000	19.083	14.743	.111	1
4.588	-.203							
4	2.000	.750	136.293	-8.000	20.233	14.743	.113	1
4.590	-.186							
5	2.000	1.000	137.823	-9.000	20.977	14.743	.109	1
4.586	-.220							
6	2.000	1.250	135.653	-8.000	23.599	14.743	.111	1
4.591	-.177							
7	2.000	1.500	134.506	-6.000	27.254	14.743	.111	1
4.594	-.154							
8	2.000	1.750	130.342	.000	32.902	14.743	.111	1
4.603	-.077							
9	2.000	2.000	127.358	8.000	37.165	14.743	.112	1
4.609	-.022							
10	2.000	2.250	121.656	19.000	35.322	14.743	.109	1
4.621	.074							
11	2.000	2.500	117.405	27.000	28.040	14.742	.106	1
4.629	.142							
12	2.000	2.750	115.629	28.000	20.396	14.743	.112	1
4.633	.176							
13	2.000	3.000	116.073	14.000	11.884	14.743	.109	1
4.632	.167							
14	2.000	3.250	119.315	17.000	3.472	14.743	.108	1
4.625	.112							
15	2.000	3.500	124.807	8.000	.529	14.743	.108	1
4.614	.018							
16	2.000	3.750	131.573	1.000	1.534	14.743	.108	1
4.600	-.102							
17	2.000	4.000	132.475	-2.000	4.119	14.743	.110	1
4.598	-.117							
18	2.000	4.250	134.709	-4.000	6.642	14.743	.108	1
4.593	-.161							
19	2.000	4.500	136.228	-5.000	8.425	14.742	.107	1
4.589	-.191							
20	2.000	4.750	136.170	-6.000	9.841	14.743	.111	1
4.590	-.186							
21	2.000	5.000	138.069	-7.000	10.800	14.743	.109	1
4.585	-.224							
22	2.000	5.250	137.440	-7.000	11.649	14.743	.113	1
4.587	-.208							
23	2.000	5.500	136.740	-7.000	12.133	14.743	.110	1
4.589	-.198							
1	2.250	.000	135.362	-8.000	18.392	14.742	.107	1
4.591	-.175							

2	2.250	.250	136.262	-8.000	18.740	14.742	.106	1
4.589	-.193							
3	2.250	.500	135.637	-7.000	19.325	14.742	.105	1
4.590	-.182							
4	2.250	.750	135.107	-6.000	20.334	14.743	.109	1
4.592	-.167							
5	2.250	1.000	134.338	-6.000	21.686	14.742	.106	1
4.593	-.156							
6	2.250	1.250	132.534	-6.000	23.747	14.742	.106	1
4.597	-.122							
7	2.250	1.500	131.471	-4.000	26.193	14.742	.106	1
4.600	-.103							
8	2.250	1.750	128.279	-2.000	29.454	14.742	.107	1
4.607	-.044							
9	2.250	2.000	124.259	7.000	30.897	14.742	.105	1
4.615	.025							
10	2.250	2.250	120.398	13.000	30.254	14.742	.105	1
4.623	.091							
11	2.250	2.500	117.111	18.000	25.819	14.742	.106	1
4.629	.147							
12	2.250	2.750	115.876	18.000	21.013	14.742	.107	1
4.632	.168							
13	2.250	3.000	115.611	18.000	15.443	14.742	.105	1
4.632	.170							
14	2.250	3.250	120.879	12.000	9.187	14.742	.107	1
4.622	.085							
15	2.250	3.500	123.448	8.000	6.053	14.742	.104	1
4.616	.038							
16	2.250	3.750	127.522	3.000	5.719	14.742	.106	1
4.608	-.031							
17	2.250	4.000	131.820	.000	6.437	14.743	.108	1
4.599	-.107							
18	2.250	4.250	132.895	-3.000	7.990	14.742	.106	1
4.597	-.129							
19	2.250	4.500	134.755	-4.000	9.152	14.742	.106	1
4.593	-.164							
20	2.250	4.750	135.773	-6.000	10.432	14.743	.108	1
4.590	-.181							
21	2.250	5.000	135.463	-6.000	11.203	14.743	.108	1
4.591	-.175							
22	2.250	5.250	136.525	-7.000	12.045	14.743	.108	1
4.589	-.195							
23	2.250	5.500	136.245	-7.000	12.418	14.743	.109	1
4.590	-.189							
1	2.500	.000	133.212	-7.000	18.899	14.742	.107	1
4.596	-.134							
2	2.500	.250	134.589	-7.000	19.150	14.743	.114	1
4.594	-.153							
3	2.500	.500	135.737	-8.000	19.506	14.744	.118	1
4.592	-.171							
4	2.500	.750	134.186	-7.000	20.348	14.743	.116	1
4.595	-.144							
5	2.500	1.000	132.180	-6.000	21.764	14.743	.112	1
4.599	-.110							
6	2.500	1.250	130.867	-6.000	23.229	14.743	.112	1
4.602	-.086							
7	2.500	1.500	129.322	-3.000	24.708	14.743	.113	1
4.605	-.057							
8	2.500	1.750	128.325	.000	26.047	14.743	.112	1
4.607	-.040							

9	2.500	2.000	124.946	3.000	26.810	14.743	.115	1
4.615	.023							
10	2.500	2.250	121.848	0.000	26.057	14.743	.115	1
4.621	.077							
11	2.500	2.500	118.980	12.000	23.961	14.743	.115	1
4.627	.125							
12	2.500	2.750	118.270	13.000	20.871	14.744	.116	1
4.628	.138							
13	2.500	3.000	119.701	12.000	16.567	14.744	.116	1
4.625	.114							
14	2.500	3.250	121.593	10.000	12.813	14.743	.113	1
4.621	.079							
15	2.500	3.500	124.659	5.000	10.150	14.743	.114	1
4.615	.027							
16	2.500	3.750	126.673	2.000	8.682	14.743	.115	1
4.611	-.007							
17	2.500	4.000	130.092	-1.000	8.662	14.744	.116	1
4.604	-.067							
18	2.500	4.250	132.067	-3.000	9.495	14.743	.116	1
4.600	-.104							
19	2.500	4.500	133.770	-4.000	10.173	14.743	.116	1
4.596	-.136							
20	2.500	4.750	134.656	-5.000	10.938	14.743	.113	1
4.594	-.155							
21	2.500	5.000	134.945	-6.000	11.654	14.743	.112	1
4.593	-.162							
22	2.500	5.250	135.749	-7.000	12.251	14.743	.113	1
4.591	-.176							
23	2.500	5.500	135.960	-7.000	12.703	14.743	.114	1
4.591	-.179							
1	2.750	.000	134.168	-8.000	18.668	14.743	.108	1
4.594	-.151							
2	2.750	.250	135.286	-8.000	18.770	14.743	.111	1
4.592	-.169							
3	2.750	.500	133.362	-7.000	19.800	14.743	.112	1
4.596	-.132							
4	2.750	.750	133.330	-7.000	20.206	14.743	.112	1
4.596	-.131							
5	2.750	1.000	132.317	-6.000	21.125	14.743	.113	1
4.599	-.111							
6	2.750	1.250	128.822	-4.000	22.820	14.743	.113	1
4.606	-.048							
7	2.750	1.500	127.548	-2.000	23.608	14.743	.112	1
4.609	-.026							
8	2.750	1.750	126.496	.000	24.278	14.743	.111	1
4.611	-.008							
9	2.750	2.000	124.958	3.000	24.495	14.743	.114	1
4.614	.022							
10	2.750	2.250	121.745	7.000	24.064	14.743	.111	1
4.621	.074							
11	2.750	2.500	120.189	10.000	22.501	14.743	.114	1
4.624	.103							
12	2.750	2.750	119.673	10.000	20.362	14.743	.112	1
4.625	.110							
13	2.750	3.000	120.237	9.000	17.457	14.743	.114	1
4.624	.103							
14	2.750	3.250	122.532	7.000	14.598	14.743	.112	1
4.619	.062							
15	2.750	3.500	124.683	4.000	12.629	14.743	.109	1
4.614	.022							

16	2.750	3.750	127.432	1.000	11.250	14.743	.111	1
4.609	-.025							
17	2.750	4.000	129.310	-1.000	10.685	14.743	.111	1
4.605	-.059							
18	2.750	4.250	130.544	-2.000	10.684	14.743	.109	1
4.602	-.082							
19	2.750	4.500	132.113	-3.000	11.232	14.743	.112	1
4.599	-.109							
20	2.750	4.750	134.199	-4.000	11.598	14.743	.111	1
4.594	-.149							
21	2.750	5.000	134.250	-5.000	12.084	14.743	.111	1
4.594	-.150							
22	2.750	5.250	134.819	-6.000	12.688	14.743	.109	1
4.593	-.162							
23	2.750	5.500	135.451	-6.000	12.928	14.743	.113	1
4.592	-.171							
1	3.000	.000	133.856	-6.000	18.782	14.743	.114	1
4.595	-.140							
2	3.000	.250	131.943	-5.000	19.493	14.743	.111	1
4.599	-.107							
3	3.000	.500	132.324	-5.000	19.619	14.743	.111	1
4.598	-.114							
4	3.000	.750	132.137	-6.000	20.044	14.743	.109	1
4.599	-.112							
5	3.000	1.000	130.158	-4.000	21.078	14.743	.110	1
4.603	-.075							
6	3.000	1.250	128.937	-3.000	21.836	14.742	.107	1
4.605	-.055							
7	3.000	1.500	126.693	-1.000	22.696	14.743	.113	1
4.611	-.010							
8	3.000	1.750	125.627	1.000	23.022	14.743	.111	1
4.613	.007							
9	3.000	2.000	123.270	3.000	23.437	14.743	.108	1
4.617	.046							
10	3.000	2.250	121.979	5.000	22.902	14.743	.109	1
4.620	.069							
11	3.000	2.500	120.487	7.000	21.763	14.743	.111	1
4.623	.095							
12	3.000	2.750	120.773	8.000	19.838	14.743	.111	1
4.623	.091							
13	3.000	3.000	122.215	6.000	17.752	14.743	.112	1
4.620	.067							
14	3.000	3.250	124.387	4.000	15.308	14.743	.113	1
4.615	.030							
15	3.000	3.500	125.427	2.000	13.911	14.743	.114	1
4.613	.014							
16	3.000	3.750	127.281	1.000	12.724	14.743	.113	1
4.609	-.020							
17	3.000	4.000	128.661	.000	12.058	14.743	.109	1
4.606	-.048							
18	3.000	4.250	130.582	-2.000	11.948	14.743	.111	1
4.602	-.082							
19	3.000	4.500	132.377	-3.000	12.096	14.743	.110	1
4.598	-.116							
20	3.000	4.750	132.726	-4.000	12.532	14.743	.111	1
4.598	-.121							
21	3.000	5.000	133.751	-5.000	12.591	14.743	.112	1
4.595	-.139							
22	3.000	5.250	133.585	-5.000	13.246	14.743	.108	1
4.595	-.140							
23	3.000	5.500	133.965	-6.000	13.427	14.743	.110	1
4.595	-.145							

## APPENDIX H. RESULT 3C.DAT

299									
1	.000	.000	96.737	-11.000	13.372	14.690	.172	1	
4.614	.303								
2	.000	.250	97.806	-12.000	12.936	14.690	.168	1	
4.612	.279								
3	.000	.500	99.054	-13.000	12.116	14.690	.170	1	
4.610	.259								
4	.000	.750	99.880	-14.000	11.094	14.690	.169	1	
4.609	.243								
5	.000	1.000	100.846	-16.000	10.170	14.690	.169	1	
4.607	.225								
6	.000	1.250	100.238	-15.000	8.460	14.681	.065	1	
4.599	.133								
7	.000	1.500	98.974	-3.000	-4.648	14.653	-.250	1	
4.573	-.160								
8	.000	1.750	98.912	15.000	-13.092	14.633	-.478	1	
4.553	-.386								
9	.000	2.000	94.907	37.000	-22.132	14.602	-.837	1	
4.528	-.673								
10	.000	2.250	99.870	65.000	-13.838	14.619	-.639	1	
4.538	-.565								
11	.000	2.500	104.963	73.000	2.199	14.640	-.403	1	
4.550	-.426								
12	.000	2.750	108.612	71.000	10.560	14.636	-.452	1	
4.539	-.547								
13	.000	3.000	103.958	59.000	15.672	14.602	-.837	1	
4.513	-.840								
14	.000	3.250	102.772	30.000	19.279	14.595	-.907	1	
4.509	-.888								
15	.000	3.500	103.466	11.000	21.003	14.625	-.567	1	
4.538	-.561								
16	.000	3.750	101.685	-4.000	12.623	14.635	-.457	1	
4.551	-.417								
17	.000	4.000	107.602	-15.000	10.328	14.676	.011	1	
4.582	-.064								
18	.000	4.250	104.468	-16.000	13.372	14.683	.083	1	
4.593	.070								
19	.000	4.500	103.733	-14.000	12.835	14.688	.143	1	
4.600	.144								
20	.000	4.750	101.574	-13.000	12.751	14.687	.138	1	
4.603	.180								
21	.000	5.000	99.819	-12.000	12.832	14.687	.135	1	
4.606	.210								
22	.000	5.250	98.659	-11.000	12.899	14.687	.130	1	
4.607	.226								
23	.000	5.500	96.949	-10.000	13.331	14.686	.125	1	
4.609	.252								
1	.250	.000	96.502	-11.000	14.210	14.688	.148	1	
4.612	.284								
2	.250	.250	98.184	-13.000	13.427	14.689	.157	1	
4.610	.261								
3	.250	.500	99.601	-14.000	12.825	14.690	.161	1	
4.608	.240								
4	.250	.750	102.050	-16.000	11.671	14.690	.168	1	
4.605	.201								
5	.250	1.000	103.829	-17.000	10.458	14.689	.161	1	
4.601	.160								

6	.250	1.250	104.395	-17.000	8.573	14.682	.074	1
4.593	.063							
7	.250	1.500	103.435	-7.000	-.823	14.653	-.249	1
4.566	-.242							
8	.250	1.750	103.086	-1.000	-7.788	14.624	-.587	1
4.537	-.574							
9	.250	2.000	94.559	39.000	-22.304	14.579	-1.093	1
4.506	-.923							
10	.250	2.250	100.821	68.000	-13.193	14.601	-.842	1
4.518	-.786							
11	.250	2.500	110.243	77.000	.516	14.640	-.396	1
4.541	-.524							
12	.250	2.750	113.049	74.000	5.440	14.633	-.475	1
4.529	-.662							
13	.250	3.000	101.824	61.000	3.994	14.575	-1.139	1
4.490	-.102							
14	.250	3.250	101.485	26.000	4.513	14.558	-.1329	1
4.474	-.1285							
15	.250	3.500	106.355	6.000	11.286	14.606	-.792	1
4.513	-.843							
16	.250	3.750	107.919	-9.000	8.127	14.639	-.408	1
4.544	-.490							
17	.250	4.000	106.988	-17.000	10.581	14.673	-.023	1
4.580	-.086							
18	.250	4.250	104.264	-18.000	12.185	14.685	-.110	1
4.596	.101							
19	.250	4.500	102.121	-16.000	12.377	14.687	.138	1
4.602	.170							
20	.250	4.750	101.333	-14.000	12.111	14.688	.141	1
4.604	.188							
21	.250	5.000	99.732	-12.000	12.258	14.687	.137	1
4.606	.214							
22	.250	5.250	97.907	-11.000	12.518	14.687	.132	1
4.609	.242							
23	.250	5.500	96.575	-10.000	12.897	14.687	.132	1
4.611	.266							
1	.500	.000	91.565	-11.000	16.192	14.674	-.010	1
4.606	.211							
2	.500	.250	97.493	-12.000	14.454	14.686	.126	1
4.609	.244							
3	.500	.500	100.384	-14.000	13.25	14.688	.147	1
4.606	.211							
4	.500	.750	103.031	-16.000	12.529	14.688	.148	1
4.602	.163							
5	.500	1.000	105.289	-18.000	11.701	14.688	.147	1
4.598	.118							
6	.500	1.250	107.485	-18.000	10.302	14.683	.083	1
4.588	.010							
7	.500	1.500	108.919	-10.000	4.025	14.661	-.164	1
4.564	-.266							
8	.500	1.750	99.871	5.000	-1.323	14.612	-.719	1
4.531	-.645							
9	.500	2.000	92.828	33.000	-15.353	14.558	-1.331	1
4.488	-.1.131							
10	.500	2.250	105.376	77.000	-8.410	14.605	-.804	1
4.514	-.835							
11	.500	2.500	114.442	78.000	1.004	14.651	-.277	1
4.544	-.493							
12	.500	2.750	115.768	75.000	.447	14.642	-.375	1
4.533	-.619							

13	.500	3.000	106.614	61.000	-8.569	14.579	-1.088	1
4.487	-1.144							
14	.500	3.250	105.033	23.000	-14.855	14.559	-1.317	1
4.469	-1.341							
15	.500	3.500	110.667	1.000	-1.026	14.609	-.753	1
4.509	-.890							
16	.500	3.750	111.552	-12.000	3.680	14.649	-.302	1
4.547	-.458							
17	.500	4.000	107.804	-18.000	8.075	14.672	-.038	1
4.577	-.117							
18	.500	4.250	105.384	-18.000	10.495	14.685	.110	1
4.594	.079							
19	.500	4.500	100.400	-16.000	11.451	14.687	.130	1
4.604	.194							
20	.500	4.750	99.509	-14.000	11.722	14.687	.127	1
4.606	.207							
21	.500	5.000	98.404	-12.000	11.801	14.686	.124	1
4.607	.225							
22	.500	5.250	97.393	-11.000	12.154	14.686	.121	1
4.608	.241							
23	.500	5.500	96.005	-10.000	12.782	14.686	.118	1
4.610	.262							
1	.750	.000	97.198	-12.000	15.176	14.688	.145	1
4.611	.268							
2	.750	.250	98.757	-13.000	14.856	14.689	.151	1
4.609	.245							
3	.750	.500	100.395	-14.000	14.467	14.689	.154	1
4.607	.219							
4	.750	.750	103.847	-15.000	13.774	14.689	.156	1
4.601	.185							
5	.750	1.000	106.623	-16.000	13.358	14.689	.151	1
4.596	.095							
6	.750	1.250	109.165	-19.000	12.820	14.683	.082	1
4.585	-.024							
7	.750	1.500	109.984	-12.000	9.363	14.663	-.142	1
4.564	-.265							
8	.750	1.750	106.534	.000	7.824	14.630	-.512	1
4.537	-.566							
9	.750	2.000	97.337	26.000	1.073	14.581	-1.075	1
4.503	-.954							
10	.750	2.250	103.220	61.000	.406	14.603	-.817	1
4.516	-.806							
11	.750	2.500	117.028	74.000	3.171	14.662	-.148	1
4.550	-.420							
12	.750	2.750	117.409	74.000	-.160	14.658	-.198	1
4.545	-.478							
13	.750	3.000	112.016	56.000	-15.666	14.605	-.799	1
4.502	-.964							
14	.750	3.250	111.196	23.000	-22.328	14.597	-.884	1
4.496	-1.032							
15	.750	3.500	115.114	-1.000	-10.267	14.626	-.564	1
4.517	-.794							
16	.750	3.750	112.534	-12.000	-1.891	14.659	-.184	1
4.556	-.360							
17	.750	4.000	109.175	-16.000	4.855	14.680	.055	1
4.583	-.052							
18	.750	4.250	104.321	-15.000	8.493	14.685	.111	1
4.596	.101							
19	.750	4.500	99.889	-13.000	10.106	14.687	.130	1
4.605	.204							

20	.750	4.750	98.034	-12.000	11.079	14.687	.134	1
4.609	.241							
21	.750	5.000	97.562	-11.000	11.411	14.686	.126	1
4.609	.242							
22	.750	5.250	97.200	-10.000	11.755	14.687	.132	1
4.610	.255							
23	.750	5.500	96.015	-9.000	12.364	14.686	.125	1
4.611	.270							
1	1.000	.000	92.973	-11.000	16.732	14.679	.045	1
4.609	.243							
2	1.000	.250	97.219	-12.000	15.783	14.686	.125	1
4.609	.247							
3	1.000	.500	99.888	-13.000	15.442	14.688	.145	1
4.607	.218							
4	1.000	.750	102.472	-15.000	15.370	14.688	.148	1
4.602	.173							
5	1.000	1.000	105.913	-16.000	15.095	14.688	.141	1
4.596	.099							
6	1.000	1.250	109.237	-18.000	15.245	14.685	.115	1
4.588	.007							
7	1.000	1.500	110.946	-14.000	14.219	14.675	-.008	1
4.574	-.151							
8	1.000	1.750	108.157	-3.000	13.826	14.646	-.332	1
4.550	-.418							
9	1.000	2.000	99.929	21.000	13.533	14.612	-.721	1
4.530	-.648							
10	1.000	2.250	101.992	51.000	8.347	14.616	-.669	1
4.531	-.635							
11	1.000	2.500	105.643	69.000	6.770	14.654	-.239	1
4.563	-.275							
12	1.000	2.750	111.612	71.000	1.544	14.671	-.046	1
4.569	-.203							
13	1.000	3.000	109.155	54.000	-15.730	14.629	-.521	1
4.532	-.627							
14	1.000	3.250	107.114	22.000	-25.062	14.619	-.635	1
4.526	-.701							
15	1.000	3.500	108.876	-1.000	-18.298	14.637	-.433	1
4.540	-.534							
16	1.000	3.750	108.996	-12.000	-6.883	14.666	-.101	1
4.569	-.204							
17	1.000	4.000	105.868	-13.000	2.447	14.682	.072	1
4.590	.032							
18	1.000	4.250	102.374	-14.000	6.782	14.686	.117	1
4.600	.143							
19	1.000	4.500	98.241	-12.000	9.184	14.686	.121	1
4.607	.225							
20	1.000	4.750	96.145	-11.000	10.421	14.686	.122	1
4.611	.264							
21	1.000	5.000	96.077	-10.000	11.098	14.686	.123	1
4.611	.266							
22	1.000	5.250	96.339	-10.000	11.624	14.685	.115	1
4.610	.253							
23	1.000	5.500	94.905	-9.000	12.157	14.685	.114	1
4.612	.278							
1	1.250	.000	96.335	-11.000	15.709	14.686	.121	1
4.610	.260							
2	1.250	.250	97.455	-13.000	15.844	14.686	.123	1
4.609	.242							
3	1.250	.500	98.732	-13.000	16.025	14.686	.126	1
4.607	.221							

4	1.250	.750	101.681	-14.000	15.953	14.686	.125	1
4.602	.165						.121	1
5	1.250	1.000	104.803	-16.000	16.256	14.686		
4.596	.102						.114	1
6	1.250	1.250	107.173	-17.000	17.238	14.685		
4.592	.048						.059	1
7	1.250	1.500	108.121	-16.000	18.968	14.681		
4.585	-.026						-.252	1
8	1.250	1.750	101.937	-7.000	21.148	14.653		
4.568	-.217						-.531	1
9	1.250	2.000	95.570	12.000	21.238	14.629		
4.554	-.379						-.563	1
10	1.250	2.250	93.882	41.000	15.812	14.626		
4.554	-.381						-.041	1
11	1.250	2.500	100.797	61.000	11.438	14.672		
4.589	.015						.129	1
12	1.250	2.750	102.990	62.000	4.491	14.687		
4.600	.144						-.119	1
13	1.250	3.000	106.615	50.000	-12.738	14.665		
4.572	-.175						-.399	1
14	1.250	3.250	101.650	20.000	-28.102	14.640		
4.556	-.359						-.137	1
15	1.250	3.500	105.706	.000	-22.013	14.663		
4.572	-.174						.023	1
16	1.250	3.750	105.923	-10.000	-9.544	14.677		
4.586	-.018						.092	1
17	1.250	4.000	102.964	-13.000	.221	14.683		
4.597	.107						.110	1
18	1.250	4.250	.99.508	-12.000	5.272	14.685		
4.604	.191						.106	1
19	1.250	4.500	96.297	-11.000	7.984	14.685		
4.609	.244						.104	1
20	1.250	4.750	96.357	-11.000	9.495	14.685		
4.609	.242						.103	1
21	1.250	5.000	95.758	-10.000	10.397	14.684		
4.609	.251						.102	1
22	1.250	5.250	96.329	-10.000	10.988	14.684		
4.608	.240						.097	1
23	1.250	5.500	95.217	-10.000	11.729	14.684		
4.610	.255						.123	1
1	1.500	.000	95.007	-10.000	16.130	14.686		
4.612	.285						.123	1
2	1.500	.250	96.037	-11.000	16.911	14.686		
4.611	.267						.125	1
3	1.500	.500	97.264	-12.000	17.110	14.686		
4.609	.247						.128	1
4	1.500	.750	99.451	-13.000	17.358	14.687		
4.606	.210						.124	1
5	1.500	1.000	100.871	-14.000	18.126	14.686		
4.603	.179						.121	1
6	1.500	1.250	102.806	-14.000	19.671	14.686		
4.600	.140						.094	1
7	1.500	1.500	102.248	-13.000	22.922	14.684		
4.598	.124						-.004	1
8	1.500	1.750	100.171	-7.000	26.166	14.675		
4.593	.064						-.247	1
9	1.500	2.000	93.062	9.000	28.769	14.654		
4.583	-.051						-.312	1
10	1.500	2.250	87.502	34.000	26.085	14.648		
4.585	-.023							

11	1.500	2.500	88.434	51.000	20.498	14.673	-.028	1
4.609	.246							
12	1.500	2.750	87.630	52.000	11.521	14.683	.091	1
4.621	.378							
13	1.500	3.000	92.393	41.000	-6.264	14.682	.070	1
4.612	.278							
14	1.500	3.250	95.325	21.000	-19.830	14.672	-.034	1
4.598	.122							
15	1.500	3.500	97.392	4.000	-17.915	14.676	.003	1
4.598	.123							
16	1.500	3.750	98.584	-5.000	-8.052	14.681	.066	1
4.602	.164							
17	1.500	4.000	97.081	-8.000	.147	14.684	.099	1
4.607	.224							
18	1.500	4.250	95.480	-9.000	5.111	14.685	.105	1
4.610	.258							
19	1.500	4.500	94.482	-10.000	7.935	14.684	.103	1
4.611	.275							
20	1.500	4.750	94.502	-9.000	9.457	14.685	.104	1
4.611	.275							
21	1.500	5.000	94.006	-9.000	10.302	14.684	.099	1
4.612	.278							
22	1.500	5.250	94.448	-9.000	10.910	14.684	.098	1
4.611	.270							
23	1.500	5.500	93.488	-8.000	11.756	14.684	.094	1
4.612	.282							
1	1.750	.000	92.894	-9.000	17.627	14.683	.088	1
4.612	.286							
2	1.750	.250	94.517	-10.000	17.520	14.685	.112	1
4.612	.283							
3	1.750	.500	95.581	-11.000	17.955	14.686	.116	1
4.611	.268							
4	1.750	.750	96.595	-11.000	18.597	14.685	.115	1
4.609	.249							
5	1.750	1.000	97.845	-11.000	19.581	14.686	.125	1
4.608	.236							
6	1.750	1.250	97.916	-11.000	21.410	14.686	.120	1
4.608	.230							
7	1.750	1.500	95.953	-10.000	25.644	14.685	.111	1
4.610	.256							
8	1.750	1.750	94.386	-6.000	30.707	14.682	.074	1
4.609	.247							
9	1.750	2.000	90.723	8.000	35.600	14.673	-.024	1
4.606	.212							
10	1.750	2.250	86.236	26.000	32.641	14.672	-.042	1
4.611	.268							
11	1.750	2.500	83.219	39.000	25.691	14.680	.054	1
4.624	.411							
12	1.750	2.750	81.682	40.000	16.561	14.686	.121	1
4.631	.502							
13	1.750	3.000	83.031	32.000	3.477	14.685	.111	1
4.629	.471							
14	1.750	3.250	87.326	18.000	-7.288	14.682	.081	1
4.620	.373							
15	1.750	3.500	91.390	7.000	-8.551	14.683	.086	1
4.615	.310							
16	1.750	3.750	92.676	-1.000	-3.705	14.683	.091	1
4.613	.294							
17	1.750	4.000	92.762	-5.000	1.497	14.684	.099	1
4.614	.300							

18	1.750	4.250	93.135	-6.000	5.401	14.684	.101	1
4.613	.295							
19	1.750	4.500	93.124	-8.000	7.974	14.684	.098	1
4.613	.293							
20	1.750	4.750	93.009	-8.000	9.260	14.684	.095	1
4.613	.292							
21	1.750	5.000	93.389	-8.000	10.438	14.683	.092	1
4.612	.284							
22	1.750	5.250	93.368	-8.000	11.150	14.684	.097	1
4.613	.288							
23	1.750	5.500	93.181	-8.000	11.886	14.683	.092	1
4.612	.286							
1	2.000	.000	93.140	-8.000	17.710	14.683	.086	1
4.612	.280							
2	2.000	.250	94.026	-8.000	17.834	14.685	.110	1
4.613	.289							
3	2.000	.500	94.754	-9.000	18.071	14.685	.114	1
4.612	.281							
4	2.000	.750	94.910	-9.000	18.865	14.685	.114	1
4.612	.277							
5	2.000	1.000	95.039	-9.000	19.911	14.685	.112	1
4.611	.274							
6	2.000	1.250	93.587	-8.000	22.007	14.685	.115	1
4.614	.302							
7	2.000	1.500	91.878	-7.000	25.237	14.685	.108	1
4.616	.324							
8	2.000	1.750	90.137	-2.000	29.506	14.684	.099	1
4.618	.345							
9	2.000	2.000	86.717	7.000	34.178	14.682	.077	1
4.621	.378							
10	2.000	2.250	83.605	18.000	33.172	14.681	.068	1
4.624	.419							
11	2.000	2.500	80.851	28.000	26.148	14.683	.085	1
4.629	.478							
12	2.000	2.750	80.075	30.000	18.652	14.686	.123	1
4.634	.527							
13	2.000	3.000	80.632	24.000	9.609	14.684	.097	1
4.631	.493							
14	2.000	3.250	83.079	15.000	1.474	14.683	.087	1
4.627	.446							
15	2.000	3.500	86.533	9.000	-1.162	14.683	.084	1
4.622	.389							
16	2.000	3.750	89.123	1.000	.640	14.683	.084	1
4.618	.347							
17	2.000	4.000	90.442	-3.000	3.640	14.683	.086	1
4.616	.326							
18	2.000	4.250	91.362	-5.000	6.351	14.683	.086	1
4.615	.311							
19	2.000	4.500	92.002	-6.000	8.271	14.683	.085	1
4.614	.299							
20	2.000	4.750	92.287	-7.000	9.510	14.682	.079	1
4.613	.288							
21	2.000	5.000	93.240	-7.000	10.354	14.682	.081	1
4.611	.273							
22	2.000	5.250	92.851	-7.000	11.256	14.682	.077	1
4.612	.277							
23	2.000	5.500	92.639	-7.000	11.871	14.682	.076	1
4.612	.279							
1	2.250	.000	92.403	-8.000	18.107	14.683	.091	1
4.614	.298							

2	2.250	.250	93.692	-8.000	18.184	14.686	.121	1
4.614	.306							
3	2.250	.500	93.746	-8.000	18.877	14.686	.121	1
4.614	.305							
4	2.250	.750	93.966	-8.000	19.615	14.686	.122	1
4.614	.302							
5	2.250	1.000	93.590	-7.000	20.713	14.686	.121	1
4.614	.308							
6	2.250	1.250	91.805	-6.000	22.343	14.686	.125	1
4.617	.343							
7	2.250	1.500	90.291	-4.000	24.914	14.686	.122	1
4.619	.365							
8	2.250	1.750	88.769	-1.000	27.282	14.686	.123	1
4.622	.392							
9	2.250	2.000	85.854	1.000	30.087	14.685	.105	1
4.624	.420							
10	2.250	2.250	82.768	13.000	28.943	14.685	.107	1
4.629	.471							
11	2.250	2.500	80.886	20.000	25.116	14.685	.107	1
4.631	.499							
12	2.250	2.750	80.979	21.000	19.520	14.687	.137	1
4.634	.528							
13	2.250	3.000	81.587	18.000	13.444	14.686	.120	1
4.631	.502							
14	2.250	3.250	82.561	13.000	7.897	14.684	.100	1
4.628	.467							
15	2.250	3.500	85.327	6.000	4.955	14.684	.098	1
4.624	.422							
16	2.250	3.750	88.056	2.000	4.944	14.684	.101	1
4.621	.381							
17	2.250	4.000	90.051	-2.000	6.074	14.684	.098	1
4.618	.345							
18	2.250	4.250	91.463	.000	7.592	14.684	.099	1
4.616	.323							
19	2.250	4.500	92.141	-5.000	8.893	14.684	.098	1
4.615	.310							
20	2.250	4.750	92.377	-6.000	10.016	14.684	.096	1
4.614	.303							
21	2.250	5.000	92.780	-6.000	10.764	14.684	.094	1
4.613	.295							
22	2.250	5.250	92.515	-6.000	11.521	14.684	.097	1
4.614	.303							
23	2.250	5.500	92.687	-7.000	12.127	14.684	.097	1
4.614	.300							
1	2.500	.000	90.377	-8.000	18.355	14.679	.045	1
4.612	.286							
2	2.500	.250	92.261	-8.000	18.384	14.684	.094	1
4.614	.303							
3	2.500	.500	92.515	-8.000	18.957	14.684	.099	1
4.614	.304							
4	2.500	.750	92.688	-7.000	19.447	14.684	.099	1
4.614	.302							
5	2.500	1.000	91.432	-6.000	20.727	14.684	.100	1
4.616	.324							
6	2.500	1.250	90.060	-5.000	22.253	14.684	.096	1
4.617	.343							
7	2.500	1.500	88.704	-3.000	23.742	14.684	.097	1
4.620	.367							
8	2.500	1.750	86.956	.000	25.346	14.683	.090	1
4.621	.388							

9	2.500	2.000	85.017	3.000	26.416	14.683	.086	1
4.624	.414							
10	2.500	2.250	82.750	8.000	25.923	14.683	.084	1
4.627	.448							
11	2.500	2.500	80.820	12.000	23.480	14.683	.086	1
4.629	.479							
12	2.500	2.750	81.486	14.000	19.431	14.685	.106	1
4.630	.490							
13	2.500	3.000	81.651	12.000	15.271	14.683	.087	1
4.628	.468							
14	2.500	3.250	82.508	10.000	11.210	14.682	.072	1
4.626	.440							
15	2.500	3.500	85.286	5.000	8.610	14.683	.082	1
4.623	.407							
16	2.500	3.750	87.315	1.000	7.650	14.683	.083	1
4.620	.376							
17	2.500	4.000	89.155	-1.000	8.057	14.683	.082	1
4.618	.344							
18	2.500	4.250	90.679	-3.000	8.715	14.683	.086	1
4.616	.322							
19	2.500	4.500	91.148	-5.000	9.540	14.682	.079	1
4.614	.307							
20	2.500	4.750	91.837	-6.000	10.196	14.682	.078	1
4.613	.295							
21	2.500	5.000	92.040	-7.000	11.007	14.682	.077	1
4.613	.290							
22	2.500	5.250	92.076	-7.000	11.834	14.682	.076	1
4.613	.289							
23	2.500	5.500	92.143	-8.000	12.116	14.682	.077	1
4.613	.288							
1	2.750	.000	91.217	-7.000	18.257	14.683	.083	1
4.615	.310							
2	2.750	.250	91.071	-6.000	18.570	14.684	.094	1
4.616	.324							
3	2.750	.500	91.242	-6.000	19.077	14.684	.097	1
4.616	.324							
4	2.750	.750	90.064	-6.000	20.103	14.684	.097	1
4.618	.343							
5	2.750	1.000	90.326	-6.000	20.643	14.684	.095	1
4.617	.338							
6	2.750	1.250	88.862	-4.000	21.857	14.684	.097	1
4.619	.363							
7	2.750	1.500	87.337	-2.000	22.948	14.684	.094	1
4.621	.386							
8	2.750	1.750	86.183	.000	23.884	14.683	.090	1
4.623	.401							
9	2.750	2.000	84.029	3.000	24.597	14.683	.087	1
4.625	.431							
10	2.750	2.250	82.292	6.000	24.046	14.683	.086	1
4.628	.457							
11	2.750	2.500	81.353	9.000	22.450	14.683	.088	1
4.629	.473							
12	2.750	2.750	81.458	10.000	19.475	14.684	.103	1
4.630	.487							
13	2.750	3.000	82.045	10.000	16.387	14.683	.086	1
4.628	.460							
14	2.750	3.250	83.289	7.000	13.230	14.682	.072	1
4.625	.428							
15	2.750	3.500	84.357	4.000	11.507	14.682	.073	1
4.624	.412							

16	2.750	3.750	86.106	1.000	10.404	14.682	.072	1
4.621	.384							
17	2.750	4.000	86.862	.000	10.048	14.681	.069	1
4.620	.368							
18	2.750	4.250	88.866	-3.000	10.242	14.681	.066	1
4.617	.333							
19	2.750	4.500	89.571	-4.000	10.572	14.682	.072	1
4.616	.327							
20	2.750	4.750	90.345	-5.000	11.021	14.681	.068	1
4.615	.310							
21	2.750	5.000	90.176	-6.000	11.803	14.681	.069	1
4.615	.314							
22	2.750	5.250	90.795	-6.000	12.137	14.681	.064	1
4.614	.299							
23	2.750	5.500	90.414	-6.000	12.509	14.681	.064	1
4.614	.305							
1	3.000	.000	90.729	-6.000	18.408	14.682	.080	1
4.615	.316							
2	3.000	.250	91.000	-6.000	18.565	14.683	.087	1
4.615	.318							
3	3.000	.500	90.794	-5.000	19.062	14.683	.086	1
4.615	.320							
4	3.000	.750	89.922	-5.000	19.655	14.683	.086	1
4.617	.335							
5	3.000	1.000	89.061	-4.000	20.550	14.683	.087	1
4.618	.350							
6	3.000	1.250	88.460	-3.000	21.208	14.683	.088	1
4.619	.362							
7	3.000	1.500	87.082	-1.000	22.031	14.683	.083	1
4.621	.379							
8	3.000	1.750	85.296	1.000	22.807	14.682	.081	1
4.623	.405							
9	3.000	2.000	84.083	3.000	22.941	14.682	.079	1
4.625	.423							
10	3.000	2.250	82.996	5.000	22.115	14.682	.079	1
4.626	.439							
11	3.000	2.500	82.411	7.000	21.137	14.682	.081	1
4.627	.450							
12	3.000	2.750	82.629	8.000	19.176	14.683	.084	1
4.627	.450							
13	3.000	3.000	83.322	6.000	16.658	14.682	.074	1
4.625	.429							
14	3.000	3.250	83.675	4.000	14.871	14.681	.065	1
4.624	.415							
15	3.000	3.500	85.012	3.000	13.020	14.681	.061	1
4.622	.390							
16	3.000	3.750	86.292	.000	11.938	14.681	.063	1
4.620	.371							
17	3.000	4.000	87.459	-1.000	11.491	14.681	.062	1
4.618	.352							
18	3.000	4.250	88.465	-2.000	11.467	14.681	.060	1
4.617	.333							
19	3.000	4.500	88.831	-3.000	11.636	14.681	.061	1
4.616	.328							
20	3.000	4.750	89.728	-5.000	11.852	14.681	.062	1
4.615	.315							
21	3.000	5.000	89.913	-6.000	12.185	14.681	.059	1
4.614	.309							
22	3.000	5.250	90.264	-6.000	12.537	14.680	.055	1
4.614	.299							
23	3.000	5.500	89.872	-6.000	12.973	14.680	.054	1
4.614	.304							

## LIST OF REFERENCES

1. Roane, D. P., *The Effect of a Turbulent Airstream on a Vertically-Launched Missile at High Angles of Attack*, M.S. Thesis, Naval Postgraduate School, Monterey, CA, December 1987.
2. Rabang, M. P., *Turbulence Effects on the High Angle of Attack Aerodynamics of a Vertically-Launched Missile*, M.S. Thesis, Naval Postgraduate School, Monterey, CA, June 1988.
3. Lung, Ming-Hung, *Flowfield Measurements in the Vortex Wake of a Missile at High Angle of Attack in Turbulence*, M.S. Thesis, Naval Postgraduate School, Monterey, CA, December 1988.
4. Dahlem, V., Flaherty, J. I., Shereda, D. E., *High Angle of Attack Missile Aerodynamics at Mach Numbers 0.3 to 1.5*, Technical Report AFWAL-TR-80-3070, Rutgers, NJ, November 1980.
5. Ericsson, L. E. and Reding, J. P., *Asymmetric Vortex Shedding From Bodies of Revolution*, Tactical Missile Aerodynamics, American Institute of Aeronautics and Astronautics, Inc., 1986.
6. Gregoriou, G., *Modern Missile Design for High Angle of Attack*, AGARD/VKI lecture series no. 121, High Angle of Attack Aerodynamics, March 1982.
7. Keener, E. R. and Chapman, G. T., *Similarity in Vortex Asymmetries Over Slender Bodies and Wings*, AIAA Journal, v. 15, no. 9., pp. 1370-1372, September 1977.
8. Deffenbaugh, F. D., and Koerner, *Asymmetric Vortex Wake Development on Missiles at High Angles of Attack*, Journal of Spacecraft, jv. 14, no. 3, pp. 155-162, March 1977.
9. Clark, W. C., and Nelson, R. C., *Body Vortex Formation on Missiles at High Angles of Attack*, AIAA Paper 76-65, January 1976.
10. Achenbach, Elmar, *Influence of Surface Roughness on the Crossflow Around a Circular Cylinder*, Journal of Fluid Mechanics, pp. 321-335, v. 46, part 2, 1971.
11. Ericsson, L. E. and Reding, J. P., *Dynamics of Forebody Flow Separation and Associated Vortices*, AIAA Paper 83-2118, August 1983.

12. Reding, J. P. and Ericsson, L. E., *Re-examination of the Maximum Normalized Vortex-Induced Side Force*, Journal of Spacecraft, v. 21, no. 5, September-October 1984.
13. Reding, J. P. and Ericsson, L. E., *Maximum Vortex-Induced Side Forces on Slender Bodies*, AIAA Paper 77-1155, 1977.
14. Lamont, P. J., *Pressure Measurements on an Ogive-Cylinder at High Angles of Attack With Laminar, Transitional, or Turbulent Separation*, AIAA Paper 80-1556, 1980.
15. Jorgensen, L. H. and Nelson, E. R., *Experimental Aerodynamic Characteristic for a Cylindrical Body Revolution with Various Noses at AOA from 0° to 58° and Mach Numbers from 0.6 to 2.0*, NASA TM X-3130, March 1975.
16. Wardlaw, A. B., Jr., and Morrison, A. M., *Induced Side Forces on Bodies of Revolution at High Angles of Attack*, NSWC/WOL/TR 75-176, November 1975.
17. Pick, George S., *Investigation of Side Forces on Ogive-Cylinder Bodies at High Angles of Attack in the M=0.5 to 1.1 Range*, AIAA Paper 71-570, 1971.
18. Keener, E. R. and others, *Side Force on Forebodies at High AOA and Mach Number from 0.1 to 0.7; Two Tangent Ogives, Paraboloid and Cone*, NASA-TM-X-3438, Moffet Field, CA, February 1977.
19. Kruse, Robert L, Keener, Earl R., and Chapman, Gary T., *Investigation of the Asymmetric Aerodynamic Characteristics of Cylindrical Bodies of Revolution With Various Variations in Nose Geometry and Rotational Orientation*, NASA-TM 78533, September 1979.
20. Yongnian, Y., Xinzhi, Y., and Jianying, L., *Active Control of Asymmetric Forces at High Incidence*, Journal of Aircraft, v. 25, no. 2, pp. 190-192, February 1988.
21. Keener, E. R. and others, *Side Forces on a Tangent Ogive Forebody with a Fineness Ratio of 3.5 at High AOA and Mach From 0.1 to 0.7*, NASA-TM-X-3437, Moffet Field, CA, February 1977.
22. Bradshaw, P., *An Introduction to Turbulence and Its Measurement*, Pergamon Press, 1971.

23. Tieleman, H. W., *A Survey of the Turbulence in the Marine Surface Layer for the Operation of Low-Reynolds Number Aircraft*, Virginia Polytechnic Institute Report VPI-E-85-10, Blacksburg, VA, March 1985.
24. Castro, I. P., *Effects of Free Stream Turbulence on Low Reynolds Number Boundary Layers*, Journal of Fluids Engineering, Volume 106, pp. 298-306, September 1984.
25. Meier, H. U. and Kreplin, H. P., *Influence of Freestream Turbulence on Boundary-Layer Development*, AIAA Journal, Volume 18, Number 1, pp. 11-15, January 1980.
26. Deane, J. R., *Missile Body Vortices and Their Interaction With Lifting Surfaces*, AGARD/VKI, lecture series, no. 121, High Angle of Attack Aerodynamics, March 1982.
27. Arya, S. P., *Atmospheric Boundary Layers Over Homogeneous Terrain*, Engineering Meteorology, Elsevier Scientific Publishing Company, 1982.
28. Healey, J. V., *Simulating the Helicopter-Ship Interface as an Alternative to Current Methods of Determining the Safe Operating Envelopes*, Naval Postgraduate School Report, NPS 67-86-003, Monterey, CA, September 1986.
29. Hancock, P. E. and Bradshaw, P., *The Effect of Free-Stream Turbulence on Turbulent Boundary Layers*, Journals of Fluids Engineering, Vol. 105, p. 285, September 1983.
30. Gregoriou, G. and Knoche, H. G., *High Incidence Aerodynamics of Missiles During Launch Phase*, MBB GMBH Report UA-523-80, January 1980.
31. Department of Aeronautics, *Laboratory Manual for Low-Speed Wind Tunnel Testing*, Naval Postgraduate School, Monterey, CA, 1983.
32. Velmex, Inc., *User's Guide to 8300 Series Stepping Motor Controller/Drivers*, East Bloomfield, NY, January 1988.
33. United Sensors, Inc., *5-Hole Probes Calibration Manual*, Watertown, MA, June 1988.
34. Hewlett-Packard, Inc., *PC Instruments System Owner's Guide Using HP 610618 System Interface*, February 1986.
35. Kindelispire, D. W., *The Effects of Freestream Turbulence on Airfoil Boundary Layer Behavior at Low Reynolds Number*, Master's Thesis, Naval Postgraduate School, Monterey, CA, September 1988.

**INITIAL DISTRIBUTION LIST**

	No. Copies
1. Defense Technical Information Center Cameron Station Alexanderia, VA 22304-6145	2
2. Library, Code 0142 Naval Postgraduate School Monterey, CA 93943-5002	2
3. Chairman Department of Aeronautics, Code 67 Naval Postgraduate School Monterey, CA 93943-5000	1
4. Commander Naval Surface Warfare Center, Code G205 Dahlgren, VA 22448-5000	1
5. Standard Missile Program Office PMS 422, G205 ATTN: Thomas McCants Dr. Jesse East Naval Surface Warfare Center Dahlgren, VA 22448-5000	2
6. Commander Naval Weapons Center, Code 406 China Lake, CA 93555	1
7. Commander Naval Surface Weapons Center Silver Spring, MD 20903-5000	1
8. Commander Pacific Missile Test Center Point Mugu, CA 93041	1
9. NASA Ames Research Center Technical Library Moffett Field, CA 94035	1

- |  |   |
|--|---|
| 10. Prof. R. M. Howard<br>Department of Aeronautics, Code 67Ho<br>Naval Postgraduate School<br>Monterey, CA 93943-5000 | 7 |
| 11. Prof. J. V. Healey<br>Department of Aeronautics, Code 67Ho<br>Naval Postgraduate School<br>Monterey, CA 93943-5000 | 1 |
| 12. LT. Lung, Ming-Hung<br>No. 114-5 Chung-Ching Rd.<br>Taichung Taiwan 400<br>Republic of China                       | 1 |
| 13. LT. J. J. Viniotis, USN<br>379 Ocean Avenue<br>Massapequa Pk, NY 11762   | 2 |